

**MOLECULAR DISSECTION OF THE MECHANISM UTILIZED BY THE
EWS/FLI ONCOGENE TO INFLUENCE THE MORPHOLOGY AND
BEHAVIOR OF EWING SARCOMA CELLS**

by

Aashi Chaturvedi

A dissertation submitted to the faculty of
The University of Utah
in partial fulfillment of the requirements for the degree of

Doctor of Philosophy

Department of Oncological Sciences

The University of Utah

August 2013

Copyright © Aashi Chaturvedi 2013

All Rights Reserved

The University of Utah Graduate School

STATEMENT OF DISSERTATION APPROVAL

The dissertation of Aashi Chaturvedi
has been approved by the following supervisory committee members:

Mary C. Beckerle, Chair 6/5/13
Date Approved

Stephen L. Lessnick, Member 6/13/13
Date Approved

Alana L. Welm, Member 6/18/13
Date Approved

Matthew K. Topham, Member 6/12/13
Date Approved

David J. Bearss, Member _____
Date Approved

and by Bradley R. Cairns, Chair of
the Department of Oncological Sciences

and by Donna M. Wight, Interim Dean of The Graduate School.

ABSTRACT

Ewing sarcoma is a devastating pediatric tumor that is particularly aggressive and highly metastatic. The current treatment regimen for this malignancy is aggressive, invasive and toxic, but with limited success. Treatment of metastatic or relapsed Ewing sarcoma is even more dismal with a low 5-year patient survival. My research is focused on identifying new mechanisms that could explain early and extensive metastasis in Ewing sarcoma potentially enabling better disease outcome in the future.

In the majority of Ewing sarcoma cases, the causal oncoprotein EWS/FLI develops from the reciprocal chromosomal translocation $t(11;22)(q24;q12)$. For this dissertation, I analyzed the effect of EWS/FLI oncoprotein on the cellular behavior of multiple patient-derived Ewing sarcoma cell lines, and discovered that EWS/FLI compromises the cytoskeletal framework of cells. As a result, Ewing sarcoma cells display small round cell morphology and low cellular adhesion. I further show that these EWS/FLI-dependent changes in cell behavior *in vitro* are pertinent to tumor cell behavior *in vivo* and could provide relevant insight into the cell of origin for Ewing sarcoma. Based on these observations, I suggest a new model where the inciting oncogenic event could affect tumor cell adhesion to permit early dissemination of tumor cells or increased colonization of tumor cells at a secondary site, to explain early metastasis of tumor cells.

In this dissertation the analysis of the EWS/FLI transcriptome, revealed that focal adhesion proteins, extracellular matrix components, and actin cytoskeletal modulators were most downregulated by EWS/FLI expression. Two focal adhesion proteins namely

zyxin and the fibronectin receptor $\alpha 5$ integrin were shown to play vital roles in modulating Ewing sarcoma cell morphology, cytoskeletal structure, spreading and adhesion.

To adequately study the tumor progression and metastasis of Ewing sarcoma, I developed an intratibial orthotopic mouse model. The Ewing sarcoma tumors grew aggressively in mice and spontaneously metastasized from the tibia to lungs and other bones. This model system recapitulates key features pertinent to the human disease.

Taken together, the work described in this dissertation reveals the important role of EWS/FLI mediated downregulation of adhesion proteins in modulating essential cellular features, such as cell adhesion and cytoskeletal structure, to govern oncogenic transformation and metastasis.

I dedicate this dissertation to my family, especially.....

My father, Piyush Chaturvedi, who has always inspired me to set high goals in life and gave me the confidence to achieve them.

My mother, Archana Chaturvedi, for her prayers and blessings.

My siblings, Anushi and Utkarsh, for their constant love and support.

&

My husband, Sachin Attavar, for being my best friend in this journey.

TABLE OF CONTENTS

ABSTRACT.....	iii
LIST OF FIGURES	viii
LIST OF TABLES	x
ACKNOWLEDGEMENTS.....	xi
CHAPTERS	
1. INTRODUCTION.....	1
Cancer metastasis.....	1
Ewing sarcoma is a highly metastatic tumor	3
Role of studying tumor microenvironment in Ewing sarcoma.....	5
Importance of cellular context to the study of Ewing sarcoma	8
EWS/FLI-driven changes in cell behavior are essential to Ewing sarcoma biology	11
Extracellular matrix, integrins and focal adhesions influence cell behavior	12
Goals of this dissertation.....	18
References.....	25
2. THE CLONE WARS – REVENGE OF THE METASTATIC ROGUE STATE: THE SARCOMA PARADIGM.....	34
Introduction.....	35
Metastatic Ewing sarcoma: the clinical perspective	36
The tumor microenvironment	37
Metastatic disease, instability of the clone	37
Closing remarks	38
Acknowledgments.....	38
References	38
3. THE EWS/FLI ONCOGENE DRIVES CHANGES IN CELLULAR MORPHOLOGY, ADHESION, AND MIGRATION IN EWING SARCOMA..	41
Abstract.....	42
Results.....	44
Discussion.....	49

Materials and Methods.....	52
Acknowledgments.....	54
Declaration of conflicting interests.....	54
Funding.....	54
References.....	54
4. STRETCH-INDUCED ACTIN REMODELING REQUIRES TARGETING OF ZYXIN TO STRESS FIBERS AND RECRUITMENT OF ACTIN REGULATORS.....	57
Abstract.....	58
Introduction.....	58
Results.....	59
Discussion.....	66
Materials and Methods.....	68
Acknowledgments.....	69
References.....	69
5. MOLECULAR DISSECTION OF THE MECHANISM BY WHICH EWS/FLI EXPRESSION COMPROMISES ACTIN CYTOSKELETAL INTEGRITY AND CELL ADHESION IN EWING SARCOMA.....	72
Abstract.....	73
Introduction.....	74
Results.....	76
Discussion.....	87
Materials and Methods.....	93
Acknowledgments.....	99
References.....	114
6. SUMMARY AND PERSPECTIVES.....	120
References.....	127

LIST OF FIGURES

Figure	Page
1.1 Metastatic Ewing sarcoma is a lethal disease	21
1.2 Schematic diagram of the EWS/FLI fusion transcript.....	22
1.3 Histopathology of Ewing sarcoma.....	23
1.4 Spatial distribution of ECMs, integrins and focal adhesions in a cell	24
3.1 Retroviral RNAi mediated knockdown of EWS/FLI in Ewing sarcoma cells	44
3.2 EWS/FLI expression abrogates cell adhesion and spreading	45
3.3 EWS/FLI expression compromises cell adhesion <i>in vivo</i>	46
3.4 Expression of EWS/FLI results in reduced cellular migration and invasion.....	47
3.5 EWS/FLI expression affects cellular morphology and cytoarchitecture	49
3.6 Ewing sarcoma cells TC71 and EWS502 exhibit EWS/FLI-dependent loss of adhesion, migration, and cytoarchitecture	50
3.7 Model for EWS/FLI-dependent coupling of transformation to acquisition of potential for tumor cell dissemination	51
4.1 Uniaxial cyclic stretch induces changes in focal adhesion constituents and actin cytoskeletal reinforcement	60
4.2 Posttranslational modification of zyxin in response to stretch	61
4.3 Zyxin responds independent of signaling molecule p130Cas.....	62
4.4 Zyxin mechanosensitivity-domain resides in the C-terminal LIM domain	63
4.5 Zyxin and α -actinin respond to stretch independently, but together they contribute to actin thickening.....	64

4.6 Stretch-induced actin cytoskeletal response is perturbed by disruption of zyxin-VASP interaction	65
4.7 Actin stress fibers formed without VASP recruitment exhibit enhanced sensitivity to actin inhibitor jasplakinolide (Jas)	66
4.8 Stretch-induced actin remodeling persists in the presence of Rho kinase inhibition	67
4.9 Model of mechanotransduction.....	67
5.1 EWS/FLI-dependent changes in the actin cytoskeleton and contributions of cytoskeletal regulators	101
5.2 Zyxin and $\alpha 5$ integrin contribute to the actin cytoskeleton, focal adhesions, cell spreading and cell adhesion in Ewing sarcoma cells	102
5.3 Intratibial orthotopic mouse model for Ewing sarcoma recapitulates features of the human disease.....	104
5.4 Zyxin and $\alpha 5$ integrin coexpression in Ewing sarcoma cells reduce tumor growth while osteolytic degradation of bone persists.....	106
5.5 Ewing sarcoma cells that express zyxin and $\alpha 5$ integrin metastasize to lungs and bones	108
5.6 Ewing sarcoma cells that express zyxin and $\alpha 5$ integrin exhibit increased adhesion to lung parenchyma.....	110
S.1 Mouse tibial tumors of Ewing sarcoma cells engineered to express zyxin and $\alpha 5$ integrin maintain Ewing sarcoma histopathology (H&E and CD99)	113

LIST OF TABLES

Table	Page
4.1 Zyxin domain analysis	62
5.1 Categories of downregulated target genes of EWS/FLI oncoprotein	111
S.1 List of EWS/FLI-downregulated target genes	112

ACKNOWLEDGEMENTS

This dissertation embodies much more than just culmination of my work as a graduate student. It represents my relationships with all the remarkable and generous people who have inspired me and supported me throughout this journey. I am particularly thankful to my mentor, Dr. Mary Beckerle, for her trust in my capabilities and her willingness to let me follow my passion towards cancer research in a collaborative work environment. Her high standard of excellence always challenged my intellect and abilities to help me mature into an independent scientist. In her lab, I was surrounded by a magnificent group of people who have shown me how science can and should be done. I am thankful to all the members, past and present, of the Beckerle lab for their expertise, helpful discussions and friendship for all these years. I worked very closely with Dr. Laura Hoffman and Chris Jensen who were always willing to share their knowledge and experience. Chris would always cheer me up with his sense of humor for life. I am indebted to Laura, for teaching me many valuable lessons in science and in life. I will be forever grateful to her for lifting my spirits up and providing me extra support and encouragement that I needed to get through some very difficult times.

I have been very fortunate to work with some exceptional collaborators and members of my thesis committee, especially Dr. Stephen Lessnick and Dr. Alana Welm. I am thankful to them for their generosity to share their laboratory resources with me. I have enjoyed several conversations with Steve regarding future directions for my project and my life in graduate school. I would like to express my gratitude to Alana for

extending the scope of my project by introducing a new dimension of animal studies. Alana has always made herself available to meet with me, personally train me, perform experiments with me and discuss my findings. Steve and Alana, with their labs have been instrumental in providing me the opportunity to broaden my research focus. I have greatly benefitted from the guidance and input of my thesis committee member Matthew Topham. Words are not enough to describe my deep gratitude for the enthusiasm and interest shown by Lt. Dr. Chi-Bin Chien towards my project during all the years he was on my committee. I am thankful to David Bearss for agreeing to be on my committee since then. I am a more accomplished scientist because of their interest and scientific integrity.

I would also like to acknowledge everyone who has ever trained me with microscopy, which has been an integral part of my project: Dr. Chris Rodesch, Dr. Mark Smith, Dr. Laura Hoffman and Keith Carney. This study would not have been possible without their technical guidance and support.

Life in Salt Lake City would never have been so memorable without my friends. Studying so far away from home is never easy and I am thankful to my friends and family for making the twists and turns of graduate school much more manageable and fun. Words cannot express my deep gratitude for everything you have done and continue to do for me.

CHAPTER 1

INTRODUCTION

Cancer metastasis

Metastasis is the primary cause of death in more than 90% of cancer patients worldwide (Valastyan and Weinberg, 2011). The term “metastasis,” was coined by the French gynecologist Joseph Claude Anthelme Récamier in 1829, to describe the process where cancer cells invade the bloodstream of the patient. Now, metastasis is viewed as dissemination of cancer cells from the primary cancer site to other organs of the body which may be far removed from the primary tumor mass (Talmadge and Fidler, 2010). Although many years of research have been dedicated to understanding how cancer cells become metastatic, the mechanisms involved in the progression of cancer are still poorly understood. Since metastatic disease is associated with poor prognosis, antimetastatic drugs might improve patient survival. This ultimately requires a better understanding of the process itself to guide the next phase of cancer research.

Metastasis is considered to be a multistage process with sequential and inter-related steps. The inability of a cancer cell to complete any of these steps could compromise the success of this complex process. A cancer cell poised for metastasis is predicted to ensue the following steps: the detachment of tumor cell from the primary tumor, its invasion into the surrounding tissue, intravasation (i.e., entry into the blood stream), survival in the bloodstream and translocation to distant sites via circulation,

extravasation (i.e., exit from the blood stream), reattachment to the new site followed by acclimatization to this new tissue microenvironment so that the tumor cell can survive and proliferate to form the secondary lesion (Chaffer and Weinberg, 2011). Such a series of steps is suggestive of an active process of metastasis that is inefficient and slow. It also indicates that metastatic lesions require an established primary tumor to accumulate enough mutations over time, making it a later event in cancer progression (Poste and Fidler, 1980; Talmadge and Fidler, 2010). This active model of metastasis is based on research done on tumors of epithelial origin, especially carcinomas, and often requires an epithelial-to-mesenchymal transition (EMT) (Fearon and Vogelstein, 1990; Yang and Weinberg, 2008). However, there are certain types of cancer that are metastatic at presentation, even when the primary tumor is very small. This multistep model of metastasis suggests gradual growth and spread of tumors over a course of time and hence does not adequately explain the early stage metastasis seen in several aggressive or micrometastatic malignancies.

No single model can adequately account for occurrence of micrometastatic tumors. Several models such as genetic or epigenetic events, effect of environmental changes or possible stochastic processes determining tumor cell behavior have been suggested but not well characterized. Such tumors may also exhibit early dissemination through some yet unknown or not fully understood mechanism to achieve metastasis to neighboring and/or distant sites in the body. Especially in tumors of mesenchymal or nonepithelial origin, such as sarcomas, the mechanism regulating tumor progression and metastasis could be very different from tumors of epithelial origin. In the work described in this dissertation, we focused on examining a micrometastatic sarcoma, called Ewing

sarcoma, to discover the various factors that could instigate the rapid growth, progression and metastasis in nonepithelial tumors.

This dissertation first reviews the clinical prognosis and the effect of tumor microenvironment on the behavior of cancer cells in the primary and secondary sites based on current literature (Chapter 2). I then investigate the role that the initiating oncogenic event plays to influence the tumor cell phenotype and behavior such as appearance of the actin cytoskeleton, cell spreading and cell adhesion (Chapter 3). In Chapter 4, I describe how proteins that are present at the interface of the cell membrane and the surrounding matrix could be critical in regulating cellular features such as the actin cytoskeleton. Based on these findings, I analyzed the downstream targets of the oncoprotein that could influence tumor cell spreading, adhesion and actin cytoskeleton *in vitro* and tumor progression and metastasis *in vivo* in a relevant tissue microenvironment (Chapter 5). Together, by describing oncogene-mediated changes in tumor cell behavior and highlighting the contributions of adhesion proteins and interaction of cells with their environment, the results from this dissertation are anticipated to advance our knowledge of tumor progression and metastasis of nonepithelial tumors in general and Ewing sarcoma in particular.

Ewing sarcoma is a highly metastatic tumor

For the purpose of this dissertation, I have studied a highly metastatic non-epithelial tumor called Ewing sarcoma. Since its first description by James Ewing in 1921, Ewing sarcoma remains a paradigm for understanding and investigating sarcoma biology (Ewing, 1921). Even after decades of research, the prognosis remains extremely poor for patients with metastatic or recurrent disease. Although it is a rare pediatric

neoplasm, with only 250 new cases identified each year in the United States, it still presents a dire future to those affected (Gurney J.G., 1999). While the 5-year survival rate for patients with localized disease is 60-70%, it is a dismal 10-30% for patients that present with metastatic disease (Figure 1.1) (Kolb et al., 2003; Paulussen et al., 2008). Despite the current highly aggressive multimodality treatments that involve surgical resection of the tumor, localized radiotherapy and systemic chemotherapy, the cure rates have not improved in more than a decade (Dirksen and Jurgens, 2010). These disappointing outcomes underscore the need to dissect the molecular mechanisms controlling the metastatic or recurrent Ewing sarcoma in order to devise novel treatment modalities.

In the mid-1980s, the chromosomal translocation $t(11;22)(q24;q12)$ was identified to be critical to the pathogenesis, development and maintenance of Ewing sarcoma (Turc-Carel et al., 1984). This chromosomal rearrangement is present in almost 85% of Ewing sarcoma cases and represents the fusion transcript that encodes a portion of *EWSR1* (Ewing's sarcoma rearrangement domain 1) gene from chromosome 22, and a part of the *FLI1* (Friend Leukemia virus integration site) gene from chromosome 11 (Turc-Carel et al., 1988). The *EWSR1* gene encodes the expression of the *EWS* protein which is a member of the *TET* family of putative RNA-binding proteins and *FLI1* is a member of the *ETS* family of transcription factors (Delattre et al., 1992; Morohoshi et al., 1996). The fusion of the amino-terminus of *EWSR1* with the carboxyl-terminus of *FLI1* has several important outcomes: (i) the RNA binding portion of *EWS* is replaced by the DNA binding portion of *FLI1* protein, (ii) the weak transcriptional activation domain of *FLI1* is replaced by the strong activation domain of *EWSR1*, and (iii) the resulting fusion now encodes the *EWS/FLI* protein that is constitutively expressed to function as an aberrant

transcription factor and exhibits novel oncogenic properties (Figure 1.2) (Ben-David et al., 1990; Lessnick et al., 1995; May et al., 1993b; Potratz et al., 2012).

Although EWS/FLI1 is the most common chromosomal translocation associated with Ewing sarcoma, other TET/ETS translocations have been observed in about 15% of Ewing sarcoma cases (Delattre et al., 1992; Sankar and Lessnick, 2011). These observations emphasize the role of chromosomal rearrangements in the pathogenesis of Ewing sarcoma. Infact, genetic tests (such as karyotyping) and molecular tests (such as RT-PCR analysis) confirming the presence of chromosomal translocation are considered strong supportive evidence for diagnosing Ewing sarcoma (Szuhai et al., 2012). In addition to these, Ewing sarcoma displays a small, round, undifferentiated blue cell phenotype when stained with Hematoxylin and Eosin (Arndt and Crist, 1999) (Figure 1.3). Furthermore, to distinguish these tumors from other pediatric malignancies, such as rhabdomyosarcoma, neuroblastoma and lymphoma, and to positively diagnose the tumors as Ewing sarcoma, the presence of cell surface marker CD99 and nuclear FLI1 staining is deemed necessary (Folpe et al., 2000; Llombart-Bosch and Navarro, 2001). In this dissertation work I have only focused on evaluating the role of EWS/FLI oncoprotein and its downregulated targets in influencing Ewing sarcoma biology as shown in Chapters 3 and 5.

Role of tumor microenvironment in studying Ewing sarcoma

Ewing sarcoma is the second most common bone-associated malignancy that affects children and young adults and accounts for 34% of all bone malignancies in this age group (Gurney J.G., 1999). This osteolytic malignancy typically arises in the appendicular and axial or central skeleton. However, in less than 15% of patients it may

also arise in the soft tissues and are known as “extra-osseous Ewing sarcoma” (Arndt and Crist, 1999; Kimber et al., 1998). Ewing sarcoma has a predilection to involve the shaft of long tubular bones, pelvis, and ribs but could arise from any other bone (Kimber et al., 1998). It is critical to study Ewing sarcoma in the bones due to its distinct tissue composition and microenvironment. A brief review of bone biology below will provide a good preface for understanding bone (host)-tumor (Ewing sarcoma cell) interaction.

Structurally, bones can be long or flat, and could be comprised of various concentrations of cortical (compact and dense) and trabecular bones (loosely organized and porous or “spongy”). Long bones are comprised of epiphysis (ends of bones for elongation), diaphysis (long shaft, primarily cortical bone) or metaphysis (largely trabecular, interspersed with marrow and blood vessels) (Bussard et al., 2008; Marks, 2002). Ewing sarcoma primarily develops in the diaphysis or metaphysis of long bones (Arndt and Crist, 1999). While radiographic analysis of a bone affected by Ewing sarcoma usually reveals an ill-defined, lytic and mottled appearance, the actual extent of bone destruction may be greater. It often extends into the soft tissue surrounding the tumor, making a clean surgical resection of the tumor very difficult and also affecting metastasis.

There are many features of the bone, which make it a desirable destination for cancer cell colonization. As a connective tissue, bone is composed of 95% Type I Collagen and the rest 5% is composed of noncollagenous proteins, such as fibronectin in its organic matrix (Hancox, 1972). Different kinds of cells reside in the bone, namely osteoblasts, osteoclasts, bone marrow stromal cells and hematopoietic cells. It is required that cell-cell and cell-matrix interactions among these cells are well coordinated. For instance, the osteoblasts release several growth factors, chemokines and cytokines to help

with bone growth. Conversely, osteoclasts bind integrins present on the cell surface and release lysosomal enzymes to degrade the bone. This synergistic function of these two cell types helps the bones to remodel in response to any mechanical strain to maintain homeostasis (Bussard et al., 2008; Kanis and McCloskey, 1997). Although these factors and enzymes primarily mediate communication between osteoblasts and osteoclasts, they can also be used by tumor cells to their advantage. For example, extensive osteolysis in Ewing sarcoma could support aggressive tumor growth and metastasis. The factors that contribute to the aggressive and highly osteolytic nature of these tumor cells appear to be significant to Ewing sarcoma biology and remain to be studied in the bone. An important aim of this dissertation has been to study Ewing sarcoma tumor growth in a long bone, such as the tibia of male NOD/SCID mice.

In addition to preferred sites of tumor growth, Ewing sarcoma almost always displays tissue-specific metastasis. Despite hematogenous dissemination of Ewing sarcoma cells, the tumor cells metastasize to lungs, other bones and bone marrow but not other vital organs such as the liver (Arndt and Crist, 1999; Riggi and Stamenkovic, 2007). This suggests a fundamental role for tissue microenvironment in determining not only growth, progression, but also metastasis of Ewing sarcoma. More than a century ago, Stephen Paget proposed the ‘seed and soil’ hypothesis (Paget, 1989) for cancer metastasis suggesting that a ‘seed’ (progenitor cells, tumor cells, metastatic cells) could colonize and grow in favorable ‘soil’ (microenvironment of tumor cells at the local or distant organs, stroma, host factors, tumor cell niche) (Talmadge and Fidler, 2010). Since then, it has been shown that the availability of growth factors and matrices in the tissue microenvironment, expression of receptors on the tumor cell surface and the complex network of receptor and growth-factor interactions, could affect the malignant behavior

of tumors. The role of tumor microenvironment in the tissue specific dissemination of Ewing sarcoma cells is not well characterized. Therefore in this dissertation, we also examine the spontaneous sites of metastasis from primary Ewing sarcoma tibial tumors.

Ewing sarcoma has predilection for bones as the primary site of sarcomagenesis and also for metastasis in more than 90% of cases (Guise et al., 2006). Based on the ‘seed and soil’ hypothesis, this could be attributed to the abundance of growth factors such as basic fibroblast growth factor (b-FGF), platelet derived growth factor (PDGF), transforming growth factor β (TGF- β), stem cell factor (SCF, the ligand for c-kit receptor), adhesion molecules, cytokines and chemokines present in the bone, providing the so-called ‘rich soil’ or ‘favorable environment’ for growth of tumors in the bone (Bussard et al., 2008; Mundy, 2002). Some of these factors have been shown to be critical to the expression of EWS/FLI or to the tumor growth and metastasis of Ewing sarcoma (Girnit et al., 2000). In addition to this, changes in tumor microenvironment such as hypoxic or hypoglycemic conditions also cause phenotypic changes in Ewing sarcoma cells (Aryee et al., 2010; Knowles et al., 2010). A better understanding of interactions between Ewing sarcoma cells and the surrounding matrix will offer new insight towards preventing tumor growth and metastasis of Ewing sarcoma and might reveal new therapeutic targets.

Importance of cellular context to the study of Ewing sarcoma

In addition to the host environment, it is imperative to study the impact of the EWS/FLI oncoprotein in an appropriate cellular context. The cell of origin for Ewing Sarcoma has been the cause of considerable debate since the 1970s. James Ewing first described the tumor as a ‘diffused endothelioma of the bone’ (Ewing, 2006). This

suggested an endothelial origin for Ewing sarcoma, which was later challenged by suggestions of hematological origin, neural crest origin or that of mesenchymal or fibroblastic origin in 1980s further perplexing researchers (Cavazzana et al., 1987; Dickman et al., 1982; Kadin and Bensch, 1971). The undifferentiated appearance of Ewing sarcoma did not provide much information into the cell of origin; rather the presence of mesenchymal markers and several neuroectodermal markers further complicated the issue.

All these studies utilized either microscopic examination or immunohistochemistry to correlate the appearance of Ewing sarcoma cells to other cells in the cellular milieu present at the anatomic locations from where the tumor cells were isolated. However, these studies ignored the possibility that the chromosomal translocation $t(11;22)(q24;q12)$ that created EWS/FLI fusion could be responsible for the tumor cell phenotype independent of the cell of origin. Gain of function studies by putting EWS/FLI in murine and human fibroblasts or by the loss of function studies by knocking down EWS/FLI in patient-derived primary Ewing sarcoma cells could be used to address this question.

Through decades of research, scientists in the field have come to realize that the biological response to the EWS/FLI oncoprotein expression depends on the cellular context (Arvand and Denny, 2001; Kovar, 2005). Several heterologous model systems, human and murine alike, have been manipulated to recapitulate Ewing sarcoma, some more successful than others. Exogenous expression of EWS/FLI was performed in several cell lines, including fibroblast cell lines (human NIH3T3, rodent Rat-1 or mouse embryonic), NCM-1 rodent neural crest progenitor cells as well as murine marrow-derived stromal cells and CTR rhabdomyosarcoma cells (Hu-Lieskovan et al., 2005; May

et al., 1993a; Teitell et al., 1999; Toretsky et al., 1997). While NH3T3 cells could be transformed to resemble Ewing sarcoma cells, expressing EWS/FLI in other cell lines either inhibited cell growth or blocked cellular differentiation as seen in murine marrow-derived stromal cells (Lessnick et al., 2002; Torchia et al., 2003). Even though NIH3T3 cells could be transformed by EWS/FLI expression, gene profiling studies revealed that these cells do not recapitulate the gene expression pattern of bonafide Ewing sarcoma cells derived from patients, thereby limiting the use of this model system to study Ewing sarcoma (Braunreiter et al., 2006).

Based on the most recent body of evidence, mesenchymal stem cells (MSCs) may appear to be the true cell of origin for Ewing sarcoma (Riggi et al., 2008; Tirode et al., 2007). MSCs are an interesting candidate because they are believed to be derived from both hematopoietic and neuroectodermal cell lineages (Riggi et al., 2009). When EWS/FLI expression was silenced in Ewing sarcoma cell lines, the gene expression signature most closely resembled that of MSC (Tirode et al., 2007). Conversely, when EWS/FLI was expressed in MSCs, the gene expression signature was very similar to that of patient-derived Ewing sarcoma cells, but the MSCs did not form tumors in immunocompromised mice (Riggi et al., 2008). This finding further suggests that EWS/FLI expression is not sufficient to transform MSCs into Ewing sarcoma cells, and perhaps additional or cooperative mutations or a more permissive microenvironment are required for complete transformation. Alternatively, it should be noted that MSCs are not confirmed cell of origin for Ewing sarcoma and based on above experimental consequences it is possible that may be MSCs are not the cell of origin for Ewing sarcoma.

Controversies surrounding the cell of origin for Ewing sarcoma, prompted us to choose a loss of function approach in patient-derived Ewing sarcoma cells. The retrovirally mediated shRNA-based knockdown of endogenous EWS/FLI expression in patient-derived cell lines (such as A673, EWS502, TC71) facilitated the work described in this dissertation. Using this unique knockdown approach, the cells lost EWS/FLI-mediated oncogenic transformation *in vitro* and tumor formation *in vivo* (Smith et al., 2006). The microarray analysis performed to verify the transcriptional profile of EWS/FLI using this technique identified a core set of genes that are known dysregulated targets of EWS/FLI, thereby validating the use of this approach to study EWS/FLI mediated effects on cell behavior in Chapters 3 and 5 (Kinsey et al., 2006; Luo et al., 2009; Smith et al., 2006; Tirado et al., 2006).

EWS/FLI-driven changes in cell behavior are essential to Ewing sarcoma biology

It needs to be explored how EWS/FLI makes changes in cellular behavior to drive Ewing sarcoma metastasis, in addition to inciting oncogenic transformation. It can be assumed that, being an aberrant transcriptional factor, EWS/FLI oncoprotein affects the gene expression patterns in Ewing sarcoma cells to modulate tumor cell phenotype. We used the aforementioned EWS/FLI knockdown approach to examine the role of this oncoprotein to influence changes in cell morphology, adhesion, spreading, migration and invasion. For the progression and metastasis of tumors of epithelial origin, the role of surrounding tissue microenvironment in influencing tumor cell behavior have been deemed vital and are extensively studied (Thiery and Sleeman, 2006; Yilmaz and Christofori, 2009). It is important to explore if the matrix composition of the tissue at the primary and the secondary site are also relevant in sarcomas and other nonepithelial

cancers. This dissertation not only investigates whether EWS/FLI affects these vital cellular features and processes but also how the interaction of tumor cell with its surrounding tissue matrix influences Ewing sarcoma tumor progression and metastasis.

Extracellular matrix, integrins and focal adhesions influence cell behavior

As a tumor grows and metastasizes, the tumor cells experience several intrinsic (genetic/epigenetic modifications) or extrinsic (cues from surrounding matrix, growth factors, chemotactic and mechanical stimuli) pressures, to which they must survive, adapt and, proliferate (Hynes, 1992; Ingber et al., 1981; Lelievre et al., 1998; Yilmaz and Christofori, 2009). Cells must adhere to the surrounding extracellular matrix (ECM) for sensing and responding to specific information being conveyed to the cell. While this cell-ECM interaction is determined by a group of proteins on the cell surface called “integrins,” cell-cell communication is determined by another group of proteins called “cadherins” (not discussed in this dissertation) (Chambers et al., 2002; Frixen et al., 1991). Although these interactions are fairly complex, simply put, focal adhesion sites located on the edge of the cell house these integrins which form the link between the ECM present on the outside and the cytoskeleton present on the inside of the cell as described in Figure 1.4 (Hervy et al., 2006). This segment will touch on the roles of ECM, integrins and focal adhesions in the regulation of cellular features being studied in this dissertation.

The ECM can be described as a heterogenous meshwork of fibrillar and nonfibrillar components which can be assembled into elaborate structures such as basement membranes and interstitial matrices that are composed of laminins, collagens and glycoproteins such as fibronectin, which in turn act as ligands for cell surface

receptors such as integrins (Dubash et al., 2009; Humphries et al., 2004). The integrated mechanics and dynamics between the cell and the ECM enables cells to control their shape, generate force, and ultimately remodel the surrounding ECM (Bershadsky et al., 2003; Giancotti and Ruoslahti, 1999; Ingber, 2008; Janmey, 1998).

A significant role for integrins in bone biology was first suggested in 1986 when antibodies raised against osteoclasts were shown to inhibit bone resorption *in vitro* (Chambers et al., 1986). ‘Integrins’ were first identified as trans-membrane proteins that are ‘integral’ to the link between the cell and the ECM in 1986, hence the name (Hynes, 2004; Tamkun et al., 1986). These are comprised of an α subunit that is noncovalently bound to a β subunit, forming a large trans-membrane heterodimer, and consequently, may respond to cytoplasmic and extra cellular cues. To-date, 18 α and 8 β subunits are known to assemble in 24 different combinations of heterodimers which bind to distinct ECMs to determine outside-in and inside-out signaling in cells thereby regulating cell adhesion, survival, proliferation, migration and invasion (Hynes, 2002). To achieve so many functions, integrins can bind to multiple ligands and conversely, several ECMs can bind to multiple integrins by recognizing certain peptide sequences such as Arginine-Glycine-Aspartic acid (RGD) (Humphries et al., 2004; Ruoslahti, 1996). However, binding of integrins to the ligand is not sufficient for a meaningful functional interaction; rather, it also requires activation of these integrin heterodimers by clustering on the cell surface and/or by inducing conformational changes in the receptors. Downstream to the stimulation of integrins, the activation of Rho GTPases regulates formation of stress fibers and focal adhesions thereby allowing cells to adhere, spread and migrate (Guo and Giancotti, 2004; Salsmann et al., 2006).

One of the most well characterized integrin-ECM interactions is that between $\alpha 5\beta 1$ integrin and fibronectin (Nagae et al., 2012; Yang et al., 1999). In the case of hematological malignancies, the presence of fibronectin and its receptor in the bone and bone marrow suggest a vital role for these interactions in tumor-host signaling (Geiger et al., 2001; Wennerberg et al., 1996). Therefore, these interactions need to be evaluated in appropriate context for each malignancy. This dissertation attempts to evaluate the role of $\alpha 5$ integrin in regulating the cytoskeletal features and cell adhesion of Ewing sarcoma cells *in vitro* and *in vivo* in Chapter 5.

These sites of cell-ECM interactions correspond to the area of the plasma membrane where actin bundles terminate and are called focal adhesions (Singer, 1979). The term “focal adhesion” was first coined to describe focused regions where the cell makes contact with the substratum and anchors the actin bundles. These are dense adhesion plaques on the edge of the cells visible by light and electron microscopy (Abercrombie et al., 1971; Heath and Dunn, 1978). Apart from structural contributions, focal adhesions convey information bidirectionally between cells and their surroundings. This is reflected in a recent report that observed integrin-based focal adhesions comprised of 156 molecules forming 690 potential interactions (Zaidel-Bar and Geiger, 2010). Such complex networking at these sites of cell adhesion vary based on the organism, tissue, cell and even spatio-temporally regulated in a cell during various stages of development and/or malignancy (Guo and Giancotti, 2004; Kumar and Weaver, 2009; Mitra and Schlaepfer, 2006). During these processes, the cells required to adhere and spread on the matrix, attach and detach efficiently for directed migration and possibly invade through the surrounding membrane. The cells therefore change the number and size of their focal adhesions and use the actin stress fiber network to generate enough extensile and

contractile forces based on the composition and stiffness of the matrix (Balaban et al., 2001; Ingber, 2008; Mierke et al., 2008). In Chapter 4 of this dissertation, one such focal adhesion protein called zyxin is scrutinized in response to mechanical stimulation to affect actin stress fiber network.

It should be noted that the cells and the surrounding ECM are interdependent on each other. For example, while the integrins on the cell surface assemble fibronectin into functional fibrillar matrix and orchestrate assembly of other ECM components, this well-defined matrix in turn promotes cell adhesion, migration, signaling and regulation of cytoskeleton (Leiss et al., 2008). In Chapter 5 of this dissertation we investigate the contributions of adhesion proteins in general and two proteins zyxin and $\alpha 5$ integrin in particular, whose expression is regulated by EWS/FLI to affect the characteristics of Ewing sarcoma cells *in vitro* and *in vivo* in the context of an orthotopic mouse model.

Zyxin: a focal adhesion protein

One of the proteins in the list of downregulated targets of EWS/FLI was “zyxin,” an 84KDa focal adhesion protein that was identified 25 years ago. This protein was named based on the Greek word “*zeuxis*,” which means “joining” because it was first observed at the junction of actin stress fibers and focal adhesions (Beckerle, 1986). Zyxin is known to regulate actin assembly, possibly through its N-terminus by binding α -actinin (Crawford et al., 1992; Hirata et al., 2008). Zyxin also has nuclear export signals and 3 LIM domains in its C-terminus (Schmeichel and Beckerle, 1994). Zyxin is a protein that responds to mechanical cues, such as cyclic stretch or changes in the internal or external environment of cells, in order to maintain cytoskeletal integrity and homeostasis (Hervy et al., 2006; Hoffman et al., 2006; Yoshigi et al., 2005). In Chapter 4, domain analysis of

zyxin suggests that zyxin harbors two functionally and spatially discrete domains, a localization domain and a reinforcement domain, to collectively influence actin stress fiber reinforcement in response to cyclic stretch.

Zyxin recognizes sites of local stress and repair actin stress fiber break or thinning events by recruiting α -actinin protein and Vasodilator-stimulated phosphoprotein (VASP) to the sites of stress fiber damage (Smith et al., 2010). It has nuclear export signals, which when mutated can result in shuttling of zyxin into the cell nuclei from adhesion plaques (Hervy et al., 2006). Zyxin is actually the first focal adhesion protein that showed shuttling between nucleus and focal adhesion sites (Nix and Beckerle, 1997). Some studies have reported that zyxin can bind to a transcription factor *in vitro*, to influence osteoblast differentiation by shuttling between the nucleus and focal adhesion sites (Janssen and Marynen, 2006). Interestingly, zyxin along with its binding partners plays crucial role in regulating gene expression in two tissues, both of which need to be extremely responsive to mechanical cues, namely, smooth muscle and bone (Hervy et al., 2006). Given the above information about zyxin's role in mechano-sensitivity in bone or osteoblast differentiation, it was intriguing to us to further evaluate any potential part that zyxin may have in influencing growth and metastasis of a bone tumor, such as Ewing sarcoma.

In addition to these features, zyxin has also been previously implicated by other researchers in Ewing sarcoma. CD99 – a key cell surface receptor that is often specific to Ewing sarcoma – functions through reorganization of the actin cytoskeleton, and zyxin was critical to cell adhesion and downstream signaling cascade following CD99 engagement (Cerisano et al., 2004). It was subsequently reported that zyxin expression in Ewing sarcoma cells correlated with actin cytoskeletal rearrangements and that zyxin acts

as a tumor suppressor for Ewing sarcoma in a mouse model (Amsellem et al., 2005). These studies inspired my interest in understanding how zyxin could contribute to Ewing sarcoma cell morphology and cell behavior, such as cell adhesion and actin cytoskeleton *in vitro* and in tumor growth and progression *in vivo*.

$\alpha 5$ Integrin: fibronectin receptor subunit

$\alpha 5\beta 1$ integrin was one of the first integrin heterodimers to be discovered (Tamkun et al., 1986). To date, 11 integrin heterodimers are known to bind fibronectin (Leiss et al., 2008), but among these $\alpha 5\beta 1$ integrin is considered to be crucial for assembly of thin and long fibronectin fibrils. Upon binding fibronectin, the $\alpha 5\beta 1$ integrins pull out from focal adhesions and move along actin stress fibers towards the centre of the cell and form a new adhesion structure called fibrillar adhesions, such that the fibronectin fibrils are aligned with $\alpha 5\beta 1$ integrins and F-actin filaments (Geiger et al., 2001; Ohashi et al., 2002; Pankov et al., 2000; Zamir and Geiger, 2001). As multiple integrins can interact with many ECM molecules, in the absence of $\alpha 5\beta 1$, short and thick fibronectin fibrils can be assembled by $\alpha v\beta 3$ integrin. While $\alpha 5\beta 1$ integrin binds fibronectin via RGD and PHSRN (Pro-His-Ser-Arg-Asn) sequences to give cells their fibroblast like morphology, $\alpha v\beta 3$ integrin binds only using the RGD sequence (Truong and Danen, 2009). This kind of an integrin switching has been shown to affect both cell spreading and the kind of fibrillar and focal adhesions present in the cells. Only a double knockout of $\alpha 5$ and αv integrin can completely deplete formation of fibronectin fibrils (Yang et al., 1999).

The expression of $\alpha 5$ integrin on the cell surface is often modulated to affect different processes during development, erythropoiesis and several malignancies. However, based on the cell type and the malignancy, the role of $\alpha 5\beta 1$ integrin could be

positively correlated (Caswell et al., 2008; Kawajiri et al., 2008; Qian et al., 2005) or negatively correlated (Schirner et al., 1998; Tani et al., 2003; Taverna et al., 1998) with tumor formation, cell migration and metastasis. Such observations emphasize the need to study the role of cell surface receptors like $\alpha 5\beta 1$ integrins in appropriate cellular and environmental context. Ewing sarcoma mostly affects the bone and bone marrow of a patient, which are both rich in fibronectin matrix and therefore, studying the role of $\alpha 5$ integrin with its corresponding matrix fibronectin could provide new insights into the tumor cell behavior.

It was demonstrated that three genes in the cell adhesion pathway were modulated by triggering CD99 in Ewing sarcoma cells: zyxin (as described above), $\alpha 5\beta 1$ integrin (described in this sub section) and integrin $\beta 8$ precursors (not evaluated in this study) all of which have been associated with influencing cellular adhesion (Cerisano et al., 2004). In this dissertation we were able to investigate the contributions of two of these genes, zyxin and $\alpha 5$ integrin in Ewing sarcoma cell biology.

Goals of this dissertation

Molecular mechanisms regulating metastasis in nonepithelial cancers, mesenchymally-derived tumors or in tumors of uncertain origin are still not well characterized. This dissertation focuses on one such cryptic malignancy with uncertain histogenesis and aggressive biological behavior, Ewing sarcoma. Most of the research in this field is centered on understanding the transcriptome of the EWS/FLI fusion oncoprotein to identify and study critical targets required for pathogenesis of Ewing sarcoma. The research described here is a step towards studying the mechanisms by which EWS/FLI mediates changes in tumor cell behavior such as cytoskeletal integrity,

cell morphology, cellular spreading and adhesion. This knowledge will provide valuable information about the specific cellular features that are critical to EWS/FLI dependent cellular pathogenesis. The work described here explores the contributions of two downregulated targets of EWS/FLI to Ewing sarcoma pathogenesis. These studies have been performed using a loss-of-function approach where retrovirally infected shRNA could knockdown the expression of endogenous EWS/FLI in patient-derived Ewing sarcoma cells. This approach enabled us to address the impact of EWS/FLI expression on Ewing sarcoma cell behavior within its native cellular context more accurately, which was vital to this study.

This dissertation describes my work in the following segments:

- i. *Review of metastatic Ewing sarcoma.* In this review, I highlight the role of tumor microenvironment in Ewing sarcoma. I provide a comprehensive analysis of the possible host-tumor interactions that could influence the metastatic behavior of Ewing sarcoma cells and guide their propensity to metastasize to lungs and other bones.
- ii. *What is the impact of EWS/FLI expression on the behavior of tumor cells?* In this segment, I provide evidence that EWS/FLI expression gives the cells their round cell morphology and compromises actin cytoskeleton, cell adhesion and cell migration. I present a model that suggests loss of cell adhesion is caused by the oncogenic event which could lead to early tumor dissemination and contribute to metastasis, while simultaneously forming Ewing tumors.
- iii. *How does a focal adhesion protein sense cellular stress and remodel actin filaments?* In this collaborative study, we investigate the mechanism used by focal adhesion proteins, especially zyxin, to sense physical stress around the

cells and maintain or reinforce the actin stress fibers even in the presence of Rho inhibitors. This study was performed on fibroblasts but was vital in suggesting the possible role of adhesion proteins in regulating cytoskeletal features in Ewing sarcoma cells.

- iv. *What is the role of downregulated targets of EWS/FLI, especially zyxin and $\alpha 5$ integrin, in tumor cell behavior in vitro and in vivo?* In Chapter 5 of this dissertation, I first describe how expression of zyxin and $\alpha 5$ integrin in Ewing sarcoma cells leads to different functional contributions to the actin cytoskeleton, cell adhesion and cell spreading despite their overlapping location in the cells. Also, I describe the orthotopic tibial mouse model that I developed to study the growth, progression and metastasis of Ewing sarcoma cells. I then used *in vivo* model to dissect the contributions of zyxin and $\alpha 5$ integrin in regulating tumor progression and spontaneous metastasis of Ewing sarcoma cells to other bones and lungs.

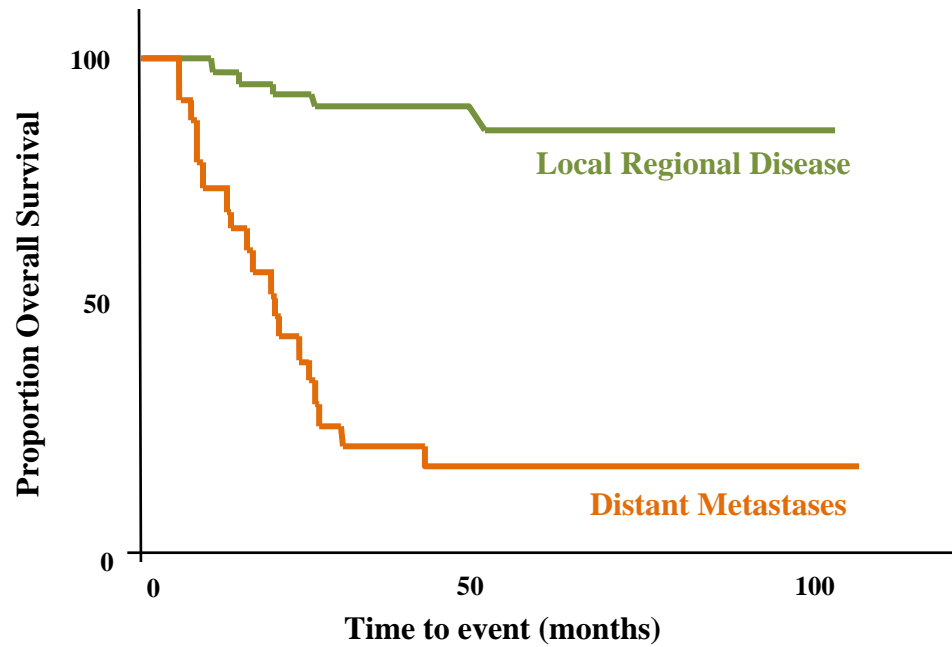


Figure 1.1: Metastatic Ewing sarcoma is a lethal disease. The 5-year overall survival rate of Ewing sarcoma patients is extremely poor when diagnosed with metastatic disease at presentation. This figure is adapted from Kolb et al., 2003.

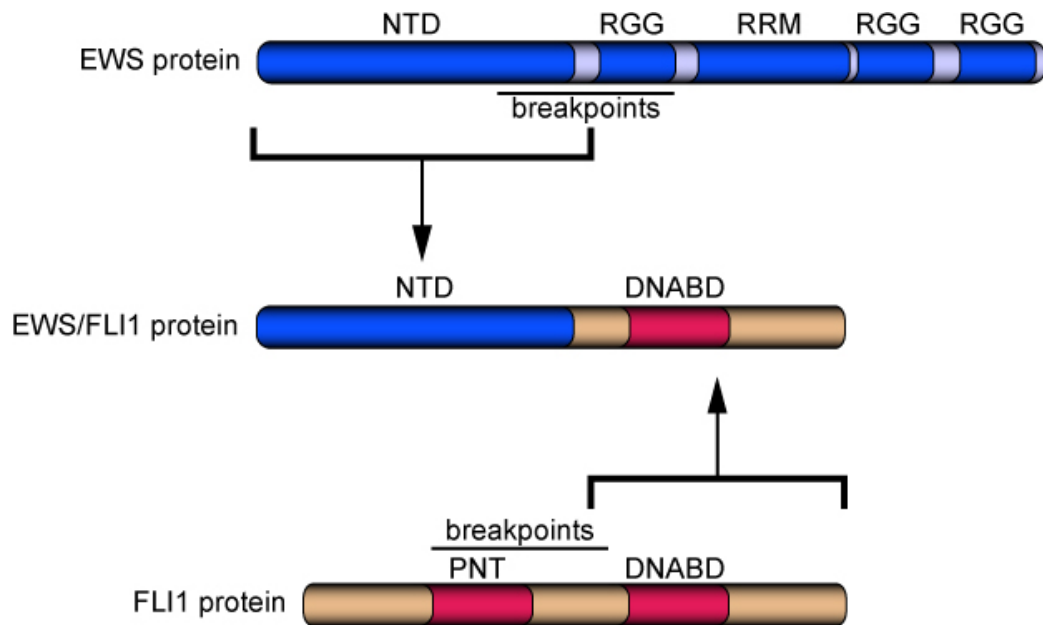


Figure 1.2: Schematic diagram of the EWS/FLI fusion transcript. The amino-terminal domain or NTD from wild-type EWS protein and the carboxyl-terminal domain containing the DNA-binding domain from the FLI protein translocate and fuse as shown above to form the EWS/FLI oncoprotein. Figure is provided as a courtesy by Dr. Stephen L. Lessnick.

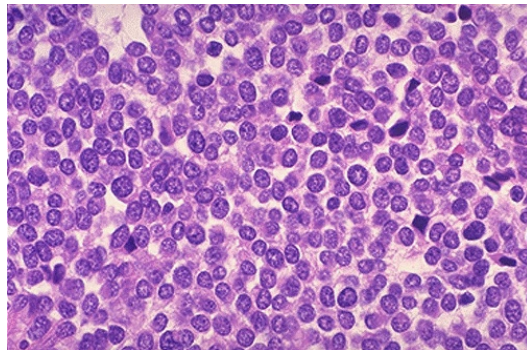


Figure 1.3: Histopathology of Ewing sarcoma. Ewing sarcoma is characterized by the appearance of monomorphic small round blue cells when stained with Hematoxylin and Eosin as shown above. Image is provided as a courtesy by Dr. Stephen L. Lessnick.

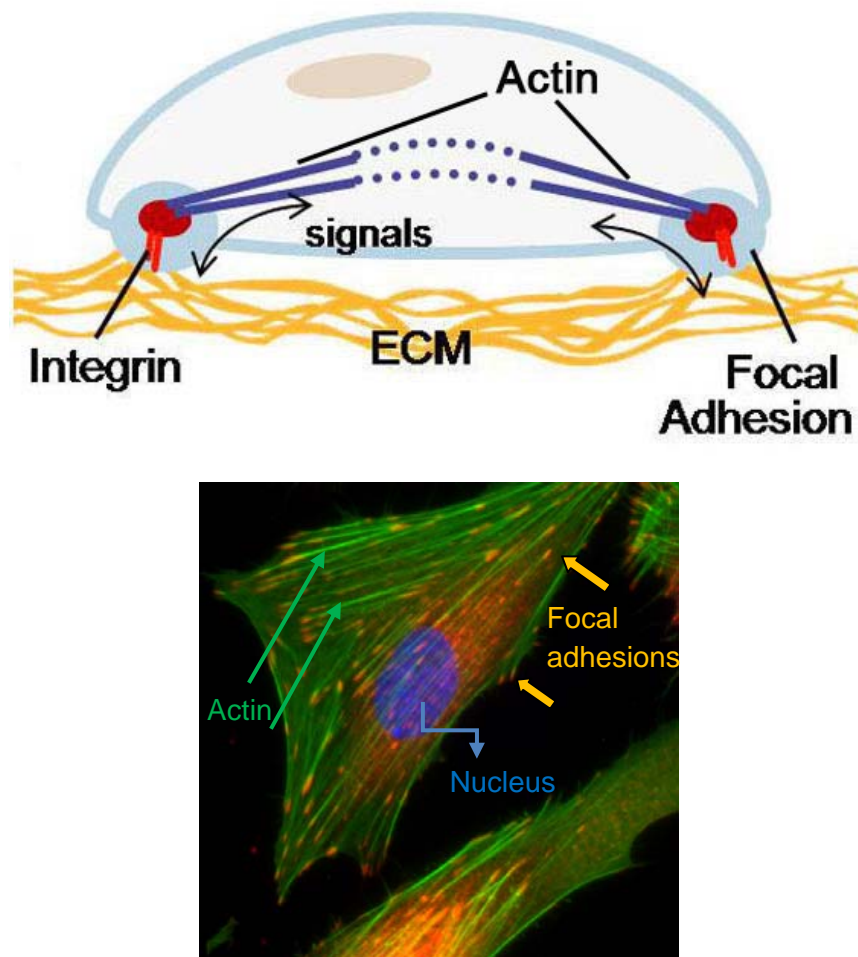


Figure 1.4: Spatial distribution of ECM, integrins and focal adhesions in cell. Integrins are transmembrane proteins localized at focal adhesion sites and transmit information between the ECM and the actin cytoskeleton or other places such as the nucleus in the cell, as represented in a cartoon (top) (Image is provided as a courtesy by Dr. Laura M. Hoffman) and in an immuno-stained cell (bottom).

References

- Abercrombie, M., Heaysman, J.E., and Pegrum, S.M. (1971). The locomotion of fibroblasts in culture. IV. Electron microscopy of the leading lamella. *Exp. Cell Res.* *67*, 359-367.
- Amsellem, V., Kryszke, M.H., Hervy, M., Subra, F., Athman, R., Leh, H., Brachet-Ducos, C., and Auclair, C. (2005). The actin cytoskeleton-associated protein zyxin acts as a tumor suppressor in Ewing tumor cells. *Exp. Cell Res.* *304*, 443-456.
- Arndt, C.A., and Crist, W.M. (1999). Common musculoskeletal tumors of childhood and adolescence. *N. Engl. J. Med.* *341*, 342-352.
- Arvand, A., and Denny, C.T. (2001). Biology of EWS/ETS fusions in Ewing's family tumors. *Oncogene* *20*, 5747-5754.
- Aryee, D.N., Niedan, S., Kauer, M., Schwentner, R., Bennani-Baiti, I.M., Ban, J., Muehlbacher, K., Kreppel, M., Walker, R.L., Meltzer, P., *et al.* (2010). Hypoxia modulates EWS-FLI1 transcriptional signature and enhances the malignant properties of Ewing's sarcoma cells in vitro. *Cancer Res.* *70*, 4015-4023.
- Balaban, N.Q., Schwarz, U.S., Riveline, D., Goichberg, P., Tzur, G., Sabanay, I., Mahalu, D., Safran, S., Bershadsky, A., Addadi, L., *et al.* (2001). Force and focal adhesion assembly: a close relationship studied using elastic micropatterned substrates. *Nat. Cell Biol.* *3*, 466-472.
- Beckerle, M.C. (1986). Identification of a new protein localized at sites of cell-substrate adhesion. *J. Cell Biol.* *103*, 1679-1687.
- Ben-David, Y., Giddens, E.B., and Bernstein, A. (1990). Identification and mapping of a common proviral integration site Fli-1 in erythroleukemia cells induced by Friend murine leukemia virus. *Proc. Natl. Acad. Sci. USA* *87*, 1332-1336.
- Bershadsky, A.D., Balaban, N.Q., and Geiger, B. (2003). Adhesion-dependent cell mechanosensitivity. *Ann. Rev. Cell Dev. Biol.* *19*, 677-695.
- Braunreiter, C.L., Hancock, J.D., Coffin, C.M., Boucher, K.M., and Lessnick, S.L. (2006). Expression of EWS-ETS fusions in NIH3T3 cells reveals significant differences to Ewing's sarcoma. *Cell Cycle* *5*, 2753-2759.
- Bussard, K.M., Gay, C.V., and Mastro, A.M. (2008). The bone microenvironment in metastasis; what is special about bone? *Cancer Metastasis Rev.* *27*, 41-55.
- Caswell, P.T., Chan, M., Lindsay, A.J., McCaffrey, M.W., Boettiger, D., and Norman, J.C. (2008). Rab-coupling protein coordinates recycling of alpha5beta1 integrin and EGFR1 to promote cell migration in 3D microenvironments. *J. Cell Biol.* *183*, 143-155.

Cavazzana, A.O., Miser, J.S., Jefferson, J., and Triche, T.J. (1987). Experimental evidence for a neural origin of Ewing's sarcoma of bone. *Am. J. Pathol.* *127*, 507-518.

Cerisano, V., Aalto, Y., Perdichizzi, S., Bernard, G., Manara, M.C., Benini, S., Cenacchi, G., Preda, P., Lattanzi, G., Nagy, B., *et al.* (2004). Molecular mechanisms of CD99-induced caspase-independent cell death and cell-cell adhesion in Ewing's sarcoma cells: actin and zyxin as key intracellular mediators. *Oncogene* *23*, 5664-5674.

Chaffer, C.L., and Weinberg, R.A. (2011). A perspective on cancer cell metastasis. *Science* *331*, 1559-1564.

Chambers, A.F., Groom, A.C., and MacDonald, I.C. (2002). Dissemination and growth of cancer cells in metastatic sites. *Nat. Rev. Cancer* *2*, 563-572.

Chambers, T.J., Fuller, K., Darby, J.A., Pringle, J.A., and Horton, M.A. (1986). Monoclonal antibodies against osteoclasts inhibit bone resorption in vitro. *Bone Miner.* *1*, 127-135.

Crawford, A.W., Michelsen, J.W., and Beckerle, M.C. (1992). An interaction between zyxin and alpha-actinin. *J. Cell Biol.* *116*, 1381-1393.

Delattre, O., Zucman, J., Plougastel, B., Desmaze, C., Melot, T., Peter, M., Kovar, H., Joubert, I., de Jong, P., Rouleau, G., *et al.* (1992). Gene fusion with an ETS DNA-binding domain caused by chromosome translocation in human tumours. *Nature* *359*, 162-165.

Dickman, P.S., Liotta, L.A., and Triche, T.J. (1982). Ewing's sarcoma. Characterization in established cultures and evidence of its histogenesis. *Lab. Invest.* *47*, 375-382.

Dirksen, U., and Jurgens, H. (2010). Approaching Ewing sarcoma. *Future Oncol.* *6*, 1155-1162.

Dubash, A.D., Menold, M.M., Samson, T., Boulter, E., Garcia-Mata, R., Doughman, R., and Burrige, K. (2009). Chapter 1. Focal adhesions: new angles on an old structure. *Int. Rev. Cell Mol. Biol.* *277*, 1-65.

Ewing, J. (2006). The Classic: Diffuse endothelioma of bone. *Proceedings of the New York Pathological Society.* 1921;12:17. *Clin. Orthop. Relat. Res.* *450*, 25-27.

Fearon, E.R., and Vogelstein, B. (1990). A genetic model for colorectal tumorigenesis. *Cell* *61*, 759-767.

Folpe, A.L., Hill, C.E., Parham, D.M., O'Shea, P.A., and Weiss, S.W. (2000). Immunohistochemical detection of FLI-1 protein expression: a study of 132 round cell tumors with emphasis on CD99-positive mimics of Ewing's sarcoma/primitive neuroectodermal tumor. *Am. J. Surg. Pathol.* *24*, 1657-1662.

Frixen, U.H., Behrens, J., Sachs, M., Eberle, G., Voss, B., Warda, A., Lochner, D., and Birchmeier, W. (1991). E-cadherin-mediated cell-cell adhesion prevents invasiveness of human carcinoma cells. *J. Cell Biol.* *113*, 173-185.

Geiger, B., Bershadsky, A., Pankov, R., and Yamada, K.M. (2001). Transmembrane crosstalk between the extracellular matrix--cytoskeleton crosstalk. *Nat. Rev. Mol. Cell Biol.* *2*, 793-805.

Giancotti, F.G., and Ruoslahti, E. (1999). Integrin signaling. *Science* *285*, 1028-1032.

Girnita, L., Girnita, A., Wang, M., Meis-Kindblom, J.M., Kindblom, L.G., and Larsson, O. (2000). A link between basic fibroblast growth factor (bFGF) and EWS/FLI-1 in Ewing's sarcoma cells. *Oncogene* *19*, 4298-4301.

Guise, T.A., Mohammad, K.S., Clines, G., Stebbins, E.G., Wong, D.H., Higgins, L.S., Vessella, R., Corey, E., Padalecki, S., Suva, L., *et al.* (2006). Basic mechanisms responsible for osteolytic and osteoblastic bone metastases. *Clinical Cancer Res.* *12*, 6213s-6216s.

Guo, W., and Giancotti, F.G. (2004). Integrin signalling during tumour progression. *Nat. Rev. Mol. Cell Biol.* *5*, 816-826.

Gurney J.G., Swensen A.R., Bulterys M. (1999). Malignant Bone Tumors. Cancer Incidence and Survival among Children and Adolescents: US SEER Prog. 1975-1995 Bethesda: NCI; 99-110.

Hancox, N.M. (1972). *Biology of the bone* (Cambridge: University Press).

Heath, J.P., and Dunn, G.A. (1978). Cell to substratum contacts of chick fibroblasts and their relation to the microfilament system. A correlated interference-reflexion and high-voltage electron-microscope study. *J. Cell Sci.* *29*, 197-212.

Hervy, M., Hoffman, L., and Beckerle, M.C. (2006). From the membrane to the nucleus and back again: bifunctional focal adhesion proteins. *Curr. Opin. Cell Biol.* *18*, 524-532.

Hirata, H., Tatsumi, H., and Sokabe, M. (2008). Mechanical forces facilitate actin polymerization at focal adhesions in a zyxin-dependent manner. *J. Cell Sci.* *121*, 2795-2804.

Hoffman, L.M., Jensen, C.C., Kloeker, S., Wang, C.L., Yoshigi, M., and Beckerle, M.C. (2006). Genetic ablation of zyxin causes Mena/VASP mislocalization, increased motility, and deficits in actin remodeling. *J. Cell Biol.* *172*, 771-782.

Hu-Lieskovan, S., Zhang, J., Wu, L., Shimada, H., Schofield, D.E., and Triche, T.J. (2005). EWS-FLI1 fusion protein up-regulates critical genes in neural crest development and is responsible for the observed phenotype of Ewing's family of tumors. *Cancer Res.* *65*, 4633-4644.

- Humphries, M.J., Travis, M.A., Clark, K., and Mould, A.P. (2004). Mechanisms of integration of cells and extracellular matrices by integrins. *Biochem. Soc. Trans.* *32*, 822-825.
- Hynes, R.O. (1992). Integrins: versatility, modulation, and signaling in cell adhesion. *Cell* *69*, 11-25.
- Hynes, R.O. (2002). Integrins: bidirectional, allosteric signaling machines. *Cell* *110*, 673-687.
- Hynes, R.O. (2004). The emergence of integrins: a personal and historical perspective. *Matrix Biol.* *23*, 333-340.
- Ingber, D.E. (2008). Tensegrity-based mechanosensing from macro to micro. *Prog. Biophys. Mol. Biol.* *97*, 163-179.
- Ingber, D.E., Madri, J.A., and Jamieson, J.D. (1981). Role of basal lamina in neoplastic disorganization of tissue architecture. *Proc. Natl. Acad. Sci. USA* *78*, 3901-3905.
- Janmey, P.A. (1998). The cytoskeleton and cell signaling: component localization and mechanical coupling. *Physiol. Rev.* *78*, 763-781.
- Janssen, H., and Marynen, P. (2006). Interaction partners for human ZNF384/CIZ/NMP4-zyxin as a mediator for p130CAS signaling? *Exp. Cell Res.* *312*, 1194-1204.
- Kadin, M.E., and Bensch, K.G. (1971). On the origin of Ewing's tumor. *Cancer* *27*, 257-273.
- Kanis, J.A., and McCloskey, E.V. (1997). Bone turnover and biochemical markers in malignancy. *Cancer* *80*, 1538-1545.
- Kawajiri, H., Yashiro, M., Shinto, O., Nakamura, K., Tendo, M., Takemura, S., Node, M., Hamashima, Y., Kajimoto, T., Sawada, T., *et al.* (2008). A novel transforming growth factor beta receptor kinase inhibitor, A-77, prevents the peritoneal dissemination of scirrhous gastric carcinoma. *Clin. Cancer Res.* *14*, 2850-2860.
- Kimber, C., Michalski, A., Spitz, L., and Pierro, A. (1998). Primitive neuroectodermal tumours: anatomic location, extent of surgery, and outcome. *J. Pediatr Surg.* *33*, 39-41.
- Kinsey, M., Smith, R., and Lessnick, S.L. (2006). NR0B1 is required for the oncogenic phenotype mediated by EWS/FLI in Ewing's sarcoma. *Mol. Cancer Res.* *4*, 851-859.
- Knowles, H.J., Schaefer, K.L., Dirksen, U., and Athanasou, N.A. (2010). Hypoxia and hypoglycaemia in Ewing's sarcoma and osteosarcoma: regulation and phenotypic effects of Hypoxia-Inducible Factor. *BMC Cancer* *10*, 372.

Kolb, E.A., Kushner, B.H., Gorlick, R., Laverdiere, C., Healey, J.H., LaQuaglia, M.P., Huvos, A.G., Qin, J., Vu, H.T., Wexler, L., *et al.* (2003). Long-term event-free survival after intensive chemotherapy for Ewing's family of tumors in children and young adults. *J. Clin. Oncol.* *21*, 3423-3430.

Kovar, H. (2005). Context matters: the hen or egg problem in Ewing's sarcoma. *Semin. Cancer Biol.* *15*, 189-196.

Kumar, S., and Weaver, V.M. (2009). Mechanics, malignancy, and metastasis: the force journey of a tumor cell. *Cancer Metastasis Rev.* *28*, 113-127.

Leiss, M., Beckmann, K., Giros, A., Costell, M., and Fassler, R. (2008). The role of integrin binding sites in fibronectin matrix assembly in vivo. *Curr. Opin. Cell Biol.* *20*, 502-507.

Lelievre, S.A., Weaver, V.M., Nickerson, J.A., Larabell, C.A., Bhaumik, A., Petersen, O.W., and Bissell, M.J. (1998). Tissue phenotype depends on reciprocal interactions between the extracellular matrix and the structural organization of the nucleus. *Proc. Natl. Acad. Sci. USA* *95*, 14711-14716.

Lessnick, S.L., Braun, B.S., Denny, C.T., and May, W.A. (1995). Multiple domains mediate transformation by the Ewing's sarcoma EWS/FLI-1 fusion gene. *Oncogene* *10*, 423-431.

Lessnick, S.L., Dacwag, C.S., and Golub, T.R. (2002). The Ewing's sarcoma oncoprotein EWS/FLI induces a p53-dependent growth arrest in primary human fibroblasts. *Cancer Cell* *1*, 393-401.

Llombart-Bosch, A., and Navarro, S. (2001). Immunohistochemical detection of EWS and FLI-1 proteins in Ewing sarcoma and primitive neuroectodermal tumors: comparative analysis with CD99 (MIC-2) expression. *Appl. Immunohistochem. Mol. Morphol.* *9*, 255-260.

Luo, W., Gangwal, K., Sankar, S., Boucher, K.M., Thomas, D., and Lessnick, S.L. (2009). GSTM4 is a microsatellite-containing EWS/FLI target involved in Ewing's sarcoma oncogenesis and therapeutic resistance. *Oncogene* *28*, 4126-4132.

Marks, S.C., & Odgren, P. R. (2002). Structure and development of the skeleton. *Principles of Bone Biology* *1*, 3-15.

May, W.A., Gishizky, M.L., Lessnick, S.L., Lunsford, L.B., Lewis, B.C., Delattre, O., Zucman, J., Thomas, G., and Denny, C.T. (1993a). Ewing sarcoma 11;22 translocation produces a chimeric transcription factor that requires the DNA-binding domain encoded by FLI1 for transformation. *Proc. Natl. Acad. Sci. USA* *90*, 5752-5756.

May, W.A., Lessnick, S.L., Braun, B.S., Klemsz, M., Lewis, B.C., Lunsford, L.B., Hromas, R., and Denny, C.T. (1993b). The Ewing's sarcoma EWS/FLI-1 fusion gene

encodes a more potent transcriptional activator and is a more powerful transforming gene than FLI-1. *Mol. Cell Biol.* *13*, 7393-7398.

Mierke, C.T., Rosel, D., Fabry, B., and Brabek, J. (2008). Contractile forces in tumor cell migration. *Eur. J. Cell Biol.* *87*, 669-676.

Mitra, S.K., and Schlaepfer, D.D. (2006). Integrin-regulated FAK-Src signaling in normal and cancer cells. *Curr. Opin. Cell Biol.* *18*, 516-523.

Morohoshi, F., Arai, K., Takahashi, E.I., Tanigami, A., and Ohki, M. (1996). Cloning and mapping of a human RBP56 gene encoding a putative RNA binding protein similar to FUS/TLS and EWS proteins. *Genomics* *38*, 51-57.

Mundy, G.R. (2002). Metastasis to bone: causes, consequences and therapeutic opportunities. *Nat. Rev. Cancer* *2*, 584-593.

Nagae, M., Re, S., Mihara, E., Nogi, T., Sugita, Y., and Takagi, J. (2012). Crystal structure of alpha5beta1 integrin ectodomain: atomic details of the fibronectin receptor. *J. Cell Biol.* *197*, 131-140.

Nix, D.A., and Beckerle, M.C. (1997). Nuclear-cytoplasmic shuttling of the focal contact protein, zyxin: a potential mechanism for communication between sites of cell adhesion and the nucleus. *J. Cell Biol.* *138*, 1139-1147.

Ohashi, T., Kiehart, D.P., and Erickson, H.P. (2002). Dual labeling of the fibronectin matrix and actin cytoskeleton with green fluorescent protein variants. *J. Cell Sci.* *115*, 1221-1229.

Paget, S. (1889). The distribution of secondary growths in cancer of the breast. 1889. *Cancer Metastasis Rev.* *8*, 98-101.

Pankov, R., Cukierman, E., Katz, B.Z., Matsumoto, K., Lin, D.C., Lin, S., Hahn, C., and Yamada, K.M. (2000). Integrin dynamics and matrix assembly: tensin-dependent translocation of alpha(5)beta(1) integrins promotes early fibronectin fibrillogenesis. *J. Cell Biol.* *148*, 1075-1090.

Paulussen, M., Bielack, S., Jurgens, H., and Jost, L. (2008). Ewing's sarcoma of the bone: ESMO clinical recommendations for diagnosis, treatment and follow-up. *Ann. Oncol.* *19 Suppl 2*, ii97-98.

Poste, G., and Fidler, I.J. (1980). The pathogenesis of cancer metastasis. *Nature* *283*, 139-146.

Potratz, J., Jurgens, H., Craft, A., and Dirksen, U. (2012). Ewing sarcoma: biology-based therapeutic perspectives. *Pediatr. Hematol. Oncol.* *29*, 12-27.

- Qian, F., Zhang, Z.C., Wu, X.F., Li, Y.P., and Xu, Q. (2005). Interaction between integrin alpha(5) and fibronectin is required for metastasis of B16F10 melanoma cells. *Biochem. Biophys. Res. Commun.* 333, 1269-1275.
- Riggi, N., and Stamenkovic, I. (2007). The Biology of Ewing sarcoma. *Cancer Lett.* 254, 1-10.
- Riggi, N., Suva, M.L., and Stamenkovic, I. (2009). Ewing's sarcoma origin: from duel to duality. *Expert Rev. Anticancer Ther.* 9, 1025-1030.
- Riggi, N., Suva, M.L., Suva, D., Cironi, L., Provero, P., Tercier, S., Joseph, J.M., Stehle, J.C., Baumer, K., Kindler, V., *et al.* (2008). EWS-FLI-1 expression triggers a Ewing's sarcoma initiation program in primary human mesenchymal stem cells. *Cancer Res.* 68, 2176-2185.
- Ruoslahti, E. (1996). RGD and other recognition sequences for integrins. *Annu. Rev. Cell Dev. Biol.* 12, 697-715.
- Salsmann, A., Schaffner-Reckinger, E., and Kieffer, N. (2006). RGD, the Rho'd to cell spreading. *Eur. J. Cell Biol.* 85, 249-254.
- Sankar, S., and Lessnick, S.L. (2011). Promiscuous partnerships in Ewing's sarcoma. *Cancer Genet.* 204, 351-365.
- Schirner, M., Herzberg, F., Schmidt, R., Streit, M., Schoning, M., Hummel, M., Kaufmann, C., Thiel, E., and Kreuser, E.D. (1998). Integrin alpha5beta1: a potent inhibitor of experimental lung metastasis. *Clin. Exp. Metastasis* 16, 427-435.
- Schmeichel, K.L., and Beckerle, M.C. (1994). The LIM domain is a modular protein-binding interface. *Cell* 79, 211-219.
- Singer, II (1979). The fibronexus: a transmembrane association of fibronectin-containing fibers and bundles of 5 nm microfilaments in hamster and human fibroblasts. *Cell* 16, 675-685.
- Smith, M.A., Blankman, E., Gardel, M.L., Luettjohann, L., Waterman, C.M., and Beckerle, M.C. (2010). A zyxin-mediated mechanism for actin stress fiber maintenance and repair. *Dev. Cell* 19, 365-376.
- Smith, R., Owen, L.A., Trem, D.J., Wong, J.S., Whangbo, J.S., Golub, T.R., and Lessnick, S.L. (2006). Expression profiling of EWS/FLI identifies NKX2.2 as a critical target gene in Ewing's sarcoma. *Cancer Cell* 9, 405-416.
- Szuhai, K., Cleton-Jansen, A.M., Hogendoorn, P.C., and Bovee, J.V. (2012). Molecular pathology and its diagnostic use in bone tumors. *Cancer Genet.* 205, 193-204.

- Talmadge, J.E., and Fidler, I.J. (2010). AACR centennial series: the biology of cancer metastasis: historical perspective. *Cancer Res.* *70*, 5649-5669.
- Tamkun, J.W., DeSimone, D.W., Fonda, D., Patel, R.S., Buck, C., Horwitz, A.F., and Hynes, R.O. (1986). Structure of integrin, a glycoprotein involved in the transmembrane linkage between fibronectin and actin. *Cell* *46*, 271-282.
- Tani, N., Higashiyama, S., Kawaguchi, N., Madarame, J., Ota, I., Ito, Y., Ohoka, Y., Shiosaka, S., Takada, Y., and Matsuura, N. (2003). Expression level of integrin alpha 5 on tumour cells affects the rate of metastasis to the kidney. *Br. J. Cancer* *88*, 327-333.
- Taverna, D., Ullman-Cullere, M., Rayburn, H., Bronson, R.T., and Hynes, R.O. (1998). A test of the role of alpha5 integrin/fibronectin interactions in tumorigenesis. *Cancer Res.* *58*, 848-853.
- Teitell, M.A., Thompson, A.D., Sorensen, P.H., Shimada, H., Triche, T.J., and Denny, C.T. (1999). EWS/ETS fusion genes induce epithelial and neuroectodermal differentiation in NIH 3T3 fibroblasts. *Lab. Invest.* *79*, 1535-1543.
- Thiery, J.P., and Sleeman, J.P. (2006). Complex networks orchestrate epithelial-mesenchymal transitions. *Nat. Rev. Mol. Cell Biol.* *7*, 131-142.
- Tirado, O.M., Mateo-Lozano, S., Villar, J., Dettin, L.E., Llorca, A., Gallego, S., Ban, J., Kovar, H., and Notario, V. (2006). Caveolin-1 (CAV1) is a target of EWS/FLI-1 and a key determinant of the oncogenic phenotype and tumorigenicity of Ewing's sarcoma cells. *Cancer Res.* *66*, 9937-9947.
- Tirode, F., Laud-Duval, K., Prieur, A., Delorme, B., Charbord, P., and Delattre, O. (2007). Mesenchymal stem cell features of Ewing tumors. *Cancer Cell* *11*, 421-429.
- Torchia, E.C., Jaishankar, S., and Baker, S.J. (2003). Ewing tumor fusion proteins block the differentiation of pluripotent marrow stromal cells. *Cancer Res.* *63*, 3464-3468.
- Toretzky, J.A., Kalebic, T., Blakesley, V., LeRoith, D., and Helman, L.J. (1997). The insulin-like growth factor-I receptor is required for EWS/FLI-1 transformation of fibroblasts. *J. Biol. Chem.* *272*, 30822-30827.
- Truong, H., and Danen, E.H. (2009). Integrin switching modulates adhesion dynamics and cell migration. *Cell Adh. Migr.* *3*, 179-181.
- Turc-Carel, C., Aurias, A., Mugneret, F., Lizard, S., Sidaner, I., Volk, C., Thiery, J.P., Olschwang, S., Philip, I., Berger, M.P., *et al.* (1988). Chromosomes in Ewing's sarcoma. I. An evaluation of 85 cases of remarkable consistency of t(11;22)(q24;q12). *Cancer Genet. Cytogenet.* *32*, 229-238.

- Turc-Carel, C., Philip, I., Berger, M.P., Philip, T., and Lenoir, G.M. (1984). Chromosome study of Ewing's sarcoma (ES) cell lines. Consistency of a reciprocal translocation t(11;22)(q24;q12). *Cancer Genet. Cytogenet.* *12*, 1-19.
- Valastyan, S., and Weinberg, R.A. (2011). Tumor metastasis: molecular insights and evolving paradigms. *Cell* *147*, 275-292.
- Wennerberg, K., Lohikangas, L., Gullberg, D., Pfaff, M., Johansson, S., and Fassler, R. (1996). Beta 1 integrin-dependent and -independent polymerization of fibronectin. *J. Cell Biol.* *132*, 227-238.
- Yang, J., and Weinberg, R.A. (2008). Epithelial-mesenchymal transition: at the crossroads of development and tumor metastasis. *Dev. Cell* *14*, 818-829.
- Yang, J.T., Bader, B.L., Kreidberg, J.A., Ullman-Cullere, M., Trevithick, J.E., and Hynes, R.O. (1999). Overlapping and independent functions of fibronectin receptor integrins in early mesodermal development. *Dev. Biol.* *215*, 264-277.
- Yilmaz, M., and Christofori, G. (2009). EMT, the cytoskeleton, and cancer cell invasion. *Cancer Metastasis Rev.* *28*, 15-33.
- Yoshigi, M., Hoffman, L.M., Jensen, C.C., Yost, H.J., and Beckerle, M.C. (2005). Mechanical force mobilizes zyxin from focal adhesions to actin filaments and regulates cytoskeletal reinforcement. *J. Cell Biol.* *171*, 209-215.
- Zaidel-Bar, R., and Geiger, B. (2010). The switchable integrin adhesome. *J. Cell Sci.* *123*, 1385-1388.
- Zamir, E., and Geiger, B. (2001). Components of cell-matrix adhesions. *J. Cell Sci.* *114*, 3577-3579.

CHAPTER 2

THE CLONE WARS - REVENGE OF THE METASTATIC ROGUE

STATE: THE SARCOMA PARADIGM

My contribution to this work is the review of tumor microenvironment in
Ewing sarcoma metastasis.

This work is reprinted with the permission of Frontiers in Oncology.

The Article was originally published in Front Oncol. 2012;2:2



The clone wars – revenge of the metastatic rogue state: the sarcoma paradigm

Holly L. Spraker^{1,2*}, Shawn L. Price^{2,3}, Aashi Chaturvedi^{2,4}, Joshua D. Schiffman^{1,2,4}, Kevin B. Jones^{2,3}, Stephen L. Lessnick^{1,2,4}, Mary Beckerle^{2,4} and R. Lor Randall^{2,3}

¹ Division of Pediatric Hematology–Oncology, Primary Children's Medical Center, University of Utah, Salt Lake City, UT, USA

² Center for Children's Cancer Research, Huntsman Cancer Institute, University of Utah, Salt Lake City, UT, USA

³ Department of Orthopedics, Sarcoma Services, Huntsman Cancer Institute, University of Utah, Salt Lake City, UT, USA

⁴ Department of Oncological Sciences, University of Utah, Salt Lake City, UT, USA

Edited by:

Douglas Hawkins, Seattle Children's Hospital, USA

Reviewed by:

Ben Braun, University of California San Francisco, USA

Scott C. Borinstein, Vanderbilt University, USA

*Correspondence:

Holly L. Spraker, Division of Pediatric Hematology–Oncology, Primary Children's Medical Center, 100 North Mario Capecchi Drive, Salt Lake City, UT 84113, USA.
e-mail: holly.spraker@imail.org

Ewing sarcoma (ES) is the second most common bone tumor affecting primarily adolescents and young adults. Despite recent advances in biological understanding, intensification of chemotherapeutic treatments, and progress in local control with surgery and/or radiation therapy, patients with metastatic or recurrent ES continue to have a dismal prognosis with less than 20% overall survival. All ES is likely metastatic at diagnosis although our methods of detection and classification may not account for this. Progressive disease may arise via a combination of: (1) selection of chemotherapy-resistant clones in primary tumor, (2) signaling from bone or lung microenvironments that may attract tumor cells to distant locations, and/or (3) genetic changes within the ES cells themselves due to DNA-damaging chemotherapeutic agents or other "hits." These possibilities and the evidence base to support them are explored.

Keywords: Ewing sarcoma, metastatic

INTRODUCTION

Ewing sarcoma (ES) is the second most common malignant bone tumor in adolescents and young adults, leading to more than 200 cases of cancer in the United States per year (SEER). Evidence of metastatic disease at diagnosis is the most clinically relevant prognostic factor, affecting ~25% of patients (Bernstein et al., 2006). Despite recent advances in biological understanding, intensification of chemotherapeutic treatments, and progress in local control with surgery and/or radiation therapy, patients with metastatic or recurrent ES continue to have a dismal prognosis with less than 20% overall survival.

Nearly every case of ES harbors a translocation of the *EWSR1* gene, found on chromosome 22, with a member of the ETS family on chromosomes 11, 21, or others. The classic ES translocation, t(11;22)(q24;q12), creates the *EWS-FLI1* fusion oncogene found in around 85% of ES tumors. Other fusion partners have also been described and account for the remaining 15% (Turc-Carel et al., 1988; Delattre et al., 1992). The *EWS-FLI1* oncogene influences the gene expression profile of tumor cells, directly or indirectly, driving aberrant expression of over 1000 genes (Smith et al., 2006). Interestingly, *EWS-FLI1* expression is associated with activation of some genes and repression of others, illustrating the complexity of cellular response to this oncogenic transcription factor (May et al., 1993).

The ES translocation is thought to be the primary mechanism for tumorigenesis, but the heterogeneous biology found in the tumors of patients with ES suggests that additional molecular mechanisms are also involved (Toomey et al., 2010). Castillero-Trejo et al. (2005) using murine primary bone derived cells (mPBDC), have shown that serial passage of retrovirally

transduced *EWS-FLI1* mPBDCs produced tumors efficiently *only* in later-passage cells (> passage 15). In addition, Lessnick et al. (2002) established human primary fibroblast cell lines expressing the *EWS-FLI1* fusion protein that underwent p53 mediated growth arrest showing that for tumor formation to proceed, there is likely a multistep process including the acquisition of other genetic changes (Lessnick et al., 2002). This research supports that the *EWS-FLI1* translocation is an initiating event in sarcomagenesis, but that other biological processes are required for full tumorigenesis to occur (Lessnick et al., 2002; Castillero-Trejo et al., 2005).

Ewing sarcoma cells spread hematogenously to distant sites. Despite negative imaging studies and bone marrow biopsies, nearly all ES is likely micro-metastatic at diagnosis. Why then are clinically detectable metastases such an important prognostic factor? Perhaps tumor cells have differing potentials to grow and develop at distant sites determined by therapy selective pressures, micro-environmental signals, and changes that are intrinsic to the tumor cell's genes. These metastatic clones may undergo genetic changes that allow them to react differently to chemotherapeutic agents as well as signals in the microenvironment (of lung or bone) leading to a more aggressive, resistant phenotype. Many questions remain regarding the presence of ES clones that may lead to occult metastatic deposits and subsequently to recurrence of disease after completion of therapy. Are all ES metastatic clones similar or are they a heterogeneous population of rogues of varying clinical threat? This paper serves to review the current clinical knowledge about metastatic ES, to highlight current areas of research regarding the molecular pathways that influence ES metastasis, and to underscore questions that persist at this time.

To survey the recently published literature in a comprehensive fashion, searches for “ES metastasis” and “metastatic ES” were performed via the PUBMED database. Results showed 586 articles that were published after 1999 on this topic. Abstracts were briefly scanned for relevance, and selected papers were reviewed in full. Original supporting data (some dated prior to 2000) were also used for the current review, based on the bibliography of the papers found.

METASTATIC EWING SARCOMA: THE CLINICAL PERSPECTIVE

Currently, metastatic disease is clinically defined by the presence of a ES specific translocation in the tissue biopsy of at least one tumor site (primary site) plus the presence of characteristic lesions (by imaging) in bones, lungs, or malignant cells identified in a staging bone marrow aspirate or biopsy. If diagnostic imaging is inconclusive for bone or lung sites, tissue biopsy may be undertaken to prove metastasis. Bone marrow is typically considered negative for metastatic disease if the cells present are morphologically hematopoietic in origin; peripheral blood is never clinically tested for ES cells. While these parameters clinically define metastatic disease and identify a high-risk sub-population of ES patients, they likely do not completely quantify a patient’s burden of disease. Nor do such tests give us information about the genetic changes in a particular patient’s ES tumor cells.

Approximately 25% of patients will present with metastatic disease, primarily with metastasis in the lungs, bony sites, and/or bone marrow. As with most cancers, the presence of metastasis is an important predictor of outcome. Patients with metastatic ES have a 5-year relapse free survival of ~30% (versus localized disease = 61.3%, $p < 0.001$; Cotterill et al., 2000). Patients with metastatic disease have a statistically significant proportion of larger primary tumors (>8 cm) than patients without metastatic disease (76.8 versus 54.3%, $p < 0.00001$) suggesting that primary tumor size may correlate with metastasis (Rodriguez-Galindo et al., 2008; Lee et al., 2010). On the other hand, some patients who present with small primary tumors do relapse with distant metastasis, indicating the propensity of ES for dissemination. In terms of outcomes, patients with primary pulmonary metastasis fare better than their counterparts with bone or bone marrow disease (5 year EFS 29–52%) signifying that not all metastasis are equal (Paulussen et al., 1998).

The approach to treating those with metastatic disease involves systemic chemotherapy and local control of the primary site of disease. With regard to systemic therapy, there have been a variety of trials attempting to optimize a chemotherapeutic regimen specifically for patients with metastatic disease. These studies have investigated more intensive, time-compressed, and high-dose chemotherapy regimens, yet there has been minimal improvement in survival of patients with metastasis at presentation (Grier et al., 2003; Granowetter et al., 2009; Huang and Lucas, 2011). First-line agents are the same as for clinically localized disease (vincristine, doxorubicin, cyclophosphamide, ifosfamide, and etoposide), but there has been interest over the last decade in the use of camptothecin agents (such as topotecan and irinotecan) for metastatic disease (Wagner, 2011). The current front line Children’s Oncology Group (COG) trial randomizes patients with localized ES

to receive topotecan in combination with cyclophosphamide to attempt to improve survival rates, as this combination has shown promise in patients with relapsed or refractory disease.

Despite systemic chemotherapy and good local control modalities, even patients with clinically localized ES have a high-risk of relapse at distant sites, giving rise to the hypothesis that micrometastasis is almost universally present but undetected at initial diagnosis. Reports have shown that 25–30% of patients with clinically localized ES have detectable tumor cells in the peripheral blood or bone marrow by polymerase chain reaction (PCR; West et al., 1997). The question then arises as to whether these metastatic cells are clinically nefarious clones or rogues presenting a limited clinical threat. No data has been reported regarding detectable tumor cells at diagnosis for patients with metastatic disease, but one can hypothesize that it would be at least equivalent to if not higher than levels seen in localized ES. Further studies using peripheral blood PCR and/or flow cytometry in the metastatic population would be of interest as the nature of the clones in patients with clinically metastatic disease may differ from those that are detected peripherally in cases of clinically isolated disease. Perhaps comparative assessment of both primary and metastatic sites at diagnosis may also add to this body of knowledge. Other, smaller studies have suggested that detection of such EWS fusion oncogene transcripts in the blood or marrow after completion of therapy may portend relapse (Avigad et al., 2004). Again, are all metastatic clones of the same clinical threat?

Ewing sarcoma relapse usually presents within 5 years following intensive multi-agent chemotherapy and aggressive local control measures (Stahl et al., 2011). The predominant type of relapse in patients with initial metastatic disease is systemic (defined as distant recurrence only) with 73% of patients presenting almost evenly with pulmonary, bone, or multisystem recurrent sites (Stahl et al., 2011). The median survival time after a first recurrence is 9 months, and the 5-year overall survival is 12% for recurrent ES overall (Leavey et al., 2008). In recent data from the COG, the median time to recurrence in patients with metastatic disease at diagnosis is slightly earlier (~1 year; Leavey et al., 2008). Late recurrence, defined as greater than 2 years after initial diagnosis, is associated with a better prognosis (currently greater than 25% overall survival) whereas early recurrence portends a grave prognosis (OS = 7–10%; Huang and Lucas, 2011). Stahl et al. (2011) have corroborated that patients with initially clinically localized disease relapsed significantly later than those with metastatic disease at diagnosis (434 versus 563 days, $p < 0.001$). In addition, the patients that relapsed earlier had a significantly worse outcome (OS 0–2 years = 0.07, 2–3 years = 0.27, >3 years = 0.30, $p < 0.001$; Stahl et al., 2011). Overall, the data suggests that *metastatic* patients are more likely to relapse *early* with *systemic* disease and have a *worse* prognosis. This leads to the hypothesis that either tumor-related OR patient-related factors may lead to these ES clone’s ability to evade destruction or removal during treatment. Disease that is cytereduced into an initial state of subclinical tumor burden, but not fully eradicated, necessarily harbors resistant clones of ES. Chemotherapy provides both selective pressure favoring such clones as well as additional DNA damage able to induce genetic alterations that may generate new resistant clones. Early clinical recurrence implies that either the clones were resistant enough to

grow during therapy or aggressive enough to rebound rapidly after therapy-suppression is lifted.

THE TUMOR MICROENVIRONMENT

The continued poor prognosis for patients with metastatic ES questions the possible need for distinctive treatment strategies designed specifically to prevent metastasis from the primary tumor site and to target and eradicate known or latent metastatic disease (Riggi and Stamenkovic, 2007). Research has focused both on understanding what triggers dissemination as well as what factors support tumor cell survival and proliferation in ectopic sites. ES cells have a propensity to metastasize to the lung, bone, and bone marrow (Arndt and Crist, 1999) suggesting an important role of tumor cell microenvironment that may direct this tissue-specific metastasis (Kerbel, 1995; Mundy, 2002). In recent years, several labs have focused their efforts on understanding the contribution of metastatic sites in attracting ES cells and supporting their growth. To prevent ES metastasis, an understanding of these unique tumor microenvironment and host-tumor interactions may offer new therapeutic targets.

Ewing sarcoma usually arises from bone, but can also metastasize to distant bones. The bone is a rich repository of growth factors including stem cell factor (SCF, the ligand for c-kit receptor), basic fibroblast growth factor (b-FGF), platelet derived growth factor (PDGF), and transforming growth factor- β (TGF- β), therefore providing chemo-attractants for metastatic disease and a favorable environment for metastatic growth of many types of tumors (Mundy, 2002; Bussard et al., 2008). For example, metastatic sites highly express SCF in the bone marrow stromal cells (BMSCs), osteoblasts, and endothelial cells. Landuzzi et al. (2000) noted the presence of substantial surface c-kit receptors in six ES cell lines; transmembrane SCF was also found on five of the six cell lines. Exposure of these ES cell lines to exogenous SCF caused down-regulation of its receptor, decreased chemoattraction of ES cell lines to SCF, and significantly reduced metastasis to lungs and other extra-pulmonary organs in a metastatic xenograft model. These data suggest that SCF expressed in potential metastatic sites may serve a chemoattractant role and that the c-kit receptor/SCF interaction is a potential target for decreasing ES metastasis (Landuzzi et al., 2000).

Fibroblast growth factor produced by BMSCs may promote a metastatic phenotype in ES tumors by increasing cell motility. Conditioned medium from BMSCs was shown to increase motility in human ES cell lines, specifically through activation of FGF receptor-1 (FGFR-1) by b-FGF and its downstream signaling cascade, phosphatidylinositol 3 kinase (PI3K)-Rac-1 (Kamura et al., 2010). Receptors for FGF and PDGF are well-characterized and small molecule inhibitors against these catalytic receptors may provide a therapeutic option in ES.

Lyn, a member of the Src family of kinases, is a known regulator of tumor cell proliferation, adhesion, motility, and invasion. Targeting Lyn using a small interfering RNA (siRNA) or the small molecule inhibitor AP23994 resulted in suppression of tumor growth, decreased bony lysis due to tumor cells, and significantly fewer lung metastases *in vivo* (in athymic nude mice injected with TC71 human ES tumor cell lines; Guan et al., 2008). Here *EWS-FLI1* was shown to upregulate Lyn expression allowing increased

bony lysis. Such lysis creates space for tumor growth, and provides easier access for tumor cells to the bone stroma where they may enter the circulation and metastasize to the lung. This data suggests that targeting Lyn upregulation may decrease the propensity of ES cells to metastasize.

Finally, ezrin, a membrane-cytoskeleton linking protein, has an effect on the development of metastasis in osteosarcoma and rhabdomyosarcoma (Khanna et al., 2004; Yu et al., 2004). Krishnan et al. (2006) have shown that this is true for ES as well. In normal cells, ezrin mediates signal transduction and cell to cell interactions, and promotes growth. Phosphorylation at threonine 567 (T567) of ezrin is essential for ezrin-mediated transduction of growth signals; mutation at this site, leading to absence of phosphorylation at T567 (so called ezrinT567A mutants), causes down-regulation of growth via the AKT/mTOR (mammalian target of rapamycin) pathway. Krishnan et al. (2006) have shown that ES cell lines (both previously established cell lines and primary cell lines from patient tumor samples) have high levels of ezrin expression, and ezrinT567A mutants maintain a significantly slower growth rate than those with wild type ezrin expression due to increased apoptosis. These data lend credence to ezrin's import in primary disease. In addition, injection of ezrinT567A mutant cells into mice produced fewer experimental metastases (2/30 mice developed metastasis) than mice injected with wild type ezrin (8/10 mice) showing that ezrin may also have a role in development and growth of metastasis in ES. Manipulation of the ezrin pathway may be explored in the future as a means to decrease the development of metastatic disease in ES (Krishnan et al., 2006).

METASTATIC DISEASE, INSTABILITY OF THE CLONE

As a tumor grows and metastasizes, its genome can continue to adapt allowing for creation of resistant clones that evade conventional therapies. Newer technologies, such as copy number analysis, rendering more detailed analysis of the genome than is possible with traditional cytogenetics, have been used to also look at genomic imbalances beyond translocation status in these tumors. As cancer genomes become more unstable, the number of copy number aberrations (CNA) increases (Jahromi et al., 2011). Copy number analysis of primary tumors may be a way to identify tumors that are at higher risk of metastasis or relapse than others. Several other tumor types have copy number changes that are being used to risk stratify therapy for patients (e.g., neuroblastoma; Attiyeh et al., 2005), but this is currently not possible for ES due to its rarity and challenge of obtaining a large enough cohort to study. Researchers continue to analyze genomic changes in ES samples (Armengol et al., 1997; Tarkkanen et al., 1999; Brisset et al., 2001; Ozaki et al., 2001; Savola et al., 2009), but the results have been discordant, possibly due to the small samples sizes used and/or the variable biology of the disease coupled with a lack of detailed clinical phenotyping.

In the late 1990s to early 2000s, several researchers described chromosomal gain in ES tumor samples – most commonly trisomy 1q [due to derivative chromosome (1:16)], trisomy 8, and trisomy 12 in 25, 35, and 25% of samples respectively (Armengol et al., 1997; Tarkkanen et al., 1999). The literature supports that 63–87% of ES tumor samples have CNAs detected by CGH

(Armengol et al., 1997; Tarkkanen et al., 1999; Brisset et al., 2001; Ozaki et al., 2001; Savola et al., 2009). The most common of these CNAs have been analyzed for possible prognostic capacity, but the results have been varied. Many groups found no statistically significant changes in event-free survival or overall survival in ES based on CNAs (Armengol et al., 1997; Tarkkanen et al., 1999; Ozaki et al., 2001). However, two different groups found that the number of aberrations did significantly predict patient survival. Ozaki et al. (2001) showed in 48 patients that tumors with lower CNAs (less than five) were significantly associated with improved survival ($p = 0.009$). In addition, Savola et al. (2009) reported that tumors with higher numbers of CNA (≥ 3) fared significantly worse in terms of OS ($p = 0.030$) and EFS ($p = 0.049$) than those with fewer CNAs. The findings to date are correlative in nature and require experimental testing to demonstrate whether CNAs reflect tumor age, behavioral attributes, and both. Currently, there is not a particular aberration or combination of changes being used to stratify patients for therapy.

The average number of CNAs in ES tumors varies in the literature. The most recent data using Agilent's 44K oligoarray platform included 0–26 aberrations per tumor with a mean of 7.2 (Savola et al., 2009). Older reports, using various CGH techniques, reported on average two aberrations per tumor (range 1.14–3.6; Armengol et al., 1997; Tarkkanen et al., 1999; Brisset et al., 2001; Ozaki et al., 2001). Much of this variation may be due to the samples and techniques available for CGH at the time the data were collected. Mean copy number changes per tumor in other sarcomas such as osteosarcoma, malignant fibrous histiocytoma, and chondrosarcoma have been reported around 11, 6, and 6 respectively (Tarkkanen et al., 1995; Larramendy et al., 1997a,b). In ES, copy number changes were low in any given tumor sample lending credence to the primary translocation in ES being a single major genetic hit of great import in development and maintenance of tumors. This supports studies on cultured human ES cells in which knockdown of *EWS-FLI* expression was shown to be sufficient to reverse transformation and tumorigenic properties (May et al., 1993). As stated earlier, however, *EWS-FLI1* expression is likely not the only genetic or epigenetic hit that is required for development and maintenance of ES (Lessnick et al., 2002; Castellero-Trejo et al., 2005). Hopefully, as the resolution of SNP microarrays increases and next-generation sequencing is introduced, more clinically relevant and cooperating CNAs may be discovered in ES.

Numbers of CNA in metastatic versus localized ES have been studied and have yielded inconclusive results. Brisset et al. (2001) found no difference between the type or average number of CNAs of primary tumor samples in patients who presented with metastasis. However, Savola et al. (2009) reported that metastatic tumors showed more CNA (mean 11.8) than primary tumors (mean 5.8). Finally, samples from relapsed tumors had greater than three times

as many copy number changes as did the samples of primary tumors (1.9 versus 4.4 per tumor sample; Armengol et al., 1997; Tarkkanen et al., 1999). From these data, it can be hypothesized that CNA appear with increased frequency as a tumor metastasizes or recurs, and that resistant clones with unstable genomes continue to gain genetic changes as such tumors progress. However, none of these studies have compared paired primary and metastatic lesion samples, so the clonal relationship of primary to metastatic tumors remains unknown in ES. Other tumor types, such as pancreatic carcinoma, have features in their metastatic deposits consistent with the parent clones, yet with the addition of newly acquired lesions reflecting that metastatic clones branched from the parent clone (Yachida et al., 2010). In patients with ES, the use of CNA on samples from both local and metastatic tumors may support such a mechanism and ultimately be an effective way to measure “fitness” of a clone for metastasis.

CLOSING REMARKS

Ewing sarcoma is an aggressive cancer of bone that targets the adolescent and young adult population. In its metastatic form, survival remains poor despite an influx of knowledge regarding tumor biology and intensification of therapy. Even if the disease is localized at diagnosis (and particularly if it is not), there are an unfortunate number of patients who will relapse; relapsed ES is very difficult to cure. Progressive disease is believed to arise via a combination of selection of chemotherapy-resistant clones, signaling from bone or lung microenvironments that may attract tumor cells to distant locations, and/or genetic changes within the ES cells themselves. Intrinsic genetic changes within the ES cells, due to a combination of therapy-related selection and DNA-damaging chemotherapeutic agents, may allow the attraction and migration of resistant ES clones to locations where they may thrive. As these clones compete to survive by evading chemotherapy and responding to signal from metastatic sites, enhanced genomic instability may favor their adaptation. While understanding the biology of the primary tumor is of utmost importance, it is also critical to understand genetic and epigenetic changes that are associated with the metastatic state in order to effectively treat sarcoma patients with systemic disease. Current advances in genetics and genomics provide new approaches to identify novel molecular markers that are associated with metastatic ES and define their clinical implications.

ACKNOWLEDGMENTS

Stephen L. Lessnick is supported by R01 CA140394, R21 CA138295, the Alex's Lemonade Stand Foundation, and the Terri Anna Perine Sarcoma Fund. Joshua D. Schiffman is supported by a SARC Career Development Award. R. Lor Randall is supported by the Terri Anna Perine Sarcoma Fund. M.C.B. is supported by R01 GM50877. The authors also acknowledge support from the Huntsman Cancer Foundation and P30CA042014.

REFERENCES

- Armengol, G., Tarkkanen, M., Viro-lainen, M., Forus, A., Valle, J., Bohling, T., Asko-Seljavaara, S., Blomqvist, C., Elomaa, I., Karaharju, E., Kivioja, A. H., Siimes, M. A., Tuikainen, E., Caballin, M. R., Myklebost, O., and Knuutila, S. (1997). Recurrent gains of 1q, 8 and 12 in the Ewing family of tumours by comparative genomic hybridization. *Br. J. Cancer* 75, 1403–1409.
- Arndt, C. A., and Crist, W. M. (1999). Common musculoskeletal tumors of childhood and adolescence. *N. Engl. J. Med.* 341, 342–352.
- Attiyeh, E. E., London, W. B., Mosse, Y. P., Wang, Q., Winter, C., Khazi, D., McGrady, P. W., Seeger, R. C., Look, A. T., Shimada, H., Brodeur, G. M., Cohn, S. L., Matthay, K. K., Maris, J. M., and Children's Oncology Group. (2005). Chromosome 1p and 11q deletions and outcome in neuroblastoma. *N. Engl. J. Med.* 353, 2243–2253.

- Avigad, S., Cohen, I. J., Zilberstein, J., Liberzon, E., Goshen, Y., Ash, S., Meller, I., Kollender, Y., Issakov, J., Zaizov, R., and Yaniv, I. (2004). The predictive potential of molecular detection in the nonmetastatic Ewing family of tumors. *Cancer* 100, 1053–1058.
- Bernstein, M., Kovar, H., Paulussen, M., Randall, R. L., Schuck, A., Teot, L. A., and Juergens, H. (2006). Ewing's sarcoma family of tumors: current management. *Oncologist* 11, 503–519.
- Briset, S., Schliepacher, G., Peter, M., Mairal, A., Oberlin, O., Delattre, O., and Aurias, A. (2001). CGH analysis of secondary genetic changes in Ewing tumors: correlation with metastatic disease in a series of 43 cases. *Cancer Genet. Cytogenet.* 130, 57–61.
- Bussard, K. M., Gay, C. V., and Mastro, A. M. (2008). The bone microenvironment in metastasis: what is special about bone? *Cancer Metastasis Rev.* 27, 41–55.
- Castillero-Trejo, Y., Eliazar, S., Xiang, L., Richardson, J. A., and Ilaria, R. L. Jr. (2005). Expression of the EWS/FLI-1 oncogene in murine primary bone-derived cells results in EWS/FLI-1-dependent, Ewing sarcoma-like tumors. *Cancer Res.* 65, 8698–8705.
- Cotterill, S. J., Ahrens, S., Paulussen, M., Juergens, H. E., Voute, P. A., Gadner, H., and Craft, A. W. (2000). Prognostic factors in Ewing's tumor of bone: analysis of 975 patients from the European Intergroup Cooperative Ewing's Sarcoma Study Group. *J. Clin. Oncol.* 18, 3108–3114.
- Delattre, O., Zucman, J., Plougastel, B., Desmaziere, C., Melot, T., Peter, M., Kovar, H., Joubert, I., de Jong, P., Rouleau, G., Aurias, A., and Thomas, G. (1992). Gene fusion with an ETS DNA-binding domain caused by chromosome translocation in human tumours. *Nature* 359, 162–165.
- Granowetter, L., Womer, R., Devidas, M., Krailo, M., Wang, C., Bernstein, M., Marina, N., Leavey, P., Gebhardt, M., Healey, J., Shamberger, R. C., Goorin, A., Miser, J., Meyer, J., Arndt, C. A., Sailer, S., Marcus, K., Perlman, E., Dickman, P., and Grier, H. E. (2009). Dose-intensified compared with standard chemotherapy for nonmetastatic Ewing sarcoma family of tumors: a Children's Oncology Group Study. *J. Clin. Oncol.* 27, 2536–2541.
- Grier, H. E., Krailo, M. D., Tarbell, N. J., Link, M. P., Fryer, C. J., Pritchard, D. J., Gebhardt, M. C., Dickman, P. S., Perlman, E. J., Meyers, P. A., Donaldson, S. S., Moore, S., Rausen, A. R., Vietti, T. J., and Miser, J. S. (2003). Addition of ifosfamide and etoposide to standard chemotherapy for Ewing's sarcoma and primitive neuroectodermal tumor of bone. *N. Engl. J. Med.* 348, 694–701.
- Guan, H., Zhou, Z., Gallick, G. E., Jia, S. F., Morales, J., Sood, A. K., Corey, S. J., and Kleinerman, E. S. (2008). Targeting Lyn inhibits tumor growth and metastasis in Ewing's sarcoma. *Mol. Cancer Ther.* 7, 1807–1816.
- Huang, M., and Lucas, K. (2011). Current therapeutic approaches in metastatic and recurrent Ewing sarcoma. *Sarcoma*. doi: 10.1155/2011/863210
- Jahromi, M. S., Jones, K. B., and Schiffman, J. D. (2011). Copy number alterations and methylation in Ewing's sarcoma. *Sarcoma* 2011, 362173.
- Kamura, S., Matsumoto, Y., Fukushi, J. I., Fujiwara, T., Iida, K., Okada, Y., and Iwamoto, Y. (2010). Basic fibroblast growth factor in the bone microenvironment enhances cell motility and invasion of Ewing's sarcoma family of tumours by activating the FGFR1-PI3K-Rac1 pathway. *Br. J. Cancer* 103, 370–381.
- Kerbel, R. S. (1995). Significance of tumor-host interactions in cancer growth and metastases. *Cancer Metastasis Rev.* 14, 259–262.
- Khanna, C., Wan, X., Bose, S., Cassaday, R., Olomou, O., Mendoza, A., Yung, C., Gorlick, R., Hewitt, S. M., and Helman, L. J. (2004). The membrane-cytoskeleton linker ezrin is necessary for osteosarcoma metastasis. *Nat. Med.* 10, 182–186.
- Krishnan, K., Bruce, B., Hewitt, S., Thomas, D., Khanna, C., and Helman, L. J. (2006). Ezrin mediates growth and survival in Ewing's sarcoma through the AKT/mTOR, but not the MAPK, signaling pathway. *Clin. Exp. Metastasis* 23, 227–236.
- Landuzzi, L., De Giovanni, C., Nicoletti, G., Rossi, I., Ricci, C., Astolfi, A., Scopecce, L., Scotlandi, K., Serra, M., Bagnara, G. P., Nanni, P., and Lollini, P. L. (2000). The metastatic ability of Ewing's sarcoma cells is modulated by stem cell factor and by its receptor c-kit. *Am. J. Pathol.* 157, 2123–2131.
- Larramendy, M. L., Tarkkanen, M., Blomqvist, C., Virolainen, M., Wiklund, T., Asko-Seljavaara, S., Elomaa, I., and Knuutila, S. (1997a). Comparative genomic hybridization of malignant fibrous histiocytoma reveals a novel prognostic marker. *Am. J. Pathol.* 151, 1153–1161.
- Larramendy, M. L., Tarkkanen, M., Valle, J., Kivioja, A. H., Ervasti, H., Karaharju, E., Salmivalli, T., Elomaa, I., and Knuutila, S. (1997b). Gains, losses, and amplifications of DNA sequences evaluated by comparative genomic hybridization in chondrosarcomas. *Am. J. Pathol.* 150, 685–691.
- Leavey, P. J., Mascarenhas, L., Marina, N., Chen, Z., Krailo, M., Miser, J., Brown, K., Tarbell, N., Bernstein, M. L., Granowetter, L., Gebhardt, M., Grier, H. E., and Children's Oncology Group. (2008). Prognostic factors for patients with Ewing sarcoma (EWS) at first recurrence following multi-modality therapy: a report from the Children's Oncology Group. *Pediatr. Blood Cancer* 51, 334–338.
- Lee, J., Hoang, B. H., Ziogas, A., and Zell, J. A. (2010). Analysis of prognostic factors in Ewing sarcoma using a population-based cancer registry. *Cancer* 116, 1964–1973.
- Lessnick, S. L., Dacwag, C. S., and Golub, T. R. (2002). The Ewing's sarcoma oncoprotein EWS/FLI induces a p53-dependent growth arrest in primary human fibroblasts. *Cancer Cell* 1, 393–401.
- May, W. A., Lessnick, S. L., Braun, B. S., Klemsz, M., Lewis, B. C., Lunsford, L. B., Hromas, R., and Denny, C. T. (1993). The Ewing's sarcoma EWS/FLI-1 fusion gene encodes a more potent transcriptional activator and is a more powerful transforming gene than FLI-1. *Mol. Cell Biol.* 13, 7393–7398.
- Mundy, G. R. (2002). Metastasis to bone: causes, consequences and therapeutic opportunities. *Nat. Rev. Cancer* 2, 584–593.
- Ozaki, T., Paulussen, M., Poremba, C., Brinkschmidt, C., Rinin, J., Ahrens, S., Hoffmann, C., Hillmann, A., Wai, D., Schaefer, K. L., Boecker, W., Juergens, H., Winkelmann, W., and Dockhorn-Dworniczak, B. (2001). Genetic imbalances revealed by comparative genomic hybridization in Ewing tumors. *Genes Chromosomes Cancer* 32, 164–171.
- Paulussen, M., Ahrens, S., Burdach, S., Craft, A., Dockhorn-Dworniczak, B., Dunst, J., Frohlich, B., Winkelmann, W., Zoubek, A., and Juergens, H. (1998). Primary metastatic (stage IV) Ewing tumor: survival analysis of 171 patients from the EICESS studies. European Intergroup Cooperative Ewing Sarcoma Studies. *Ann. Oncol.* 9, 275–281.
- Rigg, N., and Stamenkovic, I. (2007). The biology of Ewing sarcoma. *Cancer Lett.* 254, 1–10.
- Rodriguez-Galindo, C., Navid, F., Liu, T., Billups, C. A., Rao, B. N., and Krasin, M. J. (2008). Prognostic factors for local and distant control in Ewing sarcoma family of tumors. *Ann. Oncol.* 19, 814–820.
- Savola, S., Klami, A., Tripathi, A., Niini, T., Serra, M., Picci, P., Kaski, S., Zambelli, D., Scotlandi, K., and Knuutila, S. (2009). Combined use of expression and CGH arrays pinpoints novel candidate genes in Ewing sarcoma family of tumors. *BMC Cancer* 9, 17. doi:10.1186/1471-2407-9-17
- Smith, R., Owen, L. A., Trem, D. J., Wong, J. S., Whangbo, J. S., Golub, T. R., and Lessnick, S. L. (2006). Expression profiling of EWS/FLI identifies NKX2.2 as a critical target gene in Ewing's sarcoma. *Cancer Cell* 9, 405–416.
- Stahl, M., Ranft, A., Paulussen, M., Bolling, T., Vieth, V., Bielack, S., Gortitz, I., Braun-Munzinger, G., Harges, J., Jurgens, H., and Dirksen, U. (2011). Risk of recurrence and survival after relapse in patients with Ewing sarcoma. *Pediatr. Blood Cancer* 57, 549–553.
- Tarkkanen, M., Karhu, R., Kallioniemi, A., Elomaa, I., Kivioja, A. H., Nevalainen, J., Bohling, T., Karaharju, E., Hyytiainen, E., Knuutila, S., and Kallioniemi, O.-P. (1995). Gains and losses of DNA sequences in osteosarcomas by comparative genomic hybridization. *Cancer Res.* 55, 1334–1338.
- Tarkkanen, M., Kiuru-Kuhlefelt, S., Blomqvist, C., Armengol, G., Bohling, T., Ektors, T., Virolainen, M., Lindholm, P., Monge, O., Picci, P., Knuutila, S., and Elomaa, I. (1999). Clinical correlations of genetic changes by comparative genomic hybridization in Ewing sarcoma and related tumors. *Cancer Genet. Cytogenet.* 114, 35–41.
- Toomey, E. C., Schiffman, J. D., and Lessnick, S. L. (2010). Recent advances in the molecular pathogenesis of Ewing's sarcoma. *Oncogene* 29, 4504–4516.
- Turc-Carel, C., Aurias, A., Mugneret, E., Lizard, S., Sidaner, I., Volk, C., Thiery, J. P., Olschwang, S., Philip, I., Berger, M. P., Philip, T., Lenoir, G. M., and Mazabraud, A. (1988). Chromosomes in Ewing's sarcoma. I. An evaluation of 85 cases of remarkable consistency of t(11;22)(q24;q12). *Cancer Genet. Cytogenet.* 32, 229–238.
- Wagner, L. (2011). Camptothecin-based regimens for treatment of Ewing sarcoma: past studies, and future directions. *Sarcoma* 2011, 957957.


- West, D. C., Grier, H. E., Swallow, M. M., Demetri, G. D., Granowetter, L., and Sklar, J. (1997). Detection of circulating tumor cells in patients with Ewing's sarcoma and peripheral primitive neuroectodermal tumor. *J. Clin. Oncol.* 15, 583–588.
- Yachida, S., Jones, S., Bozic, I., Antal, T., Leary, R., Fu, B., Kamiyama, M., Hruban, R. H., Eshleman, J. R., Nowak, M. A., Velculescu, V. E., Kinzler, K. W., Vogelstein, B., and Iacobuzio-Donahue, C. A. (2010). Distant metastasis occurs late during the genetic evolution of pancreatic cancer. *Nature* 467, 1114–1117.
- Yu, Y., Khan, J., Khanna, C., Helman, L., Meltzer, P. S., and Merlino, G. (2004). Expression profiling identifies the cytoskeletal organizer ezrin and the developmental homeoprotein Six-1 as key metastatic regulators. *Nat. Med.* 10, 175–181.
- Conflict of Interest Statement:** The authors declare that the research was conducted in the absence of any commercial or financial relationships that could be construed as a potential conflict of interest.
- Received: 27 July 2011; paper pending published: 25 August 2011; accepted: 03 January 2012; published online: 16 January 2012.
- Citation: Spraker HL, Price SL, Chaturvedi A, Schiffman JD, Jones KB, Lessnick SL, Beckerle M and Randall RL (2012) The clone wars – revenge of the metastatic rogue state: the sarcoma paradigm. *Front. Oncol.* 2:2. doi: 10.3389/fonc.2012.00002
- This article was submitted to *Frontiers in Pediatric Oncology*, a specialty of *Frontiers in Oncology*.
- Copyright © 2012 Spraker, Price, Chaturvedi, Schiffman, Jones, Lessnick, Beckerle and Randall. This is an open-access article distributed under the terms of the Creative Commons Attribution Non Commercial License, which permits non-commercial use, distribution, and reproduction in other forums, provided the original authors and source are credited.

CHAPTER 3

THE EWS/FLI ONCOGENE DRIVES CHANGES IN CELLULAR MORPHOLOGY, ADHESION, AND MIGRATION IN EWING SARCOMA

The tail vein injections described in this chapter for the *in vivo* lung adhesion assays were performed by Dr. Alana L. Welm.

The EWS/FLI Oncogene Drives Changes in Cellular Morphology, Adhesion, and Migration in Ewing Sarcoma

Genes & Cancer
3(2) 102–116
© The Author(s) 2012
Reprints and permission:
sagepub.com/journalsPermissions.nav
DOI: 10.1177/1947601912457024
http://ganc.sagepub.com


Aashi Chaturvedi^{1,2}, Laura M. Hoffman^{1,3}, Alana L. Welm^{1,2},
Stephen L. Lessnick^{1,2,4}, and Mary C. Beckerle^{1,2,3}

Submitted 28-Mar-2012; accepted 14-Jul-2012

Abstract

Ewing sarcoma is a tumor of the bone and soft tissue caused by the expression of a translocation-derived oncogenic transcription factor, EWS/FLI. Overt metastases are associated with a poor prognosis in Ewing sarcoma, but patients without overt metastases frequently harbor micrometastatic disease at presentation. This suggests that the metastatic potential of Ewing sarcoma exists at an early stage during tumor development. We have therefore explored whether the inciting oncogenic event in Ewing sarcoma, EWS/FLI, directly modulates tumor cell features that support metastasis, such as cell adhesion, cell migration, and cytoarchitecture. We used an RNAi-based approach in patient-derived Ewing sarcoma cell lines. Although we hypothesized that EWS/FLI might induce classic metastatic features, such as increased cell adhesion, migration, and invasion (similar to the phenotypes observed when epithelial malignancies undergo an epithelial-to-mesenchymal transition during the process of metastasis), surprisingly, we found the opposite. Thus, EWS/FLI expression inhibited the adhesion of isolated cells in culture and prevented adhesion in an *in vivo* mouse lung assay. Cell migration was similarly inhibited by EWS/FLI expression. Furthermore, EWS/FLI expression caused a striking loss of organized actin stress fibers and focal adhesions and a concomitant loss of cell spreading, suggesting that EWS/FLI disrupts the mesenchymal phenotype of a putative tumor cell-of-origin. These data suggest a new paradigm for the dissemination and metastasis of mesenchymally derived tumors: these tumors may disseminate via a “passive/stochastic” model rather than via an “active” epithelial-to-mesenchymal type transition. In the case of Ewing sarcoma, it appears that the loss of cell adhesion needed to promote tumor cell dissemination might be induced by the EWS/FLI oncogene itself rather than via an accumulation of stepwise mutations.

Keywords

cell adhesion, cytoskeleton, Ewing sarcoma, EWS/FLI, metastasis

Cancer is the second leading cause of death worldwide. More than 90% of the deaths due to cancer are attributable to metastatic disease. Based on this clinical reality, it is widely argued that effective treatment of cancer will depend significantly on our ability to block the process of metastasis.¹ Indeed, many therapeutic agents in development for cancer applications are designed to interfere with aspects of the metastatic cascade.

Because of the profound impact of metastasis on cancer outcomes, significant research focus has been applied to understanding the factors that influence metastatic spread of tumor cells. Work in this area has been concentrated on tumors of epithelial origin, in large part because carcinomas are the most common cancers. Years of investigation have led to a now widely accepted multistep model for tumor metastasis that involves an “active” process including an epithelial-to-mesenchymal transition with important morphologic changes that allow for release of cells from the primary tumor site, invasion of tumor cells into the surrounding tissue, movement of tumor cells into and out of blood or lymphatic vessels, and adaptation of tumor cells to microenvironmental conditions encountered at the ectopic

site. Although different groups emphasize distinct aspects of the metastatic cascade, the process can generally be depicted as having 2 major phases: first, the translocation phase in which a tumor cell moves from the primary tumor site to a distant organ, and second, the colonization phase in which the tumor cells adapt and proliferate in the ectopic site to establish metastatic disease.^{2,3}

Substantial mechanistic detail has been deciphered for how carcinomas achieve the capacity to navigate the translocation phase. For a cell within an epithelial-derived tumor, a critical step involves an epithelial-to-mesenchymal

¹Huntsman Cancer Institute, University of Utah, Salt Lake City, UT, USA

²Department of Oncological Sciences, University of Utah, Salt Lake City, UT, USA

³Department of Biology, University of Utah, Salt Lake City, UT, USA

⁴Center for Children’s Cancer Research, Huntsman Cancer Institute, Division of Pediatric Hematology/Oncology, University of Utah School of Medicine, Salt Lake City, UT, USA

Corresponding Author:

Mary C. Beckerle, Huntsman Cancer Institute, 2000 Circle of Hope,
Room 5380, Salt Lake City, UT 84112, USA
Email: mary.beckerle@hci.utah.edu

transition with associated loss of cell surface adhesion molecules, such as E-cadherin, that would normally tether the cell to its neighbors.⁴ The loss of E-cadherin is correlated with advanced metastatic disease in several types of epithelial-derived tumors.^{5,6} Moreover, the importance of E-cadherin loss for tumor metastasis has been directly demonstrated in several preclinical models. For example, disruption of E-cadherin expression in a mouse model of pancreatic cancer leads to reduced cell-cell adhesion as well as temporally accelerated tumor invasion and metastasis.^{7,8} In addition to loss of cell-cell adhesion, the carcinoma cells also acquire enhanced migratory and invasive potential that typically involves changes in expression of cytoskeletal proteins, integrins, and proteases that help dissolve the basement membrane and promote motility.^{9,10} These changes are thought to facilitate the movement of tumor cells into the vasculature, where they can be transported throughout the body. Ultimately, the tumor cells leave the vasculature and invade a new organ site, where significant adaptation and proliferation result in colonization and formation of metastases.

The dramatic changes in cell behavior that are necessary for metastasis must ultimately be driven by changes in gene expression programs within the tumor cells. It is envisioned that cancer cells navigate the substantial environmental challenges encountered along their metastatic journeys by acquisition of genetic and epigenetic changes beyond the initial oncogenic transformation events that influence cell properties such as adhesion, migration, and survival support progression to metastasis.^{11,12} Thus, metastasis is thought to represent an important later step during tumor progression. Consistent with the view that acquisition of metastatic potential occurs over an extended time period and involves multiple genetic steps, many cancers grow for years at the primary site prior to any evidence of dissemination and metastatic behavior.¹³⁻¹⁵

However, in apparent conflict with the multistep model of metastasis, some cancers are typically metastatic upon presentation, even under conditions where the primary tumor is small.¹⁶⁻¹⁸ These examples raise the possibility that a very early event, perhaps even the initiating oncogenic event, might simultaneously influence both cell proliferation and capacity for metastasis. As discussed above, the prevailing model for metastasis is derived from study of epithelial-derived tumor cells, which undergo an epithelial-to-mesenchymal transition during acquisition of metastatic potential. This raises interesting questions about whether nonepithelial tumors, such as sarcomas, may follow a different course on their path to metastasis.

Ewing sarcoma is an important example of a tumor that usually displays early evidence of metastatic dissemination. Ewing sarcoma is a small round blue cell tumor of the bone and soft tissue with peak incidence in teenage years. Ewing

sarcoma represents the second most common bone tumor in children and adolescents. Although approximately two-thirds of patients with localized Ewing sarcoma can be cured with intensive chemotherapy, along with surgery and/or radiation therapy, patients with metastatic Ewing sarcoma have a very poor prognosis, with less than 20% 5-year disease-free survival.¹⁹ In the absence of chemotherapy, approximately 90% of patients die from disease following definitive surgery, suggesting that the vast majority of patients have micrometastatic disease at presentation.^{20,21} Furthermore, circulating tumor cells can often be identified in patients using RT-PCR or flow-cytometric techniques.²²⁻²⁹

The majority of Ewing tumors display an (11;22)(q24;q12) chromosomal translocation, encoding the chimeric transcription factor EWS/FLI,³⁰⁻³² with other EWS fusion proteins associated with the remainder of Ewing sarcoma tumors.³³ The EWS/FLI fusion protein links the amino terminus of EWS, a strong transcriptional activator, and the carboxy terminus of FLI1, a DNA-binding protein from the ETS family of transcription factors.^{31,34} EWS/FLI acts as a transcriptional regulator to modulate hundreds to thousands of genes expression, and ongoing EWS/FLI expression is required for maintenance of transformation.³⁵⁻³⁸

Although the role of EWS/FLI in transcriptional regulation is well-documented, little is understood about how EWS/FLI expression influences cell behaviors that contribute to the ultimate tumor phenotype in patients. Early studies relied on the stable expression of EWS/FLI in NIH3T3 murine fibroblasts.^{34,39-43} However, murine fibroblasts expressing EWS/FLI protein do not recapitulate the gene expression pattern of *bona fide* patient-derived Ewing sarcoma cell lines or tumors,^{44,45} highlighting the need for a cell-based model that more faithfully replicates what occurs in human Ewing sarcoma tumor cells. Efforts to develop a high fidelity experimental approach to study the consequences of EWS/FLI expression for cell behavior have been further complicated by the fact that the cell of origin that gives rise to Ewing sarcoma remains controversial.⁴⁶⁻⁴⁹

To circumvent these challenges and to achieve a cell culture model that reliably reflects the contextual properties of the patient tumor, we have used patient-derived Ewing sarcoma cells and stable RNA-interference to knock down EWS/FLI expression.^{35,38,50} This approach allowed us to study the effects of EWS/FLI on key properties related to the metastatic phenotype, such as cell adhesion, migration, invasion, and cytoarchitecture. Our initial hypothesis was that EWS/FLI might induce cellular features consistent with those observed in epithelial malignancies undergoing epithelial-to-mesenchymal transitions. Surprisingly, we observed the opposite phenotype, with EWS/FLI inhibiting cell adhesion, rather than promoting cell migration and invasion. Our results suggest that EWS/FLI expression

might stimulate the dissemination of Ewing sarcoma cells by influencing cell adhesion and raises the possibility that sarcomas might metastasize via pathways that are distinct from epithelial malignancies.

Results

Efficient knockdown of EWS/FLI using RNA interference. To characterize the impact of the EWS/FLI fusion oncoprotein on cell phenotype and behavior, we used a model system in which expression of endogenous EWS/FLI is knocked down by RNA interference (RNAi) in patient-derived Ewing sarcoma cells. Retroviral infection was used to introduce short-hairpin RNAs against luciferase as a control or against the 3' untranslated region of EWS/FLI in A673 Ewing sarcoma cells.³⁸ The A673 cell line was derived from a human tumor that was definitively diagnosed as Ewing sarcoma by molecular cytogenetic analysis⁵¹ and has been shown to establish tumors when introduced by subcutaneous injection into immunocompromised mice.³⁸ RNAi mediated knockdown of EWS/FLI resulted in efficient reduction of EWS/FLI transcript (Fig. 1A). Because wild-type FLI is not expressed in Ewing sarcoma cells,³⁸ the oncogenic fusion protein is the only protein targeted by the RNAi. Antibody directed against the carboxyl-terminus of FLI demonstrated a corresponding reduction in the level of EWS/FLI protein (Fig. 1B).

By monitoring growth in soft agar as a hallmark of oncogenic transformation, we observed nearly complete loss of colony forming efficiency when A673 cells were infected with EWS/FLI RNAi retroviruses versus those with control RNAi (Fig. 1C, D). We previously showed that EWS/FLI knockdown in A673 cells does not change cell proliferation or lead to growth arrest.³⁸ Thus, the loss of capacity to grow in soft agar illustrates the requirement for ongoing expression of EWS/FLI to sustain anchorage-independent cell growth.

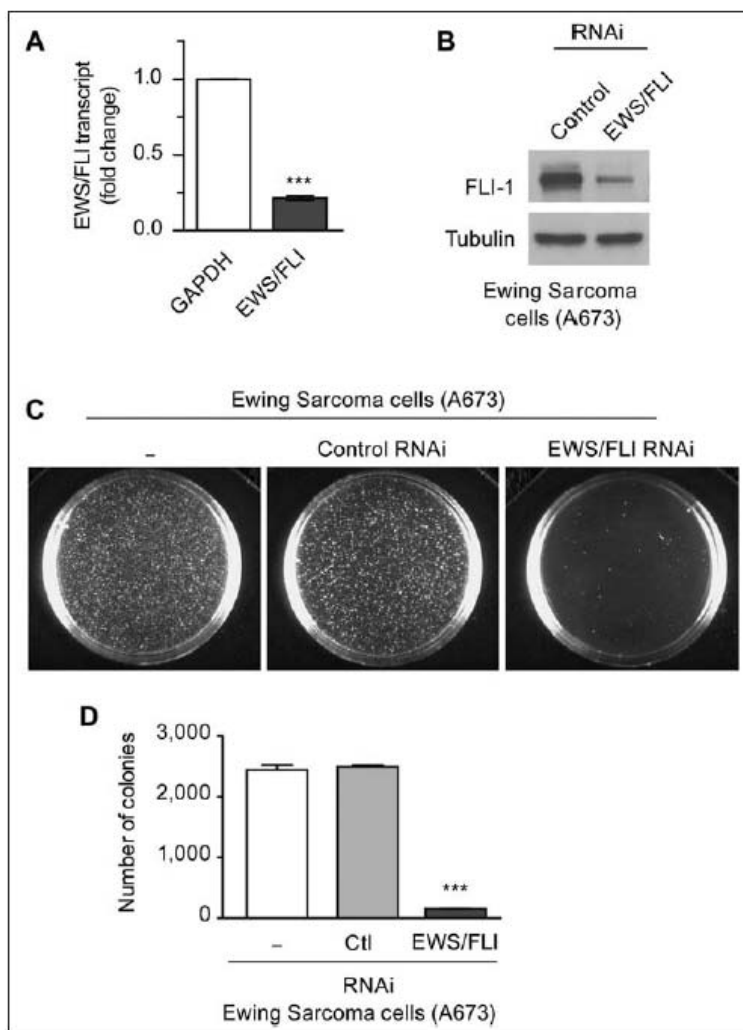


Figure 1. Retroviral RNAi mediated knockdown of EWS/FLI in Ewing sarcoma cells. (A) Retroviral mediated knockdown of endogenous EWS/FLI fusion transcripts in Ewing sarcoma A673 cells was measured by semiquantitative RT-PCR, with GAPDH transcripts as control. Transcripts were normalized as fold change compared with control A673 cells. (B) Western immunoblot with FLI-1 antibody detected EWS/FLI fusion protein in A673 cells with control RNAi and significant reduction of EWS/FLI protein with EWS/FLI RNAi. Tubulin antibody was used to show equivalent protein loading. (C) In soft agar transformation assays of A673 cells, the number of colonies formed in 4 weeks was unaffected by control RNAi but significantly reduced by EWS/FLI RNAi (D). *** $P < 0.001$.

EWS/FLI expression inhibits cell adhesion and spreading. Since an early determinant of metastatic potential is the ability of tumor cells to exit the primary tumor mass, we first evaluated the impact of EWS/FLI expression on Ewing sarcoma cell adhesion. We analyzed the ability of cells to adhere and spread on fibronectin-coated tissue culture plastic over a 2-hour time period in the presence of serum. By

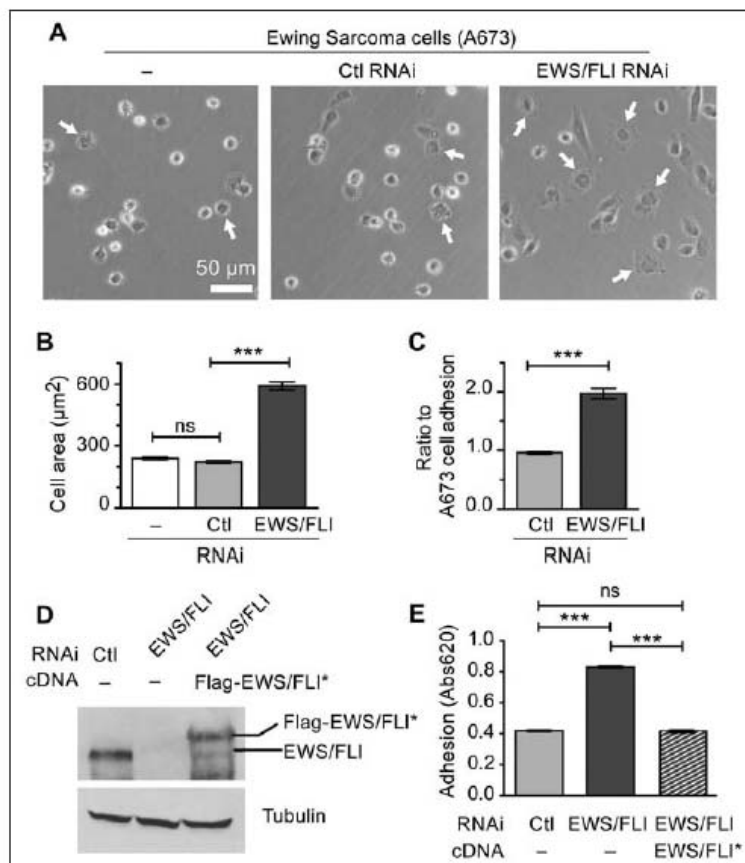


Figure 2. EWS/FLI expression abrogates cell adhesion and spreading. **(A)** Ewing sarcoma A673 cells alone or with control or EWS/FLI RNAi were plated on a tissue culture dish for 2 hours and then evaluated for cell spreading by phase contrast microscopy. Arrows indicate cells adhering to the substratum, spreading, and losing their phase brightness. **(B)** Measurement of A673 cell area following 2 hours adhesion showed that EWS/FLI RNAi enhanced cell spreading compared with cells with control RNAi. **(C)** In a colorimetric adhesion assay of cells plated for 2 hours, the compromised adhesiveness of cells with control RNAi compared with the EWS/FLI RNAi was quantitated and shown to be approximately 2-fold. **(D)** Western immunoblot for EWS/FLI protein in A673 cells with control RNAi or EWS/FLI RNAi were compared with EWS/FLI RNAi cells reconstituted with Flag-tagged EWS/FLI* cDNA that is resistant to the RNAi. The reconstituted EWS/FLI levels approached those seen in control A673 cells, and the tubulin signal shows equivalent protein loading. **(E)** Cell adhesion over 2 hours was measured by a colorimetric assay for A673 cells with control RNAi (light gray) and EWS/FLI RNAi (dark gray) and showed that EWS/FLI knockdown increased cell adhesion 2-fold over control cells. Reconstituted cells programmed to express RNAi-resistant EWS/FLI* (striped) exhibited adhesion that was not statistically different (ns) than control cells. *** $P < 0.001$.

visual inspection using phase contrast microscopy, we noted that Ewing sarcoma cells in which EWS/FLI expression was subject to RNA interference displayed more robust adhesion and spreading compared with Ewing sarcoma cells that retained EWS/FLI expression (Fig. 2A). Cell

spreading requires the establishment of progressive, circumferential substratum adhesion zones as the cell periphery extends its reach. Direct measurement of cell area revealed that control Ewing sarcoma cells display a statistically significant reduction in their capacity to spread compared with Ewing sarcoma cells in which EWS/FLI expression is compromised (Fig. 2B), further suggesting that EWS/FLI induces a reduction in cell adhesion, which can be measured *in vitro*. Quantitative colorimetric adhesion assays confirmed these results, demonstrating that suppression of EWS/FLI expression results in a 200% increase in adherent cells compared with the parental A673 cells, whereas treatment with a control RNAi construct had no impact on cell adhesion (Fig. 2C).

To ascertain that these changes in cell adhesion and spreading are EWS/FLI-dependent and not due to an off-target effect of the RNAi, we performed a knockdown-rescue experiment. We reconstituted expression of EWS/FLI in Ewing sarcoma cells that had been subjected to oncogene knockdown; expression of EWS/FLI was achieved using a previously published Flag-EWS/FLI-cDNA construct that is insensitive to our RNAi construct (Fig. 2D).³⁸ Re-expression of EWS/FLI induced a statistically significant reduction in cellular adhesion (Fig. 2E), thereby confirming that EWS/FLI expression influences cell adhesion. Cells that were programmed to re-express EWS/FLI after knockdown displayed adhesion properties comparable to the parental Ewing sarcoma cells (Fig. 2E).

EWS/FLI expression compromises in vivo cell adhesion. To assess whether the *in vitro* finding that EWS/FLI

expression compromises cell adhesion is relevant in a physiological setting, we tested the ability of Ewing sarcoma cells harboring control or EWS/FLI-directed RNAi constructs to adhere in a mouse lung colonization assay. Equal numbers of differentially labeled fluorescent Ewing sarcoma cells that

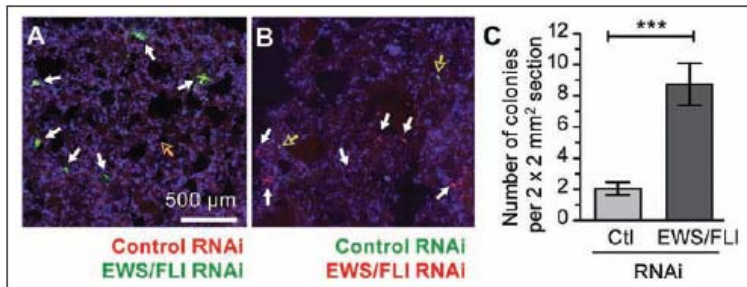


Figure 3. EWS/FLI expression compromises cell adhesion *in vivo*. A673 cells with control RNAi were colored red (DiI) and cells with EWS/FLI RNAi were colored green (DiO), mixed in 1:1 ratio, and then injected into mouse lateral tail veins. Twenty-four hours later the lungs were harvested and cryosectioned, and the red and green cells were counted. (A) Maximum intensity projection of confocal images of lung sections showing differentially labeled A673 cells with control RNAi (red, hollow arrows) and EWS/FLI RNAi (green, solid white arrows). Nuclei are stained with DAPI (blue). (B) Lung sections from additional experiment of mice injected with the cell colors switched to avoid bias of dyes (green-control RNAi, red-EWS/FLI RNAi). (C) Cell colonies were counted for 4 mm² sections in 15 representative sections and showed more cells with EWS/FLI RNAi (solid white arrows in A and B) accumulated in lung parenchyma compared with cells with control RNAi (hollow arrows in A and B). ****P* < 0.001.

had been selected after infection with retroviruses harboring either control or EWS/FLI RNAi constructs were introduced into the circulation of NOD SCID mouse recipients via tail vein injection. In our initial experiments, control RNAi treated cells were labeled with the lipophilic carbocyanine dye, DiI, which displays an emission maximum of 565nm (red); EWS/FLI RNAi treated cells were labeled with DiO, which displays an emission maximum of 501nm (green). The appearance of fluorescently labeled cells in the lungs of the recipient mice was monitored by fluorescence microscopy of lung sections derived from animals sacrificed 24 hours after tumor cell inoculation.

Consistent with the *in vitro* findings described above, A673 cells harboring the EWS/FLI knockdown construct (DiO labeled green fluorescent colonies in Fig. 3A) were found in greater abundance in the mouse lungs compared with cells harboring the control RNAi construct (DiI-labeled red fluorescent colonies in Fig. 3A). Six animals were examined for each RNAi construct. To control for potential differences in the lipophilic labels, such as fluorescence intensity or stability, we repeated this experiment, labeling the RNAi-treated Ewing sarcoma cells with the reciprocal dye, with similar results (Fig. 3B). Quantitative analysis was performed by counting the numbers of DiI- and DiO-labeled cell colonies in multiple lung sections as described in Materials and Methods. We found a statistically significant 4-fold reduction in the number of lung colonies derived from control Ewing sarcoma cells compared with those in which EWS/FLI expression was knocked down (Fig. 3C). These findings illustrate that cells expressing EWS/FLI are less adhesive *in vivo*, as measured by a lung colonization assay.

EWS/FLI expression adversely impacts both cellular migration and invasion. The finding that EWS/FLI expression caused decreased adhesion raised the possibility that cell migration might also be affected by EWS/FLI expression. Therefore, we next examined the impact of EWS/FLI expression on the inherent migratory and invasive ability of A673 Ewing sarcoma cells compared with A673 Ewing sarcoma cells in which EWS/FLI expression had been abrogated. Using a monolayer wound healing assay, we observed that the parental A673 Ewing sarcoma cells or A673 cells with control RNAi migrate more slowly than cells with EWS/FLI RNAi (Fig. 4A). Ewing sarcoma cells in which EWS/FLI expression was knocked down were able to reach the midline of the

wound as early as 24 hours, whereas control RNAi expressing cells did not close the wound even after 48 hours.

In an effort to dissect the mechanism underlying alteration in monolayer wound healing capacity associated with EWS/FLI expression, we performed time lapse microscopic analysis of individual cells to measure speed, distance, and displacement of cells over a 24 hour period in a random migration assay (Fig. 4B-F). By inspection of the motility tracks of individual cells, it was evident that expression of EWS/FLI inhibited the ability of the A673 cells to migrate on tissue culture plastic (Fig. 4B). Quantitative measurement of the individual cellular tracks revealed a statistically significant decrease in total distance traveled by control A673 cells compared with those in which EWS/FLI expression was knocked down (Fig. 4C). The mean cell velocity also reduced to 7 μm/h for control RNAi expressing cells compared with 19 μm/h for EWS/FLI RNAi expressing cells (Fig. 4D). The net displacement, defined as the length of a straight line drawn from the starting cell position to the ending position after the 8 hour migration interval had elapsed, was 92 μm for the A673 cells in which EWS/FLI was knocked down compared with 21 μm for the cells with control RNAi (Fig. 4E).

Cells can migrate randomly or in a directed fashion. To evaluate whether the expression of EWS/FLI also influences the directionality of Ewing sarcoma cell migration, we assessed the persistence of the migrating cells by calculating the ratio of net cell displacement to total path length travelled by the cell. Our analysis shows that A673 cells treated with either control RNAi or EWS/FLI RNAi exhibit comparable persistence (Fig. 4F). No statistically significant differences

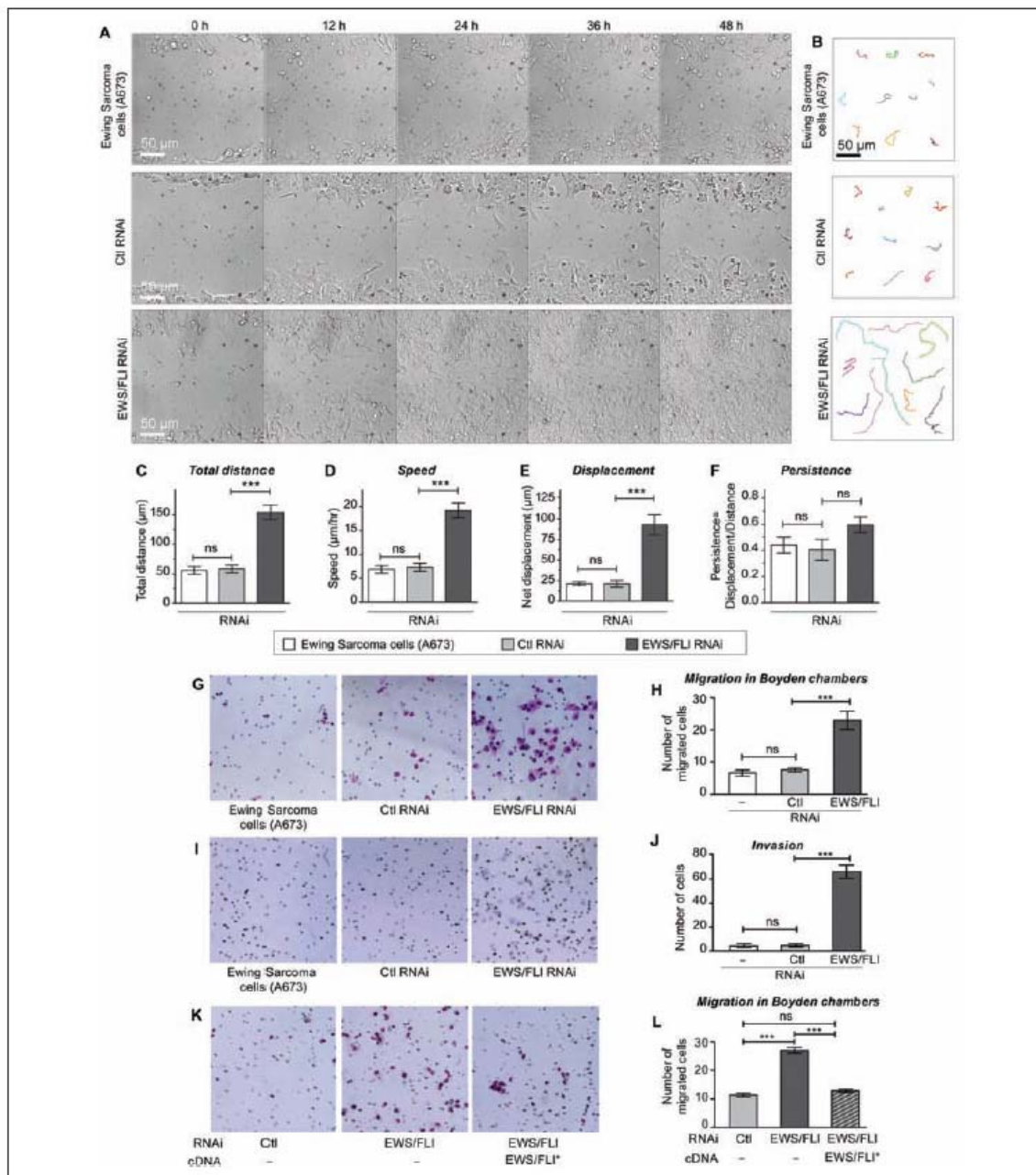


Figure 4. Expression of EWS/FLI results in reduced cellular migration and invasion. Ewing sarcoma A673 cells with control RNAi or EWS/FLI RNAi were evaluated for directed cell migration, random motility, chemotaxis, and invasion. (A) Cell migration into wounds scraped across cell monolayers was monitored by time lapse microscopy for 48 hours. A673 cells with EWS/FLI RNAi reached the midline of the wound within 24 hours, whereas the other A673 cells did not migrate effectively. (B) Random cell motility was tracked by time lapse microscopy (15-minute intervals for 8 hours), and representative cells tracks are shown. Analysis for total distance (C), speed (D), displacement (E), and persistence (F) was performed with MetaMorph software, and showed enhanced motility but no EWS/FLI-dependent difference in persistence in A673 cells with EWS/FLI RNAi. (G, H) Cells in serum-free media were plated onto Boyden transwell migration filters and then given 24 hours to migrate through pores (small circles on images) toward a high serum environment, fixed, and stained (blue). Compared with control cells, significantly more cells with EWS/FLI RNAi migrated. (I, J) Transwell invasion through Matrigel matrix (24 hours) indicated significant increase in cellular invasiveness upon knockdown of EWS/FLI. (K, L) A673 cells with control (light gray bar) or EWS/FLI RNAi (dark gray bar) were compared with EWS/FLI RNAi cells reconstituted with Flag-tagged EWS/FLI* cDNA (striped bar) that is resistant to the RNAi in transwell migration assays. Quantitation of the number of migrated cells indicated the EWS/FLI-dependence of this cell migration difference. *** $P < 0.001$, ns is not significantly different.

in distance, velocity, or net displacement were observed when comparing untreated A673 cells with those treated with control RNAi (Fig. 4C-F).

Consistent with the monolayer wound healing and single cell migration assays, we found that EWS/FLI expression in Ewing sarcoma cells also inhibited translocation through a porous membrane in a chemotactic Boyden Chamber assay in which cells are stimulated to migrate towards high serum gradient (Fig. 4G, H). Whereas EWS/FLI knockdown cells exhibited significantly increased capacity for invasion in a Matrigel invasion assay, expression of EWS/FLI, as occurred in the parental cell line, was associated with a striking lack of invasiveness by Ewing sarcoma cells (Fig. 4I, J). Confirmation that the effects of EWS/FLI knockdown on cell migration are due specifically to the loss of EWS/FLI was achieved by knockdown-rescue experiments in which we expressed an RNAi-insensitive EWS/FLI cDNA in the knockdown cells. We observed that expression of EWS/FLI causes reduced haptotactic cell migration in a Boyden chamber cell migration assay (Fig. 4K, L). Collectively, these results illustrate that EWS/FLI expression inhibits cell migration.

EWS/FLI expression induces deficiencies in the actin cytoskeleton and focal adhesions. The decreased adhesion and migration associated with EWS/FLI expression suggested that EWS/FLI expression might induce an underlying change in cytoarchitecture that is responsible for the observed alterations in cell behavior. To assess this possibility, we compared the cytoskeletal organization in A673 Ewing sarcoma cells and A673 cells in which EWS/FLI expression was knocked down by studying subcellular localization of cytoskeletal proteins. The cells were plated on fibronectin-coated coverslips in the presence of serum. Ewing sarcoma cells that express EWS/FLI displayed a small round cell morphology with thin and short actin stress fibers (Fig. 5A). In contrast, knocking down EWS/FLI resulted in cells with robust actin stress fibers that were distributed throughout the well spread Ewing sarcoma cells, seemingly consistent with a mesenchymal/fibroblastic morphology of a putative sarcoma cell-of-origin (Fig. 5B).

Actin stress fibers terminate at specialized regions of the cell membrane called focal adhesions, which support integrin-dependent adhesion to extracellular matrix proteins. Adherent mesenchymal cells typically display robust focal adhesions. The deficit in cell adhesion and actin stress fiber organization in Ewing sarcoma cells raised the possibility that expression of EWS/FLI might affect the establishment or maturation of focal adhesions. To test the impact of EWS/FLI expression on integrin-anchored focal adhesion sites, we compared focal adhesions in Ewing sarcoma cells treated with control or EWS/FLI directed RNAi by indirect immunofluorescence with primary antibody directed against the focal adhesion marker protein, paxillin (Fig.

5A,B,C,E,F).⁵² Quantitative analysis of focal adhesion number revealed that control A673 cells expressing EWS/FLI had fewer focal adhesions than A673 cells treated with EWS/FLI RNAi, displaying an average of 50 ± 15 focal adhesions per cell compared with 177 ± 50 focal adhesions for cells in which EWS/FLI expression was compromised (Fig. 5E). In addition to the reduced number of focal adhesions, cells with wild-type EWS/FLI expression had smaller focal adhesions, with average focal adhesion areas of $1.3 \mu\text{m}^2 \pm 0.3 \mu\text{m}^2$ compared with an average focal adhesion area of $1.8 \mu\text{m}^2 \pm 0.3 \mu\text{m}^2$ for Ewing sarcoma cells treated with EWS/FLI RNAi (Fig. 5F).

Consistent with our observations that cells with EWS/FLI expression have compromised actin stress fibers and focal adhesions, these cells also exhibited an average cell area of $916 \mu\text{m}^2$ after 24 hours of plating, compared with an area of $2218 \mu\text{m}^2$ for A673 cells with reduced EWS/FLI expression (Fig. 5D, G). This finding complements the cell adhesion and cell spreading analysis presented in Fig. 2, which showed that Ewing sarcoma cells display deficits in adhesion and spread more slowly than Ewing sarcoma cells in which EWS/FLI expression is knocked down. Analysis of cell area 24 hours after plating illustrates that the Ewing sarcoma cells are not simply slow to spread; rather, they have lost their cytoskeletal organization and adhesive capacity, leading to a steady-state decline in cell area. As we demonstrated with the adhesion and motility measurements, EWS/FLI expression is specifically required for inducing the alterations in the actin cytoskeleton and cellular morphology observed in Ewing sarcoma cells. When an RNAi-insensitive variant of EWS/FLI cDNA is expressed in A673 sarcoma cells along with EWS/FLI RNAi, the cells lose their well-formed actin stress fibers and revert to small and round morphology (Fig. 5H).

EWS/FLI-dependent reduction in cell adhesion, cell migration, and actin stress fibers is seen in several patient-derived Ewing sarcoma cell lines. To confirm that our findings using A673 cells were providing generalizable insights regarding the influence of EWS/FLI on cellular phenotype, we replicated our experiments using 2 additional primary tumor-derived Ewing sarcoma cell lines, TC71 and EWS502. Both of these cell lines displayed similar phenotypic changes upon RNAi based knockdown of EWS/FLI (Fig. 6A). Adhesion (Fig. 6B) and migration (Fig. 6C) of TC71 and EWS502 cells increased upon knockdown of EWS/FLI, illustrating that EWS/FLI expression abrogates both cell adhesion and motility. As we observed for A673 cells, EWS/FLI expression is associated with loss of actin filaments, reduced cell spreading, and compromised focal adhesions in both TC71 and EWS502 cells (Fig. 6D, E). It is striking that even with the baseline morphological heterogeneity among the Ewing sarcoma cell lines, all 3 display robust and parallel phenotypic responses to

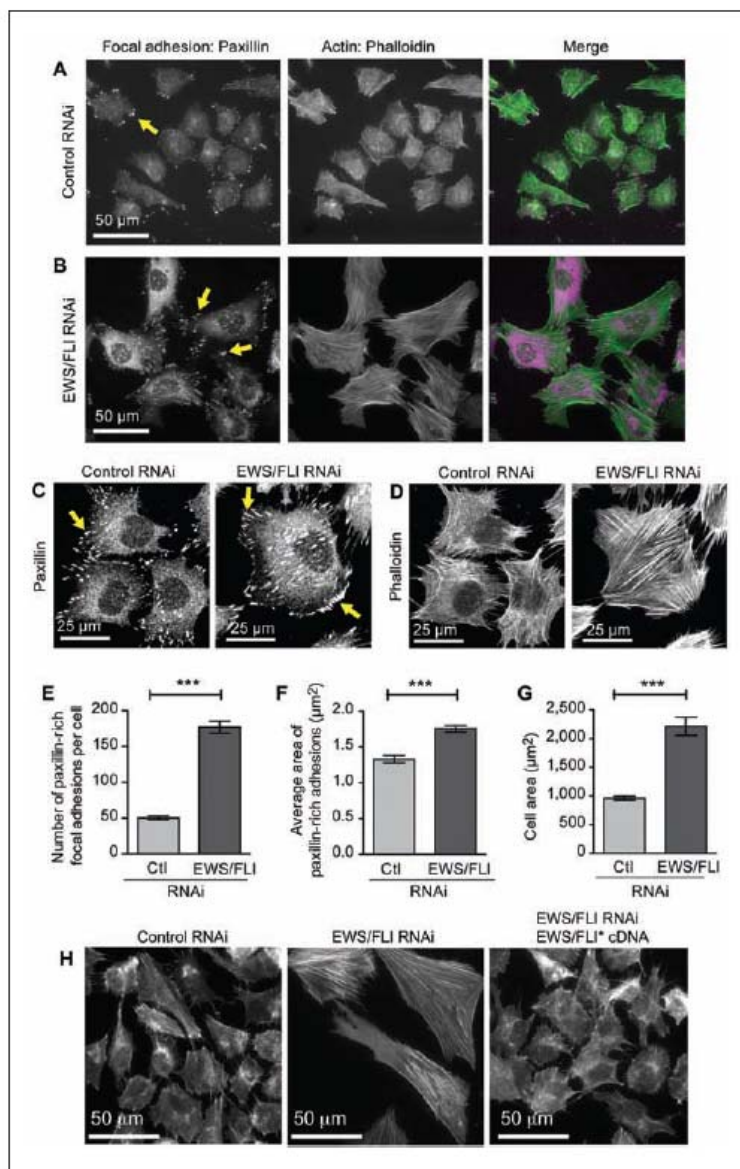


Figure 5. EWS/FLI expression affects cellular morphology and cytoarchitecture. Widefield immunofluorescent images of A673 cells with (A) control RNAi or (B) EWS/FLI RNAi stained for focal adhesions (paxillin antibody) and for actin filaments (phalloidin) showed a striking EWS/FLI-dependent difference in cellular morphology, the actin cytoskeleton network, and focal adhesions. (C) Paxillin-rich focal adhesions and actin cytoskeletons (D) in cells with EWS/FLI or with EWS/FLI knockdown were analyzed. Both the number (E) and size (F) of focal adhesions were lower in A673 cells with control RNAi compared with cells with EWS/FLI RNAi, consistent with the compromised adhesion phenotype of Ewing sarcoma cells. (G) Cell area was measured in cells with control RNAi or EWS/FLI RNAi plated for 24 hours and then fixed and stained with phalloidin. Cell area of Ewing sarcoma A673 cells was significantly smaller than for cells with EWS/FLI knockdown. (H) Phalloidin-stained actin cytoskeleton in A673 cells with control RNAi, EWS/FLI RNAi, or EWS/FLI RNAi plus reconstituted Flag-EWS/FLI^{*} showed that the loss of actin stress fibers is EWS/FLI-dependent. *** $P < 0.001$.

EWS/FLI knockdown, underscoring the fact that transformation by EWS/FLI induces dramatic changes in cell adhesion, migration, and cytoarchitecture.

The loss of adhesion, migration, and actin cytoskeletal integrity induced by EWS/FLI expression represents a constellation of effects that is generally consistent with a loss of mesenchymal cell features. To explore whether the expression of well-established mesenchymal markers is affected by EWS/FLI, we analyzed previously published gene expression profiles derived from Ewing sarcoma cells and cells in which EWS/FLI expression was compromised.^{36,38} We noted significant upregulation of mRNAs encoding mesenchymal markers upon knockdown of EWS/FLI in A673 cells. We performed an independent biological validation of 2 of these genes, N-cadherin and Slug, using qRT-PCR (Fig. 7A). Our results confirmed that the presence of EWS/FLI is associated with low expression of both N-cadherin and Slug in Ewing sarcoma cells and that knockdown of EWS/FLI expression using RNA interference results in 6- to 8-fold upregulation of transcripts encoding these mesenchymal markers. Upon expression of RNAi-resistant EWS/FLI cDNA, the levels of N-cadherin and Slug transcripts were reduced.

Discussion

Metastatic disease is an important tumor phenotype that portends poor prognosis for patients. For patients whose primary site of tumor development is adequately controlled with current local therapies (mainly surgery and/or radiation therapy), relapse at distant sites indicates that undetected metastatic disease (termed *micrometastasis*) was present before the primary tumor was controlled. In the case of epithelial malignancies (carcinomas), the development of metastatic disease is thought to

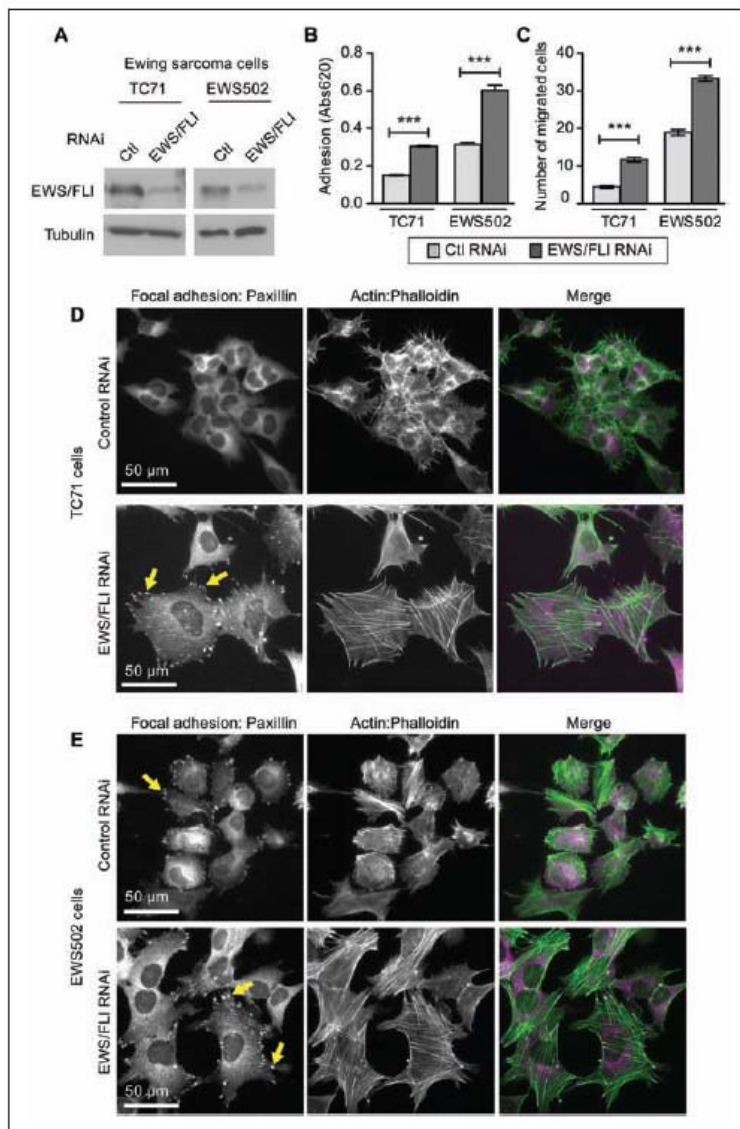


Figure 6. Ewing sarcoma cells TC71 and EWS502 exhibit EWS/FLI-dependent loss of adhesion, migration, and cytoarchitecture. (A) Cell lysates from Ewing sarcoma cell lines TC71 and EWS502 with retroviral mediated RNAi knockdown for control or EWS/FLI were evaluated by western immunoblot with FLI-1 antibody, and significant decreases in EWS/FLI expression were confirmed. (B) Ewing sarcoma cells with control RNAi (light gray bar) or EWS/FLI RNAi (dark gray bar) were seeded onto tissue culture plastic (uncoated (EWS502) or precoated with 10 μ g/ml fibronectin (TC71)) and allowed to adhere for 2 hours, and then adherent cells were quantitated by a colorimetric assay. (C) Boyden chamber transwell inserts were precoated with fibronectin (5 μ g/ml TC71; 1 μ g/ml EWS502) and seeded with cells that were allowed 24 hours to migrate through the insert pores. EWS/FLI knockdown enhanced the number of migratory cells in both cell lines. (D) TC71 and (E) EWS502 cells with EWS/FLI or with EWS/FLI knockdown were stained for paxillin-rich focal adhesions and actin stress fibers (phalloidin). Cells with EWS/FLI RNAi displayed more pronounced focal adhesions and actin stress fibers. *** $P < 0.001$

represent a stepwise progression of tumor development, following genetic and/or epigenetic alterations. These alterations are thought to culminate in the development of an epithelial-to-mesenchymal transition (EMT), with the result that tumor cells acquire the ability to escape the primary tumor, adhere, migrate, and invade through the extracellular matrix and ultimately to extravasate into the blood or lymphatic system.^{1,12}

Sarcomas are mesenchymally derived tumors of less certain origin than many carcinomas. The process of metastatic spread is less well understood for sarcomas compared with carcinomas, and whether an “EMT-equivalent” process occurs that allows for increased cellular adhesion, migration, and invasion is unknown. Furthermore, the stepwise progression model of metastatic spread occurring as a late phenotype in tumor development does not adequately explain tumors that exhibit very early metastatic (or micrometastatic) spread. We therefore evaluated Ewing sarcoma as an example with a clear propensity for early metastatic and micrometastatic spread. This also allowed us to evaluate the role of the critical oncoprotein, EWS/FLI, in modulating metastatic-relevant phenotypes in this disease.

Here we report that EWS/FLI expression has a profound effect on cell adhesion, reducing capacity for adhesion and associated cellular spreading, both *in vitro* and *in vivo*. Analysis of focal adhesion architecture and actin cytoskeletal organization revealed that EWS/FLI expression results in loss of actin stress fibers and reduced size and number of focal adhesions, 2 structural changes that likely account for the functional deficit in cell adhesion. Reciprocal changes in cellular morphology have also been observed following expression of EWS/FLI in human mesenchymal stem cells, which causes the conversion of a

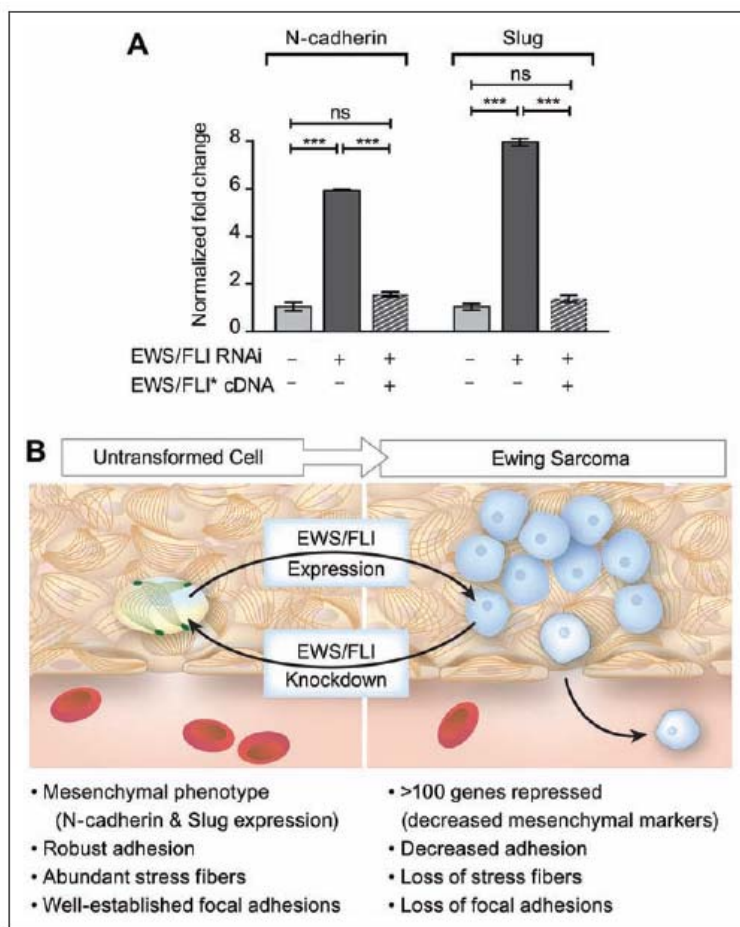


Figure 7. Model for EWS/FLI-dependent coupling of transformation to acquisition of potential for tumor cell dissemination. **(A)** RT-PCR analysis of mesenchymal markers, N-cadherin and Slug, in Ewing sarcoma cells programmed to express control RNAi, EWS/FLI RNAi, or EWS/FLI RNAi and an RNAi-insensitive EWS/FLI* construct. $***P < 0.0001$, ns is not statistically different. **(B)** In this model, EWS/FLI-induced oncogenic transformation simultaneously causes downregulation of cellular adhesion. Consistent with this model, EWS/FLI knockdown caused cells to return to a more normalized mesenchymal phenotype, including expression of mesenchymal markers, robust adhesion, pronounced stress fibers, and well-established focal adhesions. We postulate that these events prime the tumor cells for dissemination and may account for the early acquisition of metastatic potential in Ewing sarcoma.

well-spread, fibroblast-like shape to a rounded cell morphology.⁵³ Somewhat surprisingly, given the highly metastatic nature of Ewing sarcoma and results from previous studies,^{39,54} we found that EWS/FLI expression also resulted in reduced cell migration, as assayed in single cell migration studies, wound healing assays, and transwell migration studies. Similarly, we found that EWS/FLI reduces the ability of Ewing sarcoma cells to invade Matrigel matrices.

These findings suggest the possibility that active promotion of cell migration is not critical to drive the metastatic potential of Ewing sarcoma.

These data stand in direct contrast to our initial hypothesis, that EWS/FLI might stimulate metastasis by inducing increased cellular adhesion, migration, and invasion, and therefore prompt a reevaluation of how Ewing sarcoma might navigate the processes required for metastatic development. Our data (and prior data from other investigators) are consistent with the notion that Ewing sarcoma arises from a mesenchymal cell type (perhaps a mesenchymal stem or progenitor cell).^{48,53} In this view, a mesenchymal cell of origin would display strong adhesion to extracellular matrix proteins. The cell would thus be tethered to the extracellular matrix via these strong adherent properties that would constrain inappropriate release of locally resident cells. As illustrated in the model in Fig. 7B, EWS/FLI expression results in downregulation of several hundred genes (including mesenchymal markers), decreased adhesion, and significant cytoskeletal changes with loss of actin stress fibers and focal adhesions. Reciprocally, RNAi-based knockdown of EWS/FLI causes a tumor-to-mesenchymal-transition, where Ewing sarcoma cells are “normalized” to a more mesenchymal phenotype. This is demonstrated in our study by increased expression of N-cadherin and Slug, the restoration of robust actin stress fibers and focal adhesions, and increased cell adhesion.

The loss of cell adhesion induced by EWS/FLI expression could promote dissemination of the tumor cells. The histological features of the capillary beds in the bone marrow, which display a fenestrated endothelium and discontinuous basement membrane, would be expected to promote permissive transfer of nonadherent tumor cells into the circulation. If tumor cell dissemination is a rate-limiting step in progression to metastasis, EWS/FLI-dependent abrogation of adhesion may be a powerful

way to promote the early metastasis observed in this disease. Such a model might be considered “stochastic” or “passive” in contrast to the “active” process observed in epithelial tumors undergoing an EMT.

An interesting precedent for such a stochastic/passive scenario, in which loss of adhesion might be permissive for exit of cells from bone marrow, is found in the case of erythroid differentiation. In this case, mammalian reticulocytes are tethered in the bone marrow early in the erythroid differentiation process by binding to fibronectin. At later stages along the path toward maturation to erythrocytes, the cells lose adhesion to fibronectin, and it has been proposed that this allows passive release of the mature cells from the interstitial matrix of the bone marrow into the circulation.⁵⁵⁻⁵⁷ From this perspective it is interesting to note that approximately 85% of Ewing sarcoma cases arise in and around the bone (usually with extension into the marrow cavity).⁵⁸ Thus, Ewing sarcoma cells typically arise in locations that have ready access to the intravascular space. In this environment, tumor cells may not require enhanced migratory or invasive capacity to access the vasculature on the path to metastasis but rather would simply require downregulation of cell adhesion, as occurs upon expression of the EWS/FLI oncoprotein.

Although the loss of cellular adhesion that is promoted by EWS/FLI expression may help to explain how Ewing sarcoma cells are so effectively disseminated from the site of the primary tumor, it is less clear how this reduced adhesion might influence the ability of the circulating tumor cells to take up residence and survive in a secondary site. Our experiments show that Ewing sarcoma cells in which EWS/FLI is knocked down are more likely to seed the lung when introduced into the circulation compared with the parental cell line. Nevertheless, the parental Ewing sarcoma cells are also effective in colonizing the lung. It is possible that Ewing sarcoma cells, even though less adhesive than their nontransformed counterparts, have adequate capacity to adhere and grow in the lung. Alternatively, it has been shown that tissue microenvironment can influence tumor biology, including oncogene expression.^{59,60} In the case of Ewing sarcoma, growth factor availability can influence the expression of EWS/FLI itself,⁶¹ raising the possibility that microenvironmental cues might modulate the expression of EWS/FLI and thus provide a mechanism for Ewing sarcoma cells to adapt and modulate their cellular phenotypes in a location-restricted fashion.

An important conclusion from our studies is that the primary oncogene (EWS/FLI) that induces Ewing sarcoma directly modulates a cell's adhesive and cytoarchitectural phenotypes. This again stands in contrast to current models suggesting that tumor metastasis is a later effect resulting from an accumulation of secondary mutations or epigenetic changes during tumor progression. Importantly, our EWS/

FLI reconstitution studies further signified that these phenotypic changes are EWS/FLI-dependent. Our data suggest that EWS/FLI serves an even larger role than previously envisioned for Ewing sarcoma tumorigenesis. It has previously been demonstrated that ongoing EWS/FLI expression is important for oncogenic “transformation” (in this case defined as the ability to grow as colonies under anchorage-independent conditions and as the ability to form tumors when injected into immunodeficient mice).^{37,38} Downstream targets, such as *IGFBP3*, *NKX2.2*, and *NROB1*, are absolutely required for this phenotype.³⁵⁻³⁸ Subsequent studies have demonstrated that EWS/FLI also modulates drug resistance via the regulation of *GSTM4* expression.⁶² The current study adds to this growing list of EWS/FLI-regulated phenotypes by demonstrating that the fusion protein modulates cell adhesion, migration, and invasiveness and thus might affect the metastatic phenotype.

In conclusion, we suggest that the transformed growth properties of Ewing sarcoma are induced in tandem with changes in cell behavior, such as reduced adhesion, that would promote tumor cell dissemination. The molecular mechanism by which EWS/FLI expression triggers the changes in adhesion, motility, and cytoskeleton reported here is not currently understood. EWS/FLI is a chimeric transcription factor that induces many alterations in the expression of a large number of genes.^{37,38,63} Other than a few EWS/FLI targets that have been extensively studied, such as *NROB1*, *NKX2.2*, and *Caveolin1*,^{35,36,64} little is understood about the physiological influence of EWS/FLI on complex cell behaviors, but it is likely that EWS/FLI exerts its influence via both direct and indirect transcriptional targets. Inspection of the genes whose expression is modulated by EWS/FLI revealed numerous genes that encode cytoskeletal and cell adhesion factors (our unpublished results). Future work will be required to identify the critical factors that are modulated downstream of EWS/FLI to affect features such as cytoskeletal integrity and cell adhesion of the tumor cells. These studies will be a key to enable better understanding of the genesis of Ewing sarcoma cell behavior.

Materials and Methods

Reagents. Antibodies were used for western immunoblots and indirect immunofluorescence microscopy as per manufacturer's instructions: FLI-1 rabbit antibody C-19 (sc-356X Santa Cruz Biotechnology, Santa Cruz, CA), Paxillin mouse antibody (P13520 Transduction Laboratories, San Jose, CA), β -tubulin mouse monoclonal antibody clone 2-28-33 (T 5293 Sigma-Aldrich, St. Louis, MO), HRP-conjugated antibodies for immunoblots (GE Healthcare, Pittsburgh, PA), and the Alexa-Fluor antibodies and phalloidin for microscopy (Molecular Probes/Invitrogen, Eugene,

OR). Prolong Gold anti-fade reagent with DAPI (Invitrogen (Gibco, Life Technologies, Grand Island, NY), catalog #P-36931) was used for mounting lung sections. Fibronectin and Mowiol (Sigma-Aldrich, St. Louis, MO) and Vybrant Cell-Labeling solutions DiI and DiO (Molecular Probes/Invitrogen, Eugene, OR) were used as per manufacturer's instructions.

Cell culture. Ewing sarcoma cell lines A673, TC71, and EWS502 were grown in DMEM media with 10% FBS, RPMI media with 10% FBS, and RPMI media with 15% FBS, respectively, as previously published.³⁸

RNA interference. Knockdown experiments used the luciferase-RNAi (as control RNAi) and EF-2-RNAi (as EWS/FLI RNAi) constructs previously described.³⁸ Constructs were made in pSRP retroviral vector with an H1 promoter to allow expression of sh-RNAs and a puromycin resistance marker. The retrovirally infected cells were selected in 2 µg/ml puromycin containing DMEM media for 2 days prior to use and maintained in selection for up to 5 weeks.

RT-PCR analysis. Total RNA was extracted from cell pellets using QIAgen RNeasy mini kit (QIAgen, Valencia, CA, catalog #74174). Using previously established primers,³⁸ EWS/FLI and glyceraldehyde-3-phosphate dehydrogenase were amplified and detected using iScript One-Step RT-PCR kit with SYBR green (BIO-RAD, Hercules, CA, catalog #170-8893) for quantitative analysis. Specific primers were designed to analyze N-cadherin (forward primer 5'-GAG-CAGTGAGCCTGCAGATTTTAAAG G-3' and reverse primer 5'-CCTTTGTAGGTGGCCACTGTGC-3') and Slug (forward primer 5'-GCCAACTACAGCGAACTG-GACAC-3' and reverse primer 5'-GCTTTCTGAGCCAC TGTGGTCC-3') as mesenchymal markers.

Western blots. Whole cell lysates in RIPA buffer with (Complete Mini-EDTA free) protease inhibitor cocktail tablets (Roche Diagnostics GmbH, Indianapolis, IN catalog #11836153001) were electrophoresed on 10% SDS-PAGE gels transferred onto nitrocellulose membranes. Proteins were detected with primary antibodies (see Reagents) and horseradish peroxidase-conjugated antibodies and enhanced chemiluminescence (GE Healthcare, Buckinghamshire, UK).

Soft agar assays. Soft agar assays were performed as described,⁶⁵ in short, with 1.6% SeaPlaque GTG agarose (Lonza, Rockland, ME, catalog #50111) and Iscove's modification Eagle's media, penicillin/streptomycin, and glutamine making a 0.35% agar underlayer with or without 2 µg/ml puromycin. Over this layer, a layer of cells was seeded at a density of 1×10^5 cells per 6 cm plate in 0.35% agar supplied with media of similar composition as the underlayer mentioned above. Cells were grown at 37°C and

5%CO₂ for 3 to 4 weeks and imaged, and colonies were counted. Assays were performed 3 times with A673, TC-71, and EWS 502 cells.

Adhesion and spreading assays. Ewing Sarcoma cells (A673 and EWS-502) were seeded at 100,000, 300,000, or 500,000 density per well in a non-ECM coated 24 well plate. TC-71 cells were seeded onto a 24-well plate pre-coated with 5 µg/ml fibronectin. Cells were allowed to adhere to the dish for 2 hours at 37°C in their respective media, washed 3 times with PBS to remove nonadherent cells, fixed (3.7% formaldehyde for 15 minutes), washed (PBS for 5 minutes), and stained with Toluidene Blue for 1 hour. Excess stain was removed, and then cells were washed, air dried overnight, and dissolved (500 µl of 2% SDS solution). O.D. was measured in duplicates at 620 nm.⁶⁶

For the spreading assay, after 2 hours of adhesion, cells were fixed and imaged (LucPlan 40X LWD objective (NA = 0.6) on an Olympus IX70 microscope with an Olympus CCD camera and Andor acquisition system). Cell area was measured for 10 representative fields of cells using Metamorph Imaging v7.5 software.

In vivo lung adhesion assay. This assay was adapted from a lung metastasis assay.⁶⁷ The A673 cells with control RNAi and with EWS/FLI RNAi were differentially labeled with lipophilic dyes Vybrant DiI (red) and DiO (green) and diluted to 1×10^6 stained cells per 100 µl. The 2 solutions were mixed in equal amounts and verified as 1:1 ratio by FACS. The mixed cell suspension (200 µl) was then injected into the lateral tail veins of 3 NOD-SCID mice (stock #1303, Jackson Laboratories, Sacramento, CA). After 24 hours, these mice were sacrificed, and the lungs were prepared by perfusion with 4% paraformaldehyde and frozen in OCT for cryopreservation. Lungs were cryosectioned (16-20 µm), mounted on slides using Prolong Gold anti-fade reagent with DAPI, and examined by fluorescent microscopy (Nikon A1R laser scan confocal acquisition on a Ti inverted microscope and Plan Fluor 40× Oil DIC H N2 objective). A large 3 field × 3 field (2 mm × 2 mm) mosaic image was created with each field having nine 2-µm optical sections (NIS Elements v3 software). The red and green colonies were then counted along with DAPI staining, and normalized values are reported for 15 representative mosaic images. The experiments were performed 3 times, including once with the dyes switched for the respective cell types to avoid any dye-based bias. Experiments were performed following approval from the University of Utah Institutional Animal Care and Use Committee.

Migration assays: monolayer wound healing assay. A monolayer of confluent Ewing sarcoma cells (A673) was generated by seeding 1×10^6 cells per well in a 6-well dish. Cells were imaged in DMEM/F/12-HEPES media lacking Phenol

Red (Invitrogen) supplemented with 10% FBS and maintained at 37°C (LIS) for microscopy. A micropipette tip was scraped across the monolayer to create a “wound.” Migration into the wound was then monitored by time-lapse microscopy at 15-minute intervals for 48 hours (inverted Nikon TE300 microscope, Plan Fluor ELWD 20x objective) and by Ludl XY stage (Ludl Electronic Products). Images were captured with Andor DV885 EMCCD camera and Andor IQ imaging software (Andor Technologies).⁶⁶

Random cell motility assay. A673 cells were seeded at a density of 25,000 cells/well in a non-ECM coated 6-well dish. Cells were imaged at 15-minute intervals for 24 hours as described for the wound healing assay above. For generating cell tracks and analysis, the Manual tracking plugin in ImageJ software was used.

Haptotactic cell migration assay. Ewing sarcoma cells (A673 and EWS502) were seeded (30,000 cells) in serum-free media onto 24-well cell culture insert membranes (polyethylene terephthalate) with 8- μ m pores (Becton Dickinson, San Jose, CA). These inserts were precoated overnight at 4°C with 1 μ g/ml fibronectin solution. For TC-71 cells, the inserts were coated with 5 μ g/ml fibronectin. Inserts with cells were placed in a 24-well plate of media supplemented with 10% FBS, and cells were allowed to migrate for 24 hours.⁶⁶ Nonmigratory cells were scraped off the top chamber, and migratory cells on the bottom surface were fixed in 100% methanol for 15 minutes and then stained overnight at 4°C with 1:20 modified Giemsa Stain. Chambers were washed in water, and images were captured for 5 representative fields per well (Olympus IX70 microscope, Luc Plan 20x phase objective, NA = 0.45, Olympus CCD camera and Andor IQ acquisition software). Migratory cells were scored for 3 individual wells per cell line. Three biological replicates were done.

Invasion assay. BioCoat Matrigel transwell invasion chambers with 8- μ m pores (BD Biosciences, Bedford, MA catalog #354480) in 24-well plates were seeded with 150,000 cells for a 24-hour invasion assay as described above for transwell migration assays.

Immunofluorescence studies. Ethanol sterilized coverslips in 12-well plates were coated with 10 μ g/ml fibronectin overnight at 4°C, and then Ewing sarcoma cells were seeded (75,000 cells/well) and allowed to adhere for 24 hours. Cells were fixed (15 minutes in 3.7% formaldehyde), washed for 5 minutes in PBS, and permeabilized in 0.2% Triton X-100/PBS. Cells were incubated with paxillin antibody (1:100) for 1 hour at 37°C followed by a 15-minute PBS wash, stained with AlexaFluor secondary antibody (1:200) and AlexaFluor-phalloidin (1:100) for 1 hour at 37°C, washed, and mounted in Mowiol medium.⁶⁶ Cell

images were captured using a Zeiss Axioskop2 mot plus microscope with a 40 \times plan NA 0.75 NeoFluor objective, Zeiss Axiocam MR camera, and Zeiss Axiovision v4.8.1 software (Carl Zeiss MicroImaging, Inc.).

Analysis of adhesions and cell spreading. Immunofluorescence microscopy of fixed cells used Nikon A1R Ti inverted microscope, 60 \times Oil Plan Apo DIC N2 (NA 1.4) objective, and Nikon Elements v3 software. Cell area was measured using the trace tool to identify the boundary of cells, a threshold was set using the actin/phalloidin staining, and region of interest areas were recorded (Metamorph v7.5 software). To count and measure the size of the paxillin-rich focal adhesions, single-cell images were first processed in Image J to despeckle and remove the noise, and background was subtracted using rolling ball (radius 10). Using Metamorph imaging v7.5 software, image threshold was set in these single cell images, and integrated morphometric analysis was performed to count the number of focal adhesions and measure the area of the thresholded region to represent size of focal adhesions.

Acknowledgments

We thank Dr. Chris Rodesch at the University of Utah Cell Imaging and Microscopy Core Facility for help with fluorescent imaging, image processing, and analysis. We thank Savita Sankar at Huntsman Cancer Institute for providing cells for the reconstitution studies. We acknowledge Diana Lim for help with manuscript preparation.

Declaration of Conflicting Interests

The author(s) declared no potential conflicts of interest with respect to the research, authorship, and/or publication of this article.

Funding

The author(s) disclosed receipt of the following financial support for the research, authorship, and/or publication of this article: This work was supported by the NIH (R01 GM50877 to M.C.B. and R01 CA140394 to SLL) and the Huntsman Cancer Foundation. The Cancer Center Support Grant (2 P30 CA042014) awarded to the Huntsman Cancer Institute provided developmental funds and Shared Resources critical to this project.

References

1. Valastyan S, Weinberg RA. Tumor metastasis: molecular insights and evolving paradigms. *Cell*. 2011;147:275-92.
2. Chaffer CL, Weinberg RA. A perspective on cancer cell metastasis. *Science*. 2011;331:1559-64.
3. Nguyen DX, Bos PD, Massague J. Metastasis: from dissemination to organ-specific colonization. *Nat Rev Cancer*. 2009;9:274-84.
4. Yang J, Weinberg RA. Epithelial-mesenchymal transition: at the crossroads of development and tumor metastasis. *Dev Cell*. 2008;14: 818-29.

5. Guilford P, Hopkins J, Harraway J, *et al.* E-cadherin germline mutations in familial gastric cancer. *Nature*. 1998;392:402-5.
6. Vincent-Salomon A, Thiery JP. Host microenvironment in breast cancer development: epithelial-mesenchymal transition in breast cancer development. *Breast Cancer Res*. 2003;5:101-6.
7. Perl AK, Wilgenbus P, Dahl U, *et al.* A causal role for E-cadherin in the transition from adenoma to carcinoma. *Nature*. 1998;392:190-3.
8. Frixen UH, Behrens J, Sachs M, *et al.* E-cadherin-mediated cell-cell adhesion prevents invasiveness of human carcinoma cells. *J Cell Biol*. 1991;113:173-85.
9. Guo W, Giancotti FG. Integrin signalling during tumour progression. *Nat Rev Mol Cell Biol*. 2004;5:816-26.
10. Rathinam R, Alahari SK. Important role of integrins in the cancer biology. *Cancer Metastasis Rev*. 2010;29:223-37.
11. Kumar S, Weaver VM. Mechanics, malignancy, and metastasis: the force journey of a tumor cell. *Cancer Metastasis Rev*. 2009;28:113-27.
12. Talmadge JE, Fidler IJ. AACR centennial series: the biology of cancer metastasis: historical perspective. *Cancer Res*. 2010;70:5649-69.
13. Eyles J, Puaux AL, Wang X, *et al.* Tumor cells disseminate early, but immunosurveillance limits metastatic outgrowth, in a mouse model of melanoma. *J Clin Invest*. 2010;120:2030-9.
14. Fearon ER, Vogelstein B. A genetic model for colorectal tumorigenesis. *Cell*. 1990;61:759-67.
15. Fidler IJ, Kripke ML. Metastasis results from preexisting variant cells within a malignant tumor. *Science*. 1977;197:893-5.
16. Pantel K, Alix-Panabieres C, Riethdorf S. Cancer micrometastases. *Nat Rev Clin Oncol*. 2009;6:339-51.
17. Wikman H, Vessella R, Pantel K. Cancer micrometastasis and tumour dormancy. *APMIS*. 2008;116:754-70.
18. Ramaswamy S, Ross KN, Lander ES, *et al.* A molecular signature of metastasis in primary solid tumors. *Nat Genet*. 2003;33:49-54.
19. Spraker HL, Price SL, Chaturvedi A, *et al.* The clone wars—revenge of the metastatic rogue state: the sarcoma paradigm. *Front Oncol*. 2012;2:2.
20. Dahlin DC, Coventry MB, Scanlon PW. Ewing's sarcoma: a critical analysis of 165 cases. *J Bone Joint Surg Am*. 1961;43-A:185-92.
21. Wang CC, Schulz MD. Ewing's sarcoma; a study of fifty cases treated at the Massachusetts General Hospital, 1930-1952 inclusive. *N Engl J Med*. 1953;248:571-6.
22. Dubois SG, Epling CL, Teague J, *et al.* Flow cytometric detection of Ewing sarcoma cells in peripheral blood and bone marrow. *Pediatr Blood Cancer*. 2010;54:13-8.
23. Peter M, Magdelenat H, Michon J, *et al.* Sensitive detection of occult Ewing's cells by the reverse transcriptase-polymerase chain reaction. *Br J Cancer*. 1995;72:96-100.
24. Pfeleiderer C, Zoubek A, Gruber B, *et al.* Detection of tumour cells in peripheral blood and bone marrow from Ewing tumour patients by RT-PCR. *Int J Cancer*. 1995;64:135-9.
25. Zoubek A, Kovar H, Kronberger M, *et al.* Mobilization of tumour cells during biopsy in an infant with Ewing sarcoma. *Eur J Pediatr*. 1996;155:373-6.
26. West DC, Grier HE, Swallow MM, *et al.* Detection of circulating tumor cells in patients with Ewing's sarcoma and peripheral primitive neuroectodermal tumor. *J Clin Oncol*. 1997;15:583-8.
27. de Alava E, Lozano MD, Patino A, *et al.* Ewing family tumors: potential prognostic value of reverse-transcriptase polymerase chain reaction detection of minimal residual disease in peripheral blood samples. *Diagn Mol Pathol*. 1998;7:152-7.
28. Fagnou C, Michon J, Peter M, *et al.* Presence of tumor cells in bone marrow but not in blood is associated with adverse prognosis in patients with Ewing's tumor. *Societe Francaise d'Oncologie Pediatric*. *J Clin Oncol*. 1998;16:1707-11.
29. Fidelia-Lambert MN, Zhuang Z, Tsokos M. Sensitive detection of rare Ewing's sarcoma cells in peripheral blood by reverse transcriptase polymerase chain reaction. *Hum Pathol*. 1999;30:78-80.
30. Aurias A, Rimbaut C, Buffe D, *et al.* Translocation involving chromosome 22 in Ewing's sarcoma: a cytogenetic study of four fresh tumors. *Cancer Genet Cytogenet*. 1984;12:21-5.
31. Delattre O, Zucman J, Plougastel B, *et al.* Gene fusion with an ETS DNA-binding domain caused by chromosome translocation in human tumours. *Nature*. 1992;359:162-5.
32. Turc-Carel C, Philip I, Berger MP, *et al.* Chromosome study of Ewing's sarcoma (ES) cell lines: consistency of a reciprocal translocation t(11;22)(q24;q12). *Cancer Genet Cytogenet*. 1984;12:1-19.
33. Sankar S, Lessnick SL. Promiscuous partnerships in Ewing's sarcoma. *Cancer Genet*. 2011;204:351-65.
34. May WA, Lessnick SL, Braun BS, *et al.* The Ewing's sarcoma EWS/FLI-1 fusion gene encodes a more potent transcriptional activator and is a more powerful transforming gene than FLI-1. *Mol Cell Biol*. 1993;13:7393-8.
35. Kinsey M, Smith R, Lessnick SL. NR0B1 is required for the oncogenic phenotype mediated by EWS/FLI in Ewing's sarcoma. *Mol Cancer Res*. 2006;4:851-9.
36. Owen LA, Kowalewski AA, Lessnick SL. EWS/FLI mediates transcriptional repression via NKX2.2 during oncogenic transformation in Ewing's sarcoma. *PLoS One*. 2008;3:e1965.
37. Prieur A, Tirode F, Cohen P, *et al.* EWS/FLI-1 silencing and gene profiling of Ewing cells reveal downstream oncogenic pathways and a crucial role for repression of insulin-like growth factor binding protein 3. *Mol Cell Biol*. 2004;24:7275-83.
38. Smith R, Owen LA, Trem DJ, *et al.* Expression profiling of EWS/FLI identifies NKX2.2 as a critical target gene in Ewing's sarcoma. *Cancer Cell*. 2006;9:405-16.
39. Amsellem V, Kryszke MH, Hervy M, *et al.* The actin cytoskeleton-associated protein zyxin acts as a tumor suppressor in Ewing tumor cells. *Exp Cell Res*. 2005;304:443-56.
40. Jaishankar S, Zhang J, Roussel MF, *et al.* Transforming activity of EWS/FLI is not strictly dependent upon DNA-binding activity. *Oncogene*. 1999;18:5592-7.
41. Song Y, Maul RS, Gerbin CS, *et al.* Inhibition of anchorage-independent growth of transformed NIH3T3 cells by epithelial protein lost in neoplasm (EPLIN) requires localization of EPLIN to actin cytoskeleton. *Mol Biol Cell*. 2002;13:1408-16.
42. Lessnick SL, Braun BS, Denny CT, *et al.* Multiple domains mediate transformation by the Ewing's sarcoma EWS/FLI-1 fusion gene. *Oncogene*. 1995;10:423-31.
43. May WA, Gishizky ML, Lessnick SL, *et al.* Ewing sarcoma 11;22 translocation produces a chimeric transcription factor that requires the

- DNA-binding domain encoded by FLI1 for transformation. *Proc Natl Acad Sci U S A.* 1993;90:5752-6.
44. Braunreiter CL, Hancock JD, Coffin CM, *et al.* Expression of EWS-ETS fusions in NIH3T3 cells reveals significant differences to Ewing's sarcoma. *Cell Cycle.* 2006;5:2753-9.
 45. Hancock JD, Lessnick SL. A transcriptional profiling meta-analysis reveals a core EWS-FLI gene expression signature. *Cell Cycle.* 2008;7:250-6.
 46. Cavazzana AO, Miser JS, Jefferson J, *et al.* Experimental evidence for a neural origin of Ewing's sarcoma of bone. *Am J Pathol.* 1987;127:507-18.
 47. Ewing J. Diffuse endothelioma of bone. *Proc NY Pathol Soc.* 1921;21:17-24.
 48. Tirode F, Laud-Duval K, Prieur A, *et al.* Mesenchymal stem cell features of Ewing tumors. *Cancer Cell.* 2007;11:421-9.
 49. Kovar H. Context matters: the hen or egg problem in Ewing's sarcoma. *Semin Cancer Biol.* 2005;15:189-96.
 50. Owen LA, Lessnick SL. Identification of target genes in their native cellular context: an analysis of EWS/FLI in Ewing's sarcoma. *Cell Cycle.* 2006;5:2049-53.
 51. Martinez-Ramirez A, Rodriguez-Perales S, Melendez B, *et al.* Characterization of the A673 cell line (Ewing tumor) by molecular cytogenetic techniques. *Cancer Genet Cytogenet.* 2003;141:138-42.
 52. Turner CE. Paxillin and focal adhesion signalling. *Nat Cell Biol.* 2000;2:E231-6.
 53. Riggi N, Suva ML, Suva D, *et al.* EWS-FLI-1 expression triggers a Ewing's sarcoma initiation program in primary human mesenchymal stem cells. *Cancer Res.* 2008;68:2176-85.
 54. Herrero-Martin D, Osuna D, Ordonez JL, *et al.* Stable interference of EWS-FLI1 in an Ewing sarcoma cell line impairs IGF-1/IGF-1R signalling and reveals TOPK as a new target. *Br J Cancer.* 2009;101:80-90.
 55. Eshghi S, Vogelezang MG, Hynes RO, *et al.* Alpha4beta1 integrin and erythropoietin mediate temporally distinct steps in erythropoiesis: integrins in red cell development. *J Cell Biol.* 2007;177:871-80.
 56. Patel VP, Lodish HF. Loss of adhesion of murine erythroleukemia cells to fibronectin during erythroid differentiation. *Science.* 1984;224:996-8.
 57. Patel VP, Ciechanover A, Platt O, *et al.* Mammalian reticulocytes lose adhesion to fibronectin during maturation to erythrocytes. *Proc Natl Acad Sci U S A.* 1985;82:440-4.
 58. Kimber C, Michalski A, Spitz L, *et al.* Primitive neuroectodermal tumours: anatomic location, extent of surgery, and outcome. *J Pediatr Surg.* 1998;33:39-41.
 59. Shibue T, Weinberg RA. Metastatic colonization: settlement, adaptation and propagation of tumor cells in a foreign tissue environment. *Semin Cancer Biol.* 2011;21:99-106.
 60. Sterling JA, Edwards JR, Martin TJ, *et al.* Advances in the biology of bone metastasis: how the skeleton affects tumor behavior. *Bone.* 2011;48:6-15.
 61. Gimita L, Gimita A, Wang M, *et al.* A link between basic fibroblast growth factor (bFGF) and EWS/FLI-1 in Ewing's sarcoma cells. *Oncogene.* 2000;19:4298-301.
 62. Luo W, Gangwal K, Sankar S, *et al.* GSTM4 is a microsatellite-containing EWS/FLI target involved in Ewing's sarcoma oncogenesis and therapeutic resistance. *Oncogene.* 2009;28:4126-32.
 63. Kauer M, Ban J, Kofler R, *et al.* A molecular function map of Ewing's sarcoma. *PLoS One.* 2009;4:e5415.
 64. Tirado OM, Mateo-Lozano S, Villar J, *et al.* Caveolin-1 (CAV1) is a target of EWS/FLI-1 and a key determinant of the oncogenic phenotype and tumorigenicity of Ewing's sarcoma cells. *Cancer Res.* 2006;66:9937-47.
 65. Lessnick SL, Dacwag CS, Golub TR. The Ewing's sarcoma oncoprotein EWS/FLI induces a p53-dependent growth arrest in primary human fibroblasts. *Cancer Cell.* 2002;1:393-401.
 66. Hoffman LM, Jensen CC, Kloeker S, *et al.* Genetic ablation of zyxin causes Mena/VASP mislocalization, increased motility, and deficits in actin remodeling. *J Cell Biol.* 2006;172:771-82.
 67. Padua D, Zhang XH, Wang Q, *et al.* TGFbeta primes breast tumors for lung metastasis seeding through angiopoietin-like 4. *Cell.* 2008;133:66-77.

CHAPTER 4

STRETCH-INDUCED ACTIN REMODELING REQUIRES TARGETING OF ZYXIN TO STRESS FIBERS AND RECRUITMENT OF ACTIN REGULATORS

My contribution for this work is towards understanding the zyxin-dependent effect on actin cytoskeleton in the presence of Rho kinase inhibitor.

This work is reprinted with permission from Molecular Biology of the Cell.

This manuscript was originally published in Mol Biol Cell. 2012 May;23(10):1846-59.

Stretch-induced actin remodeling requires targeting of zyxin to stress fibers and recruitment of actin regulators

Laura M. Hoffman, Christopher C. Jensen, Aashi Chaturvedi, Masaaki Yoshigi, and Mary C. Beckerle

Departments of Biology and Oncological Sciences, Huntsman Cancer Institute, University of Utah, Salt Lake City, UT 84112

ABSTRACT Reinforcement of actin stress fibers in response to mechanical stimulation depends on a posttranslational mechanism that requires the LIM protein zyxin. The C-terminal LIM region of zyxin directs the force-sensitive accumulation of zyxin on actin stress fibers. The N-terminal region of zyxin promotes actin reinforcement even when Rho kinase is inhibited. The mechanosensitive integrin effector p130Cas binds zyxin but is not required for mitogen-activated protein kinase-dependent zyxin phosphorylation or stress fiber remodeling in cells exposed to uniaxial cyclic stretch. α -Actinin and Ena/VASP proteins bind to the stress fiber reinforcement domain of zyxin. Mutation of their docking sites reveals that zyxin is required for recruitment of both groups of proteins to regions of stress fiber remodeling. Zyxin-null cells reconstituted with zyxin variants that lack either α -actinin or Ena/VASP-binding capacity display compromised response to mechanical stimulation. Our findings define a bipartite mechanism for stretch-induced actin remodeling that involves mechanosensitive targeting of zyxin to actin stress fibers and localized recruitment of actin regulatory machinery.

Monitoring Editor
Paul Forscher
Yale University

Received: Dec 30, 2011
Revised: Mar 15, 2012
Accepted: Mar 23, 2012

INTRODUCTION

The ability of cells to respond to mechanical stimulation is key for normal physiology and function. Cells of the cardiovascular, respiratory, urogenital, and locomotory systems are exposed to mechanical stress under both normal and pathophysiological conditions (Jaalouk and Lammerding, 2009). Given the clear impact of mechanical signals on cell physiology, much research has focused on understanding how physical force is sensed by cells and how physical signals are converted into chemical information that can directly influence cell behavior.

Recent efforts have been made to simulate physiological conditions of mechanical stimulation in the laboratory in order to learn more about how cells sense and respond to physical cues (Eyckmans *et al.*, 2011). For example, to model the mechanical stress

experienced by vascular endothelial cells *in vivo*, flow chambers that deliver calibrated levels of shear stress have been devised (Davies, 1995). To model the cyclic stretch that occurs with inspiration or rhythmic cardiac beating, chambers have been developed in which cells are grown on elastic membranes that can be deformed according to precise experimental parameters (Banes *et al.*, 1985; Yoshigi *et al.*, 2003). By employing these devices for controlled mechanical stimulation of cells, it has been possible to demonstrate activation of signaling cascades (Orr *et al.*, 2006; Cohen *et al.*, 2010), actin remodeling and reinforcement (Wille *et al.*, 2004; Yoshigi *et al.*, 2005), and even changes in gene expression (Kessler *et al.*, 2001; Wojtowicz *et al.*, 2010) in response to physical stress.

The cell membrane defines the interface between the cell interior and the extracellular environment. It plays a central role in sensing and transducing mechanical signals. Focal adhesions (FAs)—regions of the cell surface that are specialized for cell–substratum attachment—provide sites for transmission of mechanical signals to the cell interior. Integrins—transmembrane receptors for extracellular matrix—are concentrated at FAs and play central roles influencing cell behavior downstream of physical cues (Geiger *et al.*, 2009; Puklin-Faucher and Sheetz, 2009; Wang *et al.*, 2009; Parsons *et al.*, 2010; Schwartz, 2010). Actin stress fibers (SFs) are cytoskeletal structures that terminate at FAs, where they are linked to integrins bound to extracellular matrix. Prominent in cultured cells, SFs also

This article was published online ahead of print in MBoC in Press (<http://www.molbiolcell.org/cgi/doi/10.1091/mbc.E11-12-1057>) on March 28, 2012.

Address correspondence to: Mary C. Beckerle (mary.beckerle@hci.utah.edu).

Abbreviations used: FA, focal adhesion; MAPK, mitogen-activated protein kinase; NES, nuclear export sequence; SF, stress fiber; SFT1, stress fiber thickness index.

© 2012 Hoffman *et al.* This article is distributed by The American Society for Cell Biology under license from the author(s). Two months after publication it is available to the public under an Attribution–Noncommercial–Share Alike 3.0 Unported Creative Commons License (<http://creativecommons.org/licenses/by-nc-sa/3.0>). "ASCB"™, "The American Society for Cell Biology"™, and "Molecular Biology of the Cell"™ are registered trademarks of The American Society of Cell Biology.

assemble *in vivo* in locations where cells experience mechanical stress (Wong *et al.*, 1983; Byers *et al.*, 1984). Mechanical force can also influence the conductivity of stretch-gated ion channels to directly influence signaling cascades via alterations in membrane potential or intracellular calcium levels (Sukharev and Corey, 2004).

Stretch-induced signaling is also promoted in demembrated cells, illustrating the potential for non-membrane-bound effectors to contribute to the force response (Sawada and Sheetz, 2002). For example, tyrosine phosphorylation of the integrin effector p130Cas is stimulated upon direct mechanical extension of isolated cytoskeletons (Tamada *et al.*, 2004). Tyrosine phosphorylation of p130Cas creates a docking site for the SH2-adaptor CRK, which in turn recruits a Rap1-guanine nucleotide exchange factor, C3G, to activate the Rap1 GTPase and mitogen-activated protein kinase (MAPK) signaling (Sawada *et al.*, 2001, 2006; Chodniewicz and Klemke, 2004; Defilippi *et al.*, 2006). Similarly, stretching of the integrin-binding protein talin activates its capacity to bind vinculin (del Rio *et al.*, 2009). Examples such as these provide evidence for one mechanism by which application of physical force might be converted into novel chemical information by inducing exposure of a phosphorylation site or new protein interaction site.

Several recent studies have highlighted the mechanosensitive features of the cytoskeletal protein zyxin. Zyxin is a FA constituent that mobilizes to actin SFs in cells exposed to mechanical stress (Yoshigi *et al.*, 2005). A retrograde flux of zyxin along FA-anchored actin filaments is promoted by high substratum rigidity (Guo and Wang, 2007), and live-cell imaging revealed a positive correlation between SF tension and zyxin accumulation (Colombelli *et al.*, 2009). Zyxin's retention at FAs is also sensitive to mechanical signals. Conditions that reduce the forces impinging on a FA, such as chemical inhibition of cellular contractility or laser severing of a FA-associated SF, increases the k_{OFF} of zyxin at the FA, leading to a reduced concentration of zyxin at cell-substratum adhesion sites (Lele *et al.*, 2006).

The influence of physical stress on zyxin's subcellular distribution has functional consequences for local actin remodeling. Zyxin facilitates force-induced actin polymerization at FAs (Hirata *et al.*, 2008), and zyxin contributes to actin polymerization at force-bearing cell-cell junctions (Nguyen *et al.*, 2010). Exposure of cells to either uniaxial cyclic stretch or shear stress results in dramatic reorientation and reinforcement of the actin cytoskeleton. Zyxin-null cells reorient their actin SFs in response to uniaxial cyclic stretch but fail to thicken or reinforce them normally, illustrating zyxin-independent and zyxin-dependent facets of the stretch response (Yoshigi *et al.*, 2005). The SF reinforcement response is postulated to facilitate the cell's ability to withstand the physical stress associated with a cell-stretching regimen (Yoshigi *et al.*, 2005), and, indeed, cells that lack zyxin display higher-frequency breakage of their actin SFs (Smith *et al.*, 2010).

Here we investigate the mechanism by which cells reinforce their actin SFs when exposed to mechanical stimulation. We demonstrate that stretch-induced SF reinforcement occurs independent of new transcription or translation, leading us to focus on posttranslational response mechanisms. We show that zyxin is phosphorylated in response to uniaxial cyclic stretch and that this response is independent of p130Cas, an integrin effector and zyxin-binding partner that is also posttranslationally modified in response to mechanical stress. We provide evidence that stretch-stimulated zyxin phosphorylation depends on activation of MAPK pathways and identify nonoverlapping domains in zyxin that are responsible for its force-sensitive targeting to actin SFs and recruitment of the actin-remodeling machinery. Binding of both α -actinin and Ena/VASP proteins to zyxin is

essential for robust actin reinforcement downstream of physical stimulation. Zyxin's ability to influence SF maintenance and reinforcement is retained in the presence of Rho kinase inhibitors, further highlighting the novelty of this actin-remodeling pathway.

RESULTS

Uniaxial cyclic stretch triggers mobilization of a subset of FA constituents to SFs and induces actin reinforcement independent of transcription and translation

Integrin-rich FAs provide a transmembrane molecular link between the extracellular matrix and the actin cytoskeleton. Thus they serve as conduits for bidirectional communication of mechanical stress between the interior and exterior of cells. *In vivo*, normal tidal breathing induces 10% distension in the lung, and *in vitro* a similar magnitude stretch of lung cells is sufficient to induce cytoskeletal reorganization (Geiger *et al.*, 2006; Eldib and Dean, 2011). Similarly, *in vivo* vasculature changes of 2–15% have been reported (Dobrin, 1978). By culturing fibroblasts on a pliable silicone membrane, it is possible to subject cells to uniaxial cyclic stretch of defined frequency and amplitude and induce cellular responses (Yoshigi *et al.*, 2003, 2005; Jungbauer *et al.*, 2008; Faust *et al.*, 2011). On exposure to cyclic stretch (15%, 0.5 Hz), the FA proteins zyxin (Figure 1, A and B) and Mena/VASP (Figure 1, C and D) show diminished localization at sites of substratum adhesion and accumulate on actin SFs. Many other FA constituents, including vinculin, talin, and FAK, are retained at FAs for the duration of the mechanical stimulation (unpublished data). Staining of cells with anti-phosphotyrosine antibody confirms the integrity of FAs after cyclic stretch (Figure 1, E and F) and also illustrates that integrin-dependent signaling to tyrosine kinases resident at FAs is retained, and possibly even enhanced, in stretched cells. The anti-phosphotyrosine labeling of stretched cells also reveals that whereas a subset of proteins, including zyxin and Mena/VASP, accumulate on SFs in mechanically stimulated cells, other FA constituents, including those that are tyrosine phosphorylated, remain concentrated at FAs (Figure 1F). The elongated FA distribution of tyrosine-phosphorylated proteins in stretched cells is reminiscent of the retrograde flux of focal adhesion kinase that occurs when cells are grown on a stiff substrate (Guo and Wang, 2007).

Coincident with the accumulation of zyxin and Mena/VASP proteins on the actin SFs, the SFs are reoriented perpendicular to the stretch vector and show measurable thickening, as evidenced by visual inspection (Figure 1, G and H). Stretch-induced SF reinforcement is abrogated in cells isolated from mice that harbor a targeted disruption of the gene encoding zyxin (Figure 1, I and J; Hoffman *et al.*, 2003; Yoshigi *et al.*, 2005). Calculation of the stress fiber thickness index (SFTI; Yoshigi *et al.*, 2005) provides quantitative evidence that, although detectable SF thickening occurs in stretched cells that lack zyxin, zyxin is clearly required for robust SF reinforcement downstream of uniaxial cyclic stretch (Figure 1K).

The striking labeling of SFs with anti-zyxin antibodies that is observed in cells exposed to uniaxial cyclic stretch raised the possibility that mechanical stimulation might promote expression of zyxin; however, we did not detect an increase in zyxin by Western immunoblot analysis. It should also be noted that green fluorescent protein (GFP)-zyxin can be directly observed to accumulate on SFs of cells exposed to cyclic stretch. Thus we are observing bulk movement of zyxin onto the SF compartment and not simply enhanced epitope availability and antibody accessibility. Moreover, the ability of cells to reinforce the actin cytoskeleton in response to mechanical stimulation is not abrogated by gene transcription or protein translation inhibitors (actinomycin D and cycloheximide, respectively;

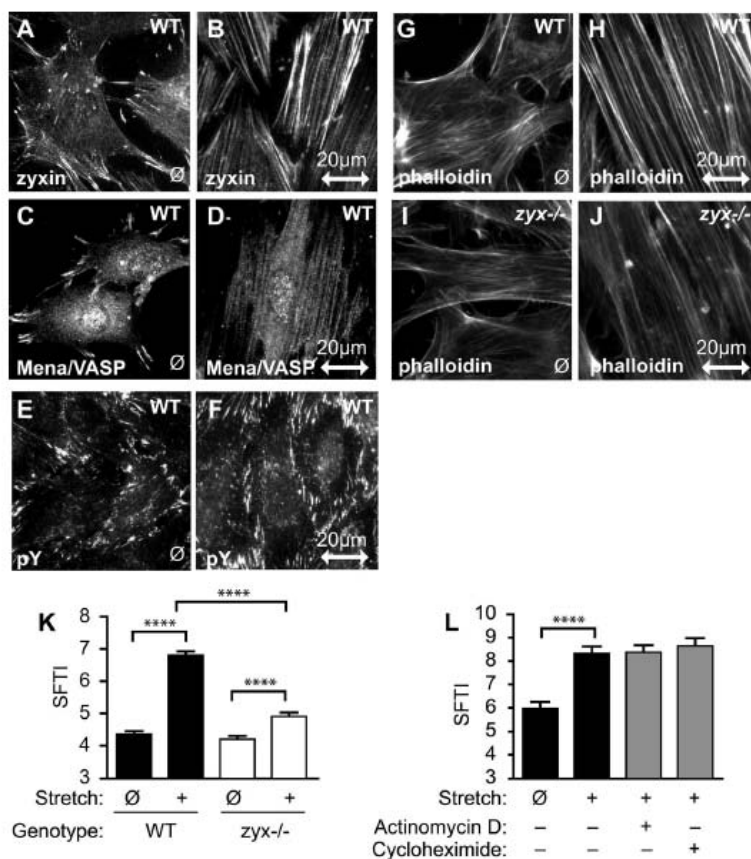


FIGURE 1: Uniaxial cyclic stretch induces changes in focal adhesion constituents and actin cytoskeletal reinforcement. Wild-type (WT) fibroblasts on unstretched membranes (\emptyset) or after uniaxial cyclic stretch (2 h, 15%, 0.5 Hz), were fixed and immunostained for zyxin (A, B), Mena/VASP (C, D), and phosphotyrosine (E, F). The direction of stretch is shown in the horizontal plane, designated by a double-headed arrow scaled to 20 μ m. Uniaxial cyclic stretch of WT (G, H) and zyxin-null (I, J) fibroblasts followed by phalloidin staining indicated abrogated actin thickening response in the absence of zyxin. (K) SFTI analysis of phalloidin-stained WT (black bars) and zyxin^{-/-} (white bars) fibroblasts, unstretched (\emptyset) and after 1 h of uniaxial cyclic stretch (+). (L) SFTI analysis of WT fibroblasts stretched in the presence of actinomycin D or cycloheximide (gray bars). **** $p < 0.0001$, $n > 100$ SFTI measurements.

Figure 1L). These results illustrate that posttranslational mechanisms are sufficient to promote the cytoskeletal changes that occur in response to mechanical stress.

Posttranslational signaling in response to uniaxial cyclic stretch

Phosphorylation is a common posttranslational modification downstream of transmembrane signaling. Because zyxin is required for the mechanical stress response and is phosphorylated *in vivo* (Beckerle, 1986; Crawford and Beckerle, 1991; Hery et al., 2010), we explored whether zyxin is phosphorylated in response to mechanical stress. Phosphorylation of zyxin affects its electrophoretic mobility (Hery et al., 2010). Therefore we used Western immunoblot analysis to explore whether uniaxial cyclic stretch is associated with altered mobility of zyxin by SDS-PAGE. As can be seen in Figure 2A (compare

lanes 1 and 2), slower-mobility zyxin isoforms displayed enhanced prominence in lysates derived from stretched cells, suggesting that stretch induced a posttranslational modification such as phosphorylation that might account for the altered electrophoretic mobility of zyxin. Incubation of lysates with phosphatase before electrophoresis results in reduced prominence of the slower-mobility isoform (Figure 2A, lanes 3 and 4), consistent with the view that stretch induces phosphorylation of zyxin. Western immunoblot analysis with antibodies specific for a phospho-zyxin isoform reveals a baseline of zyxin phosphorylation in unstretched cells with enhancement of phospho-zyxin, and the appearance of a slower-mobility phospho isoform, upon stretch (Figure 2B). Quantitative analysis reveals a 2.6-fold enhancement of phosphorylated zyxin detected by Western immunoblot (Figure 2B), whereas the total amount of zyxin remains constant during the stretch response. Immunocytochemistry illustrates the presence of phospho-zyxin at both FAs of unstretched cells (Figure 2C) and enhanced at SFs of cells exposed to uniaxial cyclic stretch (Figure 2D).

The integrin effector p130Cas is not essential for stretch-stimulated actin SF reinforcement or zyxin phosphorylation

The ability of cells to realign and reinforce actin SFs in response to uniaxial cyclic stretch was previously shown to depend on integrin-mediated adhesion (Yoshigi et al., 2005). The integrin effector p130Cas is conformationally modulated by mechanical stress and is recovered in complex with zyxin via native immunoprecipitation (Yi et al., 2002). These observations raised the possibility that p130Cas might be upstream of zyxin in the mechanical stress response pathway. If that were the case, stretch-induced actin reinforcement would be blunted in cells that lack p130Cas. To test this hypothesis,

we used cells that harbor a targeted deletion of the gene encoding p130Cas (Honda et al., 1998) and lack detectable p130Cas by Western immunoblot analysis (Figure 3A). We evaluated the capacity of these cells to mount a response to uniaxial cyclic stretch. Cells that lack p130Cas display a somewhat compromised resting SF organization, with accumulations of filamentous actin at cell borders (Figure 3B; Honda et al., 1998). Nevertheless, when stimulated by exposure to uniaxial cyclic stretch, the p130Cas^{-/-} cells realign their actin cytoskeletal arrays perpendicular to the stretch vector (Figure 3C) and reinforce their SFs (Figure 3D), illustrating that they retain the capacity to sense and respond to mechanical signals. Consistent with our demonstration that stretch-induced SF reinforcement is dependent on zyxin and independent of p130Cas, zyxin retains the ability to localize at FAs (Figure 3E) and mobilizes to SFs in response to mechanical stress (Figure 3F) in cells devoid of p130Cas. Moreover,

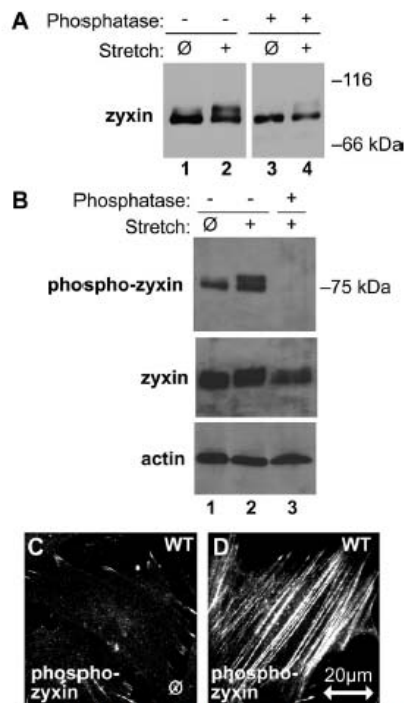


FIGURE 2: Posttranslational modification of zyxin in response to stretch. (A) Immunoblot analysis of zyxin from unstretched (ø) and stretched (+) WT fibroblasts (lanes 1 and 2) identified a stretch-induced shift of zyxin, which was reversed after incubation with phosphatase (lanes 3 and 4). (B) Immunoblot analysis with a phosphospecific zyxin antibody on unstretched (ø) and stretched (+) cell lysates (lanes 1 and 2) and elimination of the phospho-zyxin signal by incubation with phosphatase (lane 3). Immunoblots for total zyxin and β -actin show that their signals are retained following phosphatase treatment. (C, D) Indirect immunofluorescence microscopy on unstretched (ø) and stretched (+) fibroblasts with phospho-zyxin antibody. Phospho-zyxin signal is low at focal adhesions of unstretched cells, but it increases and appears along stress fibers in stretched cells. Stretch direction is in the horizontal plane (double-headed arrow; scale, 20 μ m).

the electrophoretic mobility shift between unstretched and stretched p130Cas^{-/-} cell lysates (Figure 3G), indicates that the stretch-activated signaling cascades required for phosphorylation of zyxin do not depend on p130Cas.

Stretch activation of p130Cas stimulates the GTPase Rap1, promoting the activation of MAPK signaling (Sawada *et al.*, 2001). Although p130Cas clearly contributes to Rap1 activation downstream of mechanical stress, p130Cas-independent stretch activation of Rap1 has also been observed (Sawada *et al.*, 2006). Therefore, even though p130Cas is not required for stretch-induced zyxin phosphorylation or SF realignment and reinforcement, it remained possible that zyxin phosphorylation depends on MAPK activation. Consistent with this possibility, zyxin displays multiple phosphorylation sites with sequences characteristic of MAPK consensus sites (Hervy *et al.*, 2010). Cyclic stretch activates MAPK pathways in endothelial (Kito *et al.*, 2000) and epithelial cells (Cohen *et al.*, 2010), and we find that extracellular signal-regulated kinase (ERK) activation is evident in fibroblasts exposed to uniaxial cyclic stretch

(Figure 3H). We next examined the impact of ERK activation inhibitor PD98059 on stretch-activated zyxin phosphorylation. As can be seen in Figure 3H, inhibition of ERK signaling abrogates the appearance of the activated phospho-ERK and also inhibits the zyxin phosphorylation detected by phospho-zyxin antibody. Temporal analysis of ERK and zyxin phosphorylation during the stretch response reveals that peak zyxin phosphorylation lags ERK activation (Figure 3I). Both the pharmacological inhibition studies and the phosphorylation kinetics are consistent with the conclusion that zyxin phosphorylation is directly or indirectly dependent on ERK activation.

Mapping the SF reinforcement response by molecular dissection of zyxin

Zyxin comprises 564 amino acids and is characterized by the presence of three C-terminal LIM domains, double zinc finger modules that support protein-protein interaction (Perez-Alvarado *et al.*, 1994; Schmeichel and Beckerle, 1994). Murine zyxin exhibits two nuclear export signals at residues 144–156 and 343–359 (Nix and Beckerle, 1997; Renfranz *et al.*, 2003). To define how zyxin contributes to reinforcement of SFs downstream of uniaxial cyclic stretch, we mapped the regions of zyxin that are necessary and sufficient for targeting of the protein to FAs, for recruitment to SFs in mechanically stimulated cells, and for reinforcement of the actin SFs in response to uniaxial cyclic cell stretch. We reconstituted zyxin^{-/-} mouse embryo fibroblasts with enhanced GFP (eGFP)-tagged wild-type zyxin (zyxin¹⁻⁵⁶⁴) or deletion variants (Table 1), creating a condition in which the only zyxin protein within the cells is the engineered construct, thus reducing competition or synergy that might occur if native protein were present. Because MEFs display a low DNA transfection efficiency, we used a lentiviral infection/expression system and selected cells with comparable eGFP expression by fluorescence-activated cell sorting (FACS). Western immunoblot analysis was used to verify that the proteins migrated as expected on SDS-PAGE (Figure 4A) and retained both zyxin and GFP epitopes.

We first mapped the regions of zyxin that are necessary and sufficient for FA targeting by analyzing unstretched cells. Direct fluorescence imaging of the subcellular distribution of the eGFP-tagged zyxin variants revealed that only variants containing residues 373–564 retained the capacity to target to focal adhesions (Figure 4, B, C, F, and G). The zyxin variants zyx¹⁻¹³⁸ and zyx¹⁻³⁷² (lacking LIM domains) did not exhibit significant focal adhesion accumulation (Figure 4, D and H). Although focal adhesions were clearly detectable by vinculin staining, zyxin variants zyx¹⁻¹³⁸ and zyx¹⁻³⁷² failed to accumulate at those focal adhesions (Supplemental Figure S1). As reported by others (Seibel *et al.*, 2007), eGFP alone accumulates in the nucleus (Figure 4I). Consistent with previous studies that identified two potent nuclear export sequences (NESs) in zyxin (Nix and Beckerle, 1997; Renfranz *et al.*, 2003), exclusion of the NESs results in nuclear accumulation of the zyxin variant (Figure 4, D and E). Inclusion of the zyx³⁷³⁻⁵⁶⁴ FA targeting sequence is sufficient to partially overcome the eGFP-driven nuclear localization and enable FA localization (compare Figure 4, G and I). Retention of a single NES, as in zyx³⁰⁹⁻⁵⁶⁴, eliminates the nuclear accumulation and reveals even more robust FA targeting (Figure 4F).

To identify the region(s) of zyxin that are critical for targeting of the protein to SFs in response to mechanical stimulation, we cultured the cells on elastic membranes and subjected them to uniaxial cyclic stretch before fixation and imaging (Figure 4, J–Q). Similar to what was observed for FA targeting, zyx³⁷³⁻⁵⁶⁴ harbors the sequence determinants that are necessary and sufficient for SF targeting in response to uniaxial cyclic stretch (Figure 4O). SF accumulation was not observed for constructs lacking the LIM region, such as the zyx¹⁻¹³⁸ and

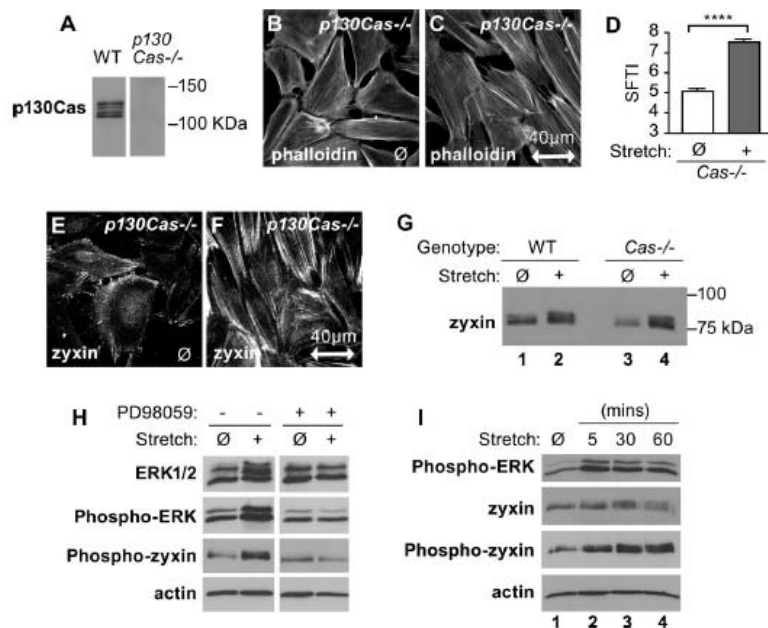


FIGURE 3: Zyxin responds independent of signaling molecule p130Cas. (A) Western immunoblot for p130Cas in WT and Cas-null fibroblasts. (B, C) Fibroblasts from p130Cas^{-/-} mice were stained for F-actin (phalloidin) on unstretched (ø) membranes or after uniaxial cyclic stretch (1 h, 15%, 0.5 Hz). Stretch direction is in the horizontal plane (double-headed arrow; scale, 40 µm). (D) SFTI analysis of the stretch-induced actin thickening in Cas^{-/-} cells, ****p < 0.0001. (E, F) Immunofluorescence microscopy of zyxin in fibroblasts from p130Cas^{-/-} mice on unstretched (ø) and stretched membranes. (G) Immunoblot analysis of zyxin in cell lysates from unstretched (ø) and stretched (+) membranes (WT, lanes 1 and 2; Cas^{-/-}, lanes 3 and 4) showed the stretch-induced zyxin shift seen in WT cells persists in p130Cas^{-/-} cells. (H) Fibroblasts on unstretched (ø) membranes or after uniaxial cyclic stretch (5 min, 15%, 0.5 Hz) with dimethyl sulfoxide control or with ERK activation inhibitor PD98059 (100 µM) were immunoblotted for total ERK1/2 (p44/p42), P-ERK, P-zyxin, and β-actin. (I) WT fibroblasts unstretched (ø) and stretched for 5, 30, and 60 min, electrophoresed, and immunoblotted for P-ERK, total zyxin, P-zyxin, and β-actin indicate maximal ERK phosphorylation at 5 min, followed by zyxin phosphorylation.

zyx¹⁻³⁷² variants (Figure 4, L and P). To ensure that the defect in SF targeting was not due to a complete lack of SFs in those cells, counterstaining with phalloidin was performed (Supplemental Figure S2).

variants provides evidence that the primary SF targeting and SF reinforcement activities of zyxin are contained in nonoverlapping areas of zyxin's primary sequence, identifying physically separable SF

Although SFs were detectable in cells with the zyxin variants zyx¹⁻¹³⁸ and zyx¹⁻³⁷², these constructs lacking the LIM domains did not accumulate on the SFs. This domain analysis provides evidence that the C-terminal LIM domains localize zyxin to FA in unstretched conditions and target zyxin to actin SFs after uniaxial cyclic stretch.

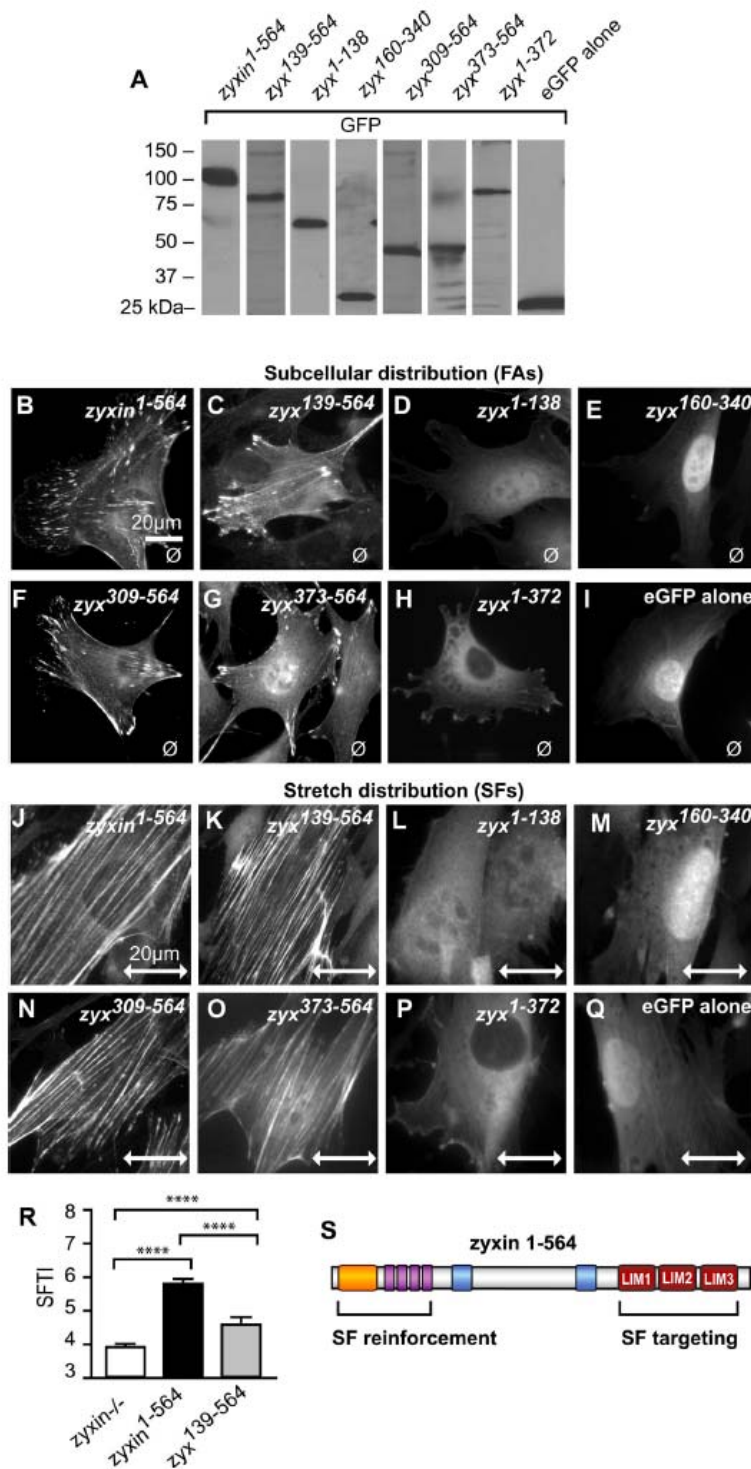
To map the region(s) of zyxin responsible for the stretch-induced SF reinforcement response, we introduced full-length zyxin or deletion variants (Table 1) into zyx^{-/-} cells, imaged filamentous actin in cells exposed to uniaxial cyclic stretch, and used our SF thickness algorithm to provide a quantitative assessment of SF reinforcement. In comparison with cells expressing full-length zyxin¹⁻⁵⁶⁴, cells expressing a zyxin deletion variant lacking the N-terminal 138 amino acids, zyx¹³⁹⁻⁵⁶⁴, display a statistically significant reduction in the SF reinforcement response (Figure 4R), suggesting that zyx¹⁻¹³⁸ contains critical information necessary for actin remodeling downstream of mechanical stimulation. We tested directly the ability of zyx¹⁻¹³⁸ to rescue the actin reinforcement response in zyx^{-/-} cells and found that it was incapable of doing so (Table 1), displaying an SFTI after stretch that was statistically indistinguishable from that observed in zyx^{-/-} cells (unpublished data). The failure of zyx¹⁻¹³⁸ to localize effectively at FAs or to SFs in stretched cells (Figure 4, D and L) is likely responsible for its lack of SF reinforcement activity. In comparison with cells lacking zyxin or reconstituted with zyx¹⁻¹³⁸, zyxin constructs harboring the C-terminal LIM domains retain some residual SF reinforcement function (Table 1), although clearly reduced relative to full-length protein.

This functional analysis of zyxin deletion

Constructs	FA	Stretch-induced SF accumulation	Stretch-induced SF thickening
zyxin ¹⁻⁵⁶⁴	+++	+++	+++
zyx ¹³⁹⁻⁵⁶⁴	+++	+++	+
zyx ¹⁻¹³⁸	+	-	-
zyx ¹⁶⁰⁻³⁴⁰	-	-	-
zyx ³⁰⁹⁻⁵⁶⁴	+++	+++	+
zyx ³⁷³⁻⁵⁶⁴	+++	+++	+
zyx ¹⁻³⁷²	+	-	-

+++ , Majority of signal/cell (comparable to wild-type zyxin); + , detectable signal/cell (minor compared with wild-type zyxin); - , not detectable as real localization.

TABLE 1: Zyxin domain analysis.



targeting and reinforcement domains that display unique structural features (Figure 4S). The C-terminal 192 amino acids, residues 373–564, a region comprising three tandemly arrayed LIM domains, is sufficient to target zyxin to SFs in stretched cells. The major sequences associated with zyxin's ability to contribute to stretch-induced SF reinforcement are found in the N-terminal 138 amino acids; however, since these sequences lack the subcellular targeting information, they are ineffective in promoting SF reinforcement. Two protein groups implicated in actin organization and dynamics— α -actinin and members of the Ena/VASP family—have been reported to associate with *zyx*¹⁻¹³⁸ (Golsteyn et al., 1997; Niebuhr et al., 1997; Reinhard et al., 1999; Drees et al., 2000; Li and Trueb, 2001). Therefore we investigated the importance of zyxin's ability to dock each of these proteins for an effective SF reinforcement response.

Deletion of zyxin's α -actinin-binding site compromises, but does not eliminate, the stress fiber reinforcement response

To define the mechanism by which zyxin residues 1–138 contribute to SF reinforcement, we first examined the importance of

FIGURE 4: Zyxin mechanosensitivity-domain resides in the C-terminal LIM domains. (A) Western immunoblot analysis of zyxin domain-GFP fusion proteins to confirm expression and relative mobility of proteins. (B–I) Subcellular distribution of GFP by fluorescence microscopy of *zyxin*¹⁻⁵⁶⁴ (B), *zyx*¹³⁹⁻⁵⁶⁴ (C), *zyx*¹⁻¹³⁸ (D), *zyx*¹⁶⁰⁻³⁴⁰ (E), *zyx*³⁰⁹⁻⁵⁶⁴ (F), *zyx*³⁷³⁻⁵⁶⁴ (G), *zyx*¹⁻³⁷² (H), and eGFP alone (I). (J–Q) After stretch stimulation (uniaxial, 15%, 0.5 Hz, 1 h), the GFP signals of *zyxin*¹⁻⁵⁶⁴ (J), *zyx*¹³⁹⁻⁵⁶⁴ (K), *zyx*³⁰⁹⁻⁵⁶⁴ (N), and *zyx*³⁷³⁻⁵⁶⁴ (O) were detected along actin stress fibers, whereas the other constructs—*zyx*¹⁻¹³⁸ (L), *zyx*¹⁶⁰⁻³⁴⁰ (M), *zyx*¹⁻³⁷² (P), and eGFP alone (Q)—were not detected on stress fibers. Stretch direction is in the horizontal plane (double-headed arrow; scale, 20 μ m). (R) Stretch-stimulated zyxin-null cells and cells expressing the *zyxin*¹⁻⁵⁶⁴ and *zyx*¹³⁹⁻⁵⁶⁴ variants were stained by phalloidin, and the SF thickening was measured. *Zyx*¹³⁹⁻⁵⁶⁴ lacking the N-terminus is insufficient for normal stress fiber thickening, although it is able to target to stress fibers; **** $p < 0.0001$. (S) Diagram of the stress fiber-targeting C-terminal LIM domains (red boxes) and the N-terminal SF reinforcement region of zyxin with α -actinin binding (yellow), Ena/VASP binding (purple), and the nuclear export sequences (blue).

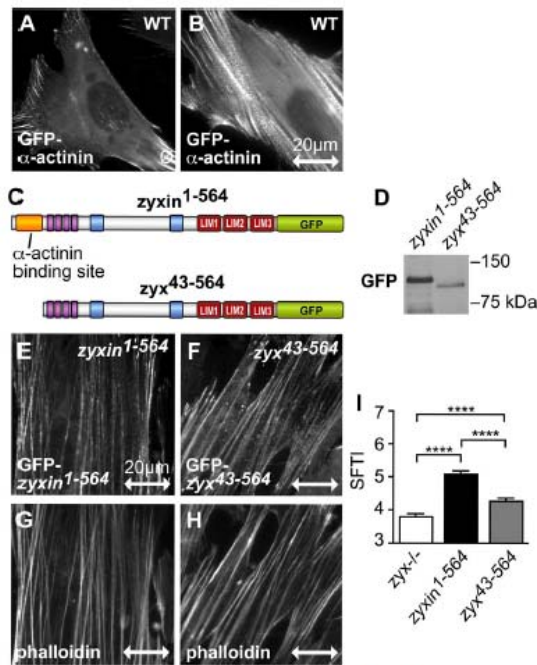


FIGURE 5: Zyxin and α -actinin respond to stretch independently, but together they contribute to actin thickening. (A, B) Fluorescence microscopy of GFP- α -actinin in WT fibroblasts on unstretched (a) and stretched membranes (uniaxial cyclic stretch, 15%, 0.5 Hz, 2 h; double-headed arrow; 20- μ m scale). (C) GFP-tagged full-length mouse zyxin (1–564) with the α -actinin interaction site (yellow box) and the N-terminal deletion mutant zyxin (43–564) missing the α -actinin interaction site. (D) Western immunoblot analysis of both zyxin constructs expressed in zyxin-null fibroblasts. (E, F) Subcellular distribution of zyxin¹⁻⁵⁶⁴ and the N-terminal mutant zyxin⁴³⁻⁵⁶⁴ along stretch-induced actin SF, coincident with phalloidin signal (G, H). (I) SFTI analysis of stretch-stimulated actin in zyxin-null cells (white bar) compared with cells expressing comparable levels of zyxin¹⁻⁵⁶⁴ (black bar) and zyxin⁴³⁻⁵⁶⁴ (gray bar). Stretch direction is in the horizontal plane (double-headed arrow; scale, 20 μ m); *****p* < 0.0001.

zyxin's α -actinin-binding capacity. The actin cross-linking protein α -actinin is prominently associated with SFs and has many binding partners (Otey and Carpen, 2004; Naumanen et al., 2008). Like zyxin, α -actinin is present at FAs of unstretched cells (Figure 5A; Pavalko et al., 1995) and accumulates on central SFs when cells are exposed to uniaxial cyclic stretch (Figure 5B). Zyxin's ability to dock α -actinin has been mapped to amino acids 1–42 (Drees et al., 1999; Reinhard et al., 1999; Li and Trueb, 2001). To probe the importance of this aspect of zyxin function for the SF reinforcement response, we expressed zyxin⁴³⁻⁵⁶⁴ in zyxin^{-/-} cells and compared this to null cells reconstituted with full-length zyxin (Figure 5, C and D). Like full-length zyxin, zyxin⁴³⁻⁵⁶⁴ accumulates on SFs in cells challenged by exposure to uniaxial cyclic stretch (Figure 5, E and F), consistent with our finding that the C-terminal LIM region of zyxin harbors the primary SF targeting information. Analysis of the SF reinforcement response revealed that deletion of zyxin's α -actinin-binding domain compromises, but does not completely abrogate, the stretch response (Figure 5, G–I).

The ability of zyxin to recruit Ena/VASP family members is crucial for cytoskeletal stability

Members of the Ena/VASP family include Mena, VASP, and EVL, all three of which are expressed in mammalian fibroblasts (Krause et al., 2003). Ena/VASP proteins are characterized by the presence of conserved EVH1 domains (Renfranz and Beckerle, 2002) that bind to ActA repeats—proline-rich sequences present in the *Listeria* cell surface protein ActA (Purich and Southwick, 1997). Zyxin⁷¹⁻¹²¹ contains four ActA repeats, each of which has the capacity to dock Ena/VASP (Golsteyn et al., 1997; Niebuhr et al., 1997; Drees et al., 2000).

An absolutely conserved phenylalanine residue present in all ActA repeats is critical to support docking of Ena/VASP proteins (Drees et al., 2000; Machner et al., 2001). Therefore, to abolish the ability of zyxin to interact with members of the Ena/VASP family while minimizing non-specific consequences that might arise with larger deletions, we mutated the individual phenylalanines (F) in each of zyxin's ActA repeats to alanine (A) to generate what we refer to as the zyxin^{F71,93,105,115A} mutant (Figure 6A). GFP-tagged wild-type zyxin or mutant zyxin^{F71,93,105,115A} was expressed in zyxin^{-/-} fibroblasts and FACS sorted for equivalent GFP expression. Western immunoblot analysis confirmed the lack of endogenous zyxin protein and the effective expression of the transgenic variants (Figure 6B). Both wild-type zyxin and zyxin^{F71,93,105,115A} localize to FAs (Figure 6, C and E); however, zyxin^{F71,93,105,115A} fails to support docking of VASP at FAs (compare Figure 6, F with D). After stretch stimulation, wild-type zyxin accumulates on SFs (Figure 6G) and recruits VASP to SFs (Figure 6H). Mutant zyxin^{F71,93,105,115A} also accumulates on SFs in stretch-challenged cells (Figure 6I) but fails to recruit VASP (Figure 6J), illustrating that VASP depends on zyxin for its appropriate targeting to both FAs and stretch-stimulated SFs.

Quantitative analysis of cells exposed to uniaxial cyclic stretch revealed that the ability of zyxin to dock Ena/VASP proteins contributes significantly to the SF reinforcement response (Figure 6, K–N). In particular, zyxin^{-/-} cells reconstituted with zyxin^{F71,93,105,115A} and subjected to cyclic stretch fail to reinforce actin SFs to the level achieved when wild-type zyxin is present (compare Figure 6, L and M, and Figure 6N). However, cells reconstituted with zyxin^{F71,93,105,115A} achieved a level of actin SF reinforcement that was superior to that observed in zyxin^{-/-} cells (Figure 6N), showing that factors in addition to zyxin's capacity to recruit Mena/VASP proteins contribute to the SF reinforcement response.

Failure of zyxin to bind Ena/VASP proteins enhances the rate of SF demise and accumulation of disorganized actin aggregates in response to jaspalkinolide

These results illustrate a role for zyxin-dependent recruitment of Ena/VASP proteins for maintenance and reinforcement of the actin cytoskeleton in the face of mechanical stress. Chemical probes provide an alternative mechanism for stressing the actin cytoskeleton in living cells and probing the functional significance of zyxin's ability to bind Ena/VASP proteins. The marine toxin jaspalkinolide reduces the critical concentration of monomeric actin required for actin assembly and increases the rate of actin nucleation in vivo (Bubb et al., 2000). Jaspalkinolide is also used to stabilize actin filaments in vivo (Lee et al., 1998; Cramer, 1999), and it may function as an inhibitor of actin depolymerization (Miyoshi et al., 2006). When applied to living cells, jaspalkinolide induces an initial thickening of SFs (Figure 7, A and B) that is associated with recruitment of zyxin to the SF compartment (Hoffman et al., 2006). Over time, there is an accumulation of disorganized filamentous actin aggregates throughout the cytoplasm (Figure 7C). The actin aggregates contain both zyxin (Figure 7, D and E) and VASP (Figure 7 F), an observation that led us to investigate

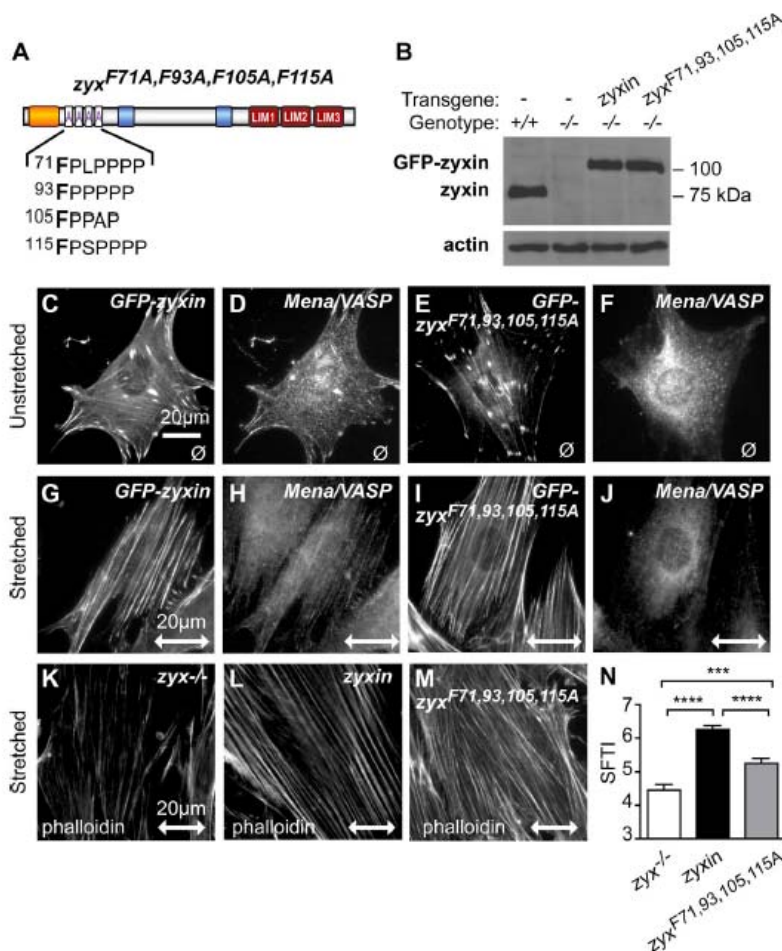


FIGURE 6: Stretch-induced actin cytoskeletal response is perturbed by disruption of zyxin-VASP interaction. (A) Diagram of mouse zyxin protein demarcates four ActA repeats for Mena/VASP interaction, targeted for site-directed mutagenesis of F71A, F93A, F105A, and F115A as zyx^{F71,93,105,115A} (purple letters). (B) Western immunoblot of zyxin from wild-type fibroblasts (+/+), zyxin-null fibroblasts (-/-), and zyxin-null fibroblasts programmed to express GFP-tagged wild-type zyxin and mutant zyx^{F71,93,105,115A}. Immunoblot for β -actin confirmed equivalent protein loading of the cell lysates. (C, D) GFP-zyxin and Mena/VASP proteins colocalized at focal adhesions. (E, F) GFP-zyx^{F71,93,105,115A} accumulated normally at focal adhesions but failed to recruit Mena/VASP. After stretch stimulation, zyxin (G) and Mena/VASP (H) accumulated along actin SF, as did zyx^{F71,93,105,115A} (I), but Mena/VASP remained mislocalized (J). Phalloidin-stained, stretch-stimulated stress fibers in zyxin-null cells (K) and cells expressing GFP-zyxin (L) and GFP-zyx^{F71,93,105,115A} (M) were analyzed for thickening. (N) SFTI analysis of zyx^{-/-} cells (white bar) and cells expressing comparable levels of zyxin (black bar) and zyx^{F71,93,105,115A} (gray bar). Stretch direction is in the horizontal plane (double-headed arrow; scale, 20 μ m); *** $p < 0.0001$.

the importance of the zyxin-VASP interaction for the cellular response to jasplakinolide.

The accumulation of actin aggregates in response to jasplakinolide treatment is both concentration and time dependent (Bubb *et al.*, 2000). Therefore we explored the kinetics of the jasplakinolide response in zyxin^{-/-} cells reconstituted with wild-type zyxin or zyx^{F71,93,105,115A}. Zyxin^{-/-} cells reconstituted with zyx^{F71,93,105,115A} display significant cytoskeletal breakdown and actin aggregate for-

mation in response to a 2-h exposure to jasplakinolide (Figure 7G) compared with cells reconstituted with wild-type zyxin, which retain many SFs under these conditions (Figure 7H).

The accumulation of actin aggregates in response to jasplakinolide has been suggested to result from the de novo polymerization of actin into amorphous masses, with the subsequent loss of SFs due to insufficient actin monomer for SF maintenance during normal remodeling and turnover (Bubb *et al.*, 2000). However, if this were the explanation, why would an inability of zyxin to bind Ena/VASP accelerate this process? We reasoned that an alternative explanation might be a failure of SF maintenance and/or repair processes when zyxin is unable to recruit Ena/VASP proteins. In that scenario, the actin aggregates might reflect the remnants of broken SFs that arise when SF maintenance is compromised. To explore this possibility directly, we imaged cells expressing GFP-tagged zyxin during exposure to jasplakinolide to determine the genesis of the actin and zyxin-rich aggregates (Figure 7I and Supplemental Video S1). From this analysis, it is evident that the amorphous aggregates of filamentous actin in the jasplakinolide-treated cells represent remnants of ruptured SFs, not newly assembled structures (Figure 7J). These results support the view that zyxin's ability to recruit Ena/VASP is important for the maintenance of SF architecture in response to both mechanical and pharmacological stress.

The zyxin-dependent actin remodeling response is independent of Rho kinase

SF assembly is triggered by activation of Rho kinase, which promotes phosphorylation and activation of myosin light chain to stimulate myosin-dependent contractility (Jaffe and Hall, 2005; Guilluy *et al.*, 2011a). We defined a zyxin, VASP, and α -actinin-dependent pathway of SF remodeling that results in SF thickening in response to uniaxial cyclic stretch. To test whether this pathway is regulated by Rho kinase, we first compared the effect of the Rho kinase inhibitor Y27632 on both zyxin^{-/-} cells and zyxin^{-/-} cells reconstituted with zyx^{F71,93,105,115A}. The eGFP-zyx^{F71,93,105,115A} cells were selected to express at levels similar to that of endogenous zyxin in wild-type cells, as seen in Figure 6B. SFs are present in untreated cells (Figure 8A), but exposure to 3 μ M Y27632 for 2 h results in loss of SFs from zyxin^{-/-} cells (Figure 8B). In contrast, although diminished compared with pretreatment, residual SFs are still present in Y27632-treated cells that express zyxin (Figure 8C). These results provide a preliminary indication that zyxin promotes SF assembly or maintenance by a mechanism that does not require Rho kinase activity.

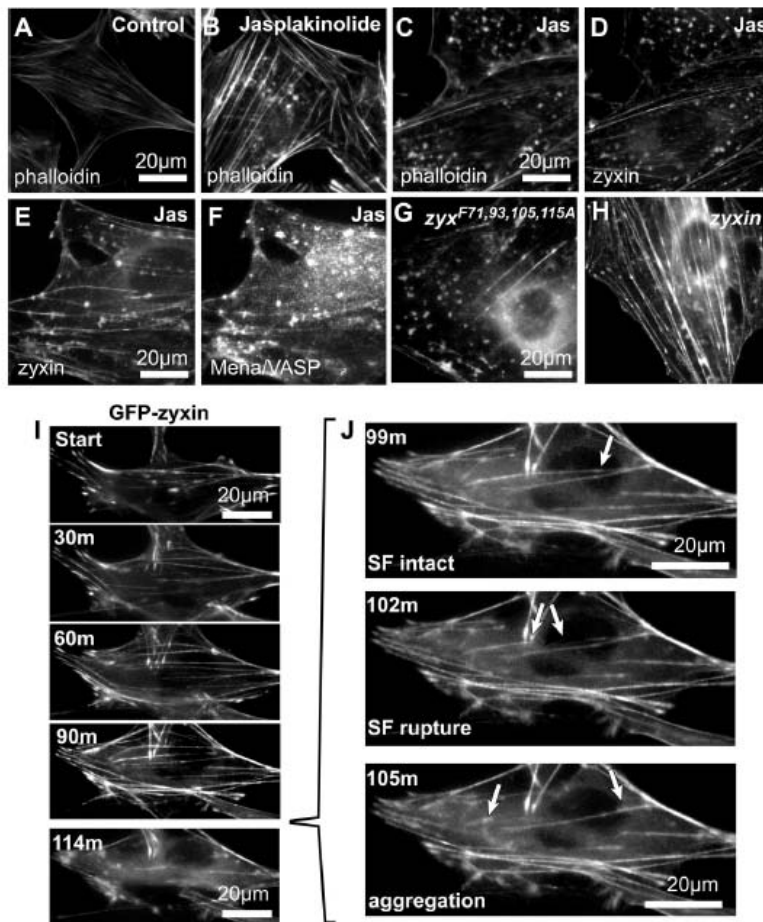


FIGURE 7: Actin stress fibers formed without VASP recruitment exhibit enhanced sensitivity to actin inhibitor jasplakinolide (Jas). (A, B) In comparison to controls, WT cells treated with jasplakinolide (100 nM, 2 h) accumulated stress fibers and aggregates of F-actin (phalloidin) visible by fluorescence microscopy. F-Actin (phalloidin); (C) and zyxin (D) colocalized within the jasplakinolide-induced aggregates. Zyxin (E) and binding partner Mena/VASP (F) also colocalized at the jasplakinolide-induced aggregates. Jasplakinolide treatment (100 nM, 2 h) of zyxin-null cells expressing either GFP-zyxin^{F71,93,105,115A} mutant (G) or GFP-zyxin (H) induced a more pronounced actin phenotype, with disruption of zyxin-Mena/VASP interaction (zyxin^{F71,93,105,115A}). (I) Time-lapse microscopy of GFP-zyxin in cells (0, 30, 60, 90, and 114 min after 200 nM jasplakinolide addition) showed mobilization from focal adhesions to actin stress fibers, followed by rupture of fiber and accumulation of aggregates (J, arrows; 99, 102, 105 min). See Supplemental Video S1.

To explore this possibility further, we tested whether inhibition of Rho kinase would influence the response of cells to uniaxial cyclic stretch (Figure 8, D–G). Unstretched cells exposed to Y27632 displayed diminished SFs relative to unstretched control cells (compare unstretched cells in Figure 8, D and E). However, cells exposed to Rho kinase inhibitor retained the capacity to launch a SF reinforcement response upon exposure to uniaxial cyclic stretch (Figure 8G). Cells treated with the Rho kinase inhibitor failed to realign their SFs perpendicular to the stretch vector (compare stretched cells in Figure 8, F and G), providing independent evidence that the Rho kinase inhibitor is interfering with the SF reorientation response while not fully eradicating the SF reinforcement response.

Zyxin displays several MAPK consensus phosphorylation sites (Hervy et al., 2010), consistent with the view that it may be a direct substrate of a MAPK.

Molecular dissection of the stretch-induced actin reinforcement response

By reconstitution of zyxin-null cells with a series of zyxin deletion variants, we defined critical functional domains of zyxin that are necessary and sufficient to support key steps in the stretch response. First, we discovered that the essential determinants of zyxin's stretch-induced actin reinforcement capacity map within the N-terminal 138 amino acids of the protein. Zyxin's N-terminus

DISCUSSION

Cells reorient and reinforce their actin cytoskeletons when exposed to mechanical force, establishing a robust interior framework composed of actin stress fibers. The LIM protein zyxin is mobilized from focal adhesions to actin stress fibers in response to mechanical stimulation, and it is required for the ensuing reinforcement of intracellular actin arrays. The results presented here refine our understanding of the pathways that lead from application of uniaxial cyclic stretch in fibroblasts and address the mechanism by which zyxin promotes SF remodeling and reinforcement.

Three mechanistically separable cellular response pathways downstream of mechanical stress can now be described (Figure 9):

1. SF reorientation. Cells align their SFs perpendicular to the stretch vector. SF reorientation is independent of zyxin and is inhibited by agents that block Rho kinase.
2. SF reinforcement. Thickening of the SFs requires zyxin. It depends on targeting of zyxin to SFs via the LIM domains and actin remodeling that involves the zyxin-binding partners α -actinin and VASP. Zyxin is phosphorylated in response to uniaxial cyclic stretch. Zyxin-dependent SF reinforcement can occur independent of Rho kinase activation.
3. p130Cas-dependent activation of MAPK signaling. p130Cas is tyrosine phosphorylated in response to mechanical stress, a modification that stimulates MAPK activation (Tamada et al., 2004; Sawada et al., 2006). Uniaxial cyclic stretch promotes both SF alignment and SF reinforcement in p130Cas^{-/-} cells, and thus there is not an obligatory link from p130Cas activation to these processes. p130Cas-independent activation of MAPK is likely responsible for stretch-induced phosphorylation of zyxin since MAPK inhibitors block this posttranslational modification and zyxin phosphorylation occurs normally in p130Cas^{-/-} cells.

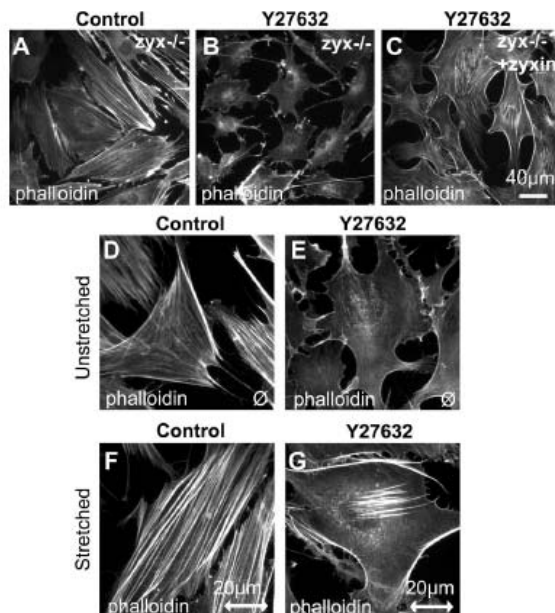


FIGURE 8: Stretch-induced actin remodeling persists in the presence of Rho kinase inhibition. *Zyx*^{-/-} cells untreated (A) or after 2 h of treatment with Y27632 (3 μ M; B) and cells expressing GFP-zyxin treated with 3 μ M Y27632 (C) were fixed and then visualized by phalloidin staining and fluorescence microscopy. Scale, 40 μ m. (D, F) WT control cells were unstretched (D) and stretch stimulated (F) for 1 h, followed by fixation, phalloidin staining, and fluorescence microscopy, and then compared with WT cells in the presence of Y27632 that were unstretched (E) and stretch stimulated (G) for 1 h. Stretch direction is in the horizontal plane (double-headed arrow; scale, 20 μ m).

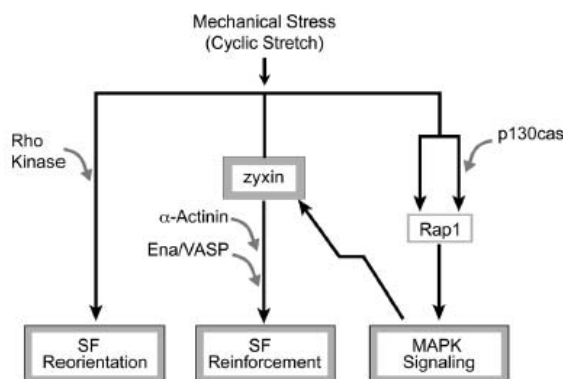


FIGURE 9: Model of mechanotransduction. Mechanical stress induces three separable responses: stress fiber reorientation, stress fiber reinforcement, and MAPK signaling. Our data support the notion that Rho kinase signaling contributes to SF reorientation, that zyxin, α -actinin, and Ena/VASP proteins contribute to SF reinforcement, and that p130Cas, Rap1, and MAPK signaling form the third response to mechanical stress applied by uniaxial cyclic stretch.

has been reported to bind a number of partners, including the actin filament cross-linker α -actinin (Drees et al., 1999; Reinhard et al., 1999; Li and Trueb, 2001), the actin assembly modulator Ena/VASP (Golsteyn et al., 1997; Niebuhr et al., 1997; Drees et al., 2000), and the cytoskeletal proteins LIM-nebulette and LASP-1 (Li et al., 2004; Grunewald et al., 2007). Because of their well-established roles in actin assembly and organization, we focused our analysis on the roles of α -actinin and Ena/VASP in the SF reinforcement response. Reconstitution of *zyxin*^{-/-} cells with constructs harboring the minimal deletion or amino acid substitution necessary to compromise *zyxin*'s ability to bind either α -actinin or Ena/VASP family members revealed that *zyxin* can be recruited to SFs in mechanically stimulated cells independent of binding to either of these partners. However, the loss of capacity to bind either α -actinin or Ena/VASP compromises the SF reinforcement response that occurs downstream of uniaxial cyclic stretch. These results illustrate the contributions of both of these binding partners to the *zyxin*-dependent actin reinforcement response. α -Actinin binding by *zyxin* could facilitate SF reinforcement by recruitment and cross-bridging of short actin filaments at sites of *zyxin* accumulation. Ena/VASP could promote actin polymerization at barbed filament ends. Alternatively, we showed previously that binding of Ena/VASP proteins to *zyxin* enhances the rate at which *zyxin* is recruited to sites of local SF damage (Smith et al., 2010). Phosphorylation promotes Ena/VASP binding by *zyxin* by inhibiting an intramolecular (head-tail) interaction within the *zyxin* protein (Moody et al., 2009; Call et al., 2011). Thus it is intriguing to consider the possibility that the MAPK-dependent phosphorylation of *zyxin* that occurs in response to uniaxial cyclic stretch might relieve an intramolecular *zyxin* interaction, simultaneously enhancing Ena/VASP binding and stabilizing a protein conformation in which the LIM region is accessible.

Distinct domains for SF targeting and remodeling

Although the core capacity of *zyxin* to promote SF reinforcement resides in the N-terminal 138 amino acids, this region of the protein on its own fails to localize to SFs in stretched cells and fails to support SF remodeling. This observation suggested that a physically separable region of *zyxin* might be responsible for targeting the protein to the SFs in mechanically stimulated cells. Here we determined that the LIM region of *zyxin* is both necessary and sufficient to promote SF localization in cells exposed to uniaxial cyclic stretch. The LIM region is also sufficient for accumulation of *zyxin* at FAs of unstretched cells (Nix et al., 2001) and migrating cells (Uemura et al., 2011). Although the LIM region of *zyxin* is capable of associating with FAs and SFs, it is not sufficient to restore the actin reinforcement response in *zyxin*-null cells exposed to mechanical stress. This observation is consistent with a report that *zyxin* LIM domains displace endogenous *zyxin* and disrupt actin polymerization at FAs (Hirata et al., 2008). Collectively, these findings support the view that *zyxin* harbors two structurally separable, discrete functional domains that contribute obligatorily to the stretch-induced actin reinforcement response: a localization or targeting domain and an actin-remodeling domain.

p130Cas is not required for stretch-induced actin reinforcement

The LIM region of *zyxin* that controls the protein's subcellular localization interacts directly with the integrin effector p130Cas (Yi et al., 2002), which has itself been shown to undergo conformational change in response to cyclic stretch (Sawada et al., 2006). *Zyxin* interacts with the same region of p130Cas that both is

modified by tyrosine phosphorylation and provides a docking site for the SH2-SH3 adaptor CRK under conditions of mechanical stimulation (Yi *et al.*, 2002; Tamada *et al.*, 2004). We were intrigued by the possibility that uniaxial cyclic stretch might simultaneously cause release of zyxin from p130Cas and enable the binding of CRK and activation of a Rap1-dependent signaling cascade to MAPK. However, in our experiments we found that both zyxin's recruitment to SFs and the actin reorientation/reinforcement that occur in response to uniaxial cyclic stretch are retained in p130Cas-null cells. Thus both zyxin and p130Cas display mechanosensitivity but appear to influence independent responses to mechanical stimulation (Figure 9).

Although p130Cas has been implicated in the stretch-induced activation of MAPK signaling, elimination of p130Cas by targeted gene disruption does not disturb zyxin's stretch-dependent phosphorylation. This is perhaps not surprising, given work showing that although knockdown of p130Cas leads to a 50% reduction in stretch-induced Rap1 activation, Rap1 activity is not completely eliminated in Cas-deficient cells exposed to cyclic stretch (Sawada *et al.*, 2006). Thus it appears that both p130Cas-dependent and -independent activation of Rap1 occurs in response to mechanical stimulation. The mechanisms by which various MAPKs influence the mechanotransduction response remain to be deciphered and will likely be complex. One recent hint regarding how MAPK signaling contributes to the response of cells to mechanical tension is the work of Guilluy *et al.* (2011b) that suggests a role for ERK activation of a particular Rho-directed guanine nucleotide exchange factor (Rho GEF-H1).

Cellular response to global or local mechanical stress

Here we show that exposure of cells to uniaxial cyclic stretch causes zyxin to accumulate on SFs, illustrating a pancellular, global mechanical stress response. Of interest, localized application of mechanical stress triggers local zyxin accumulation on individual SFs as well. For example, zyxin recruitment to a localized SF domain can be induced by targeted application of mechanical stress via direct prodding with a microprobe (Smith *et al.*, 2010) or by micromanipulation using atomic force microscopy (Colombelli *et al.*, 2009). In a complementary manner, if strain is relieved by release of an internal SF segment from its FA anchors by a pair of internal nanosurgical cuts, zyxin localization along the released SF fragment declines (Colombelli *et al.*, 2009). Thus, under a variety of conditions that exert either a positive or negative effect on zyxin accumulation on SFs, the application of force is a common factor that promotes zyxin localization. Consistent with this view, application of the nonmuscle myosin II inhibitor blebbistatin to reduce SF contractility causes release of zyxin from SFs in cultured cells (Colombelli *et al.*, 2009). It remains to be determined whether zyxin is accumulating at sites of high SF strain because it is directly detecting mechanical stress by recognizing a novel strain-induced protein conformation, for example, or whether the mechanical stress is inducing local SF damage, such as actin filament breaks, that are recruitment targets for zyxin and its partners.

SFs in cultured cells undergo strain-induced, local thinning and elongation (Smith *et al.*, 2010). Zyxin is rapidly recruited to these areas where SF integrity is compromised and is required for the restoration of SF structure via a mechanism that involves both α -actinin and VASP (Smith *et al.*, 2010). The response of cells to uniaxial cyclic stretch might reflect the accumulation of a large number of strain-induced local thinning and elongation events, which, in aggregate, would result in zyxin-coated SFs and actin remodeling and reinforcement, as we observed.

Zyxin contributes to Rho kinase-independent SF reinforcement

Activation of the small GTPase Rho stimulates SF assembly (Ridley and Hall, 1992). Rho-GTP interacts with Rho kinase, stimulating its activity and ultimately enhancing myosin-dependent contractility (Jaffe and Hall, 2005; Guilluy *et al.*, 2011a). Because zyxin promotes SF reinforcement, it was of interest to assess whether Rho kinase was an upstream modulator of the zyxin-dependent actin-remodeling response to cyclic stretch. Eliminating zyxin in concert with inhibiting Rho kinase activity results in a nearly complete loss of actin stress fibers in both stretched and unstretched cells. However, reconstitution of the cells with zyxin is sufficient to partially restore actin SFs, revealing a zyxin-dependent, Rho kinase-independent machinery that influences SF architecture. Treatment of cells with Rho kinase inhibitor abrogates the SF reorientation response downstream of uniaxial cyclic stretch, illustrating a critical role for Rho kinase-dependent actin-remodeling processes in the alignment of SFs within mechanically stimulated cells. Some new SFs are produced within stretched cells even under conditions of Rho kinase inhibition. Although the SFs are generally less abundant in cells in which Rho kinase is inhibited compared with controls, it is clear that some Rho kinase-independent mechanism contributes to SF reinforcement downstream of mechanical stress, and this likely involves zyxin. Consistent with our findings, previous studies revealed that Rho activation is required for SF reorientation in aortic endothelial cells exposed to cyclic stretch (Kaunas *et al.*, 2005; Lee *et al.*, 2010). Our work extends these studies and reveals that the zyxin/ α -actinin/VASP actin-remodeling machinery is a key contributor in a Rho kinase-independent pathway of SF reinforcement downstream of mechanical stress.

MATERIALS AND METHODS

Reagents

Mouse antibodies for vinculin hVIN-1, β -actin AC-74, and α -actinin BM75.2 (all Sigma-Aldrich, St. Louis, MO), rabbit anti-ERK1/2 and anti-phospho-ERK1/2 (4695 and 4370; Cell Signaling Technology, Beverly, MA), mouse anti-p130cas (BD Transduction Laboratories, Lexington, KY), and anti-pY 4G10 (Upstate, Millipore, Billerica, MA) were used as recommended by manufacturers. To generate the anti-Mena/VASP polyclonal rabbit serum B119, rabbits were immunized against KLH-coupled peptides GLAAAIAGAKLRKVKQK and EKPPKDESASQEESEARL (Harlan Bioproducts for Science, Indianapolis, IN). Anti-zyxin rabbit polyclonal serum B71 was previously described (Hoffman *et al.*, 2003). Phospho-zyxin (human Ser-142/143) rabbit antibody (4863; Cell Signaling Technology) detected mouse zyxin p-Ser144 (Western blots 1:2000, indirect immunofluorescence microscopy 1:200). Secondary antibodies and phalloidin were Alexa Fluor conjugates used for cell staining (Molecular Probes/Invitrogen, Carlsbad, CA) and horseradish peroxidase (HRP) conjugates used for Western blots (GE Healthcare, Piscataway, NJ). Actinomycin D and cycloheximide were from Sigma-Aldrich, jasplakinolide and Y27632 from Calbiochem (La Jolla, CA), and PD98059 from Cell Signaling Technology.

Cells and constructs

Wild type and zyxin-null fibroblasts (with or without expression constructs) were maintained in high-glucose DMEM supplemented with pyruvate, glutamine, penicillin/streptomycin (Invitrogen), and 10% fetal bovine serum (Hyclone Labs, Logan, UT) as described (Hoffman *et al.*, 2006). Wild-type and p130cas-null fibroblasts (Honda *et al.*, 1998) were cultured as recommended.

Mouse zyxin cDNA was used as template to PCR amplify domains with homologous ends for recombination cloning (Gateway Technology, Invitrogen). DNA sequencing of each entry clone confirmed the correct zyxin sequence before subcloning into a lentivirus expression system following manufacturer's recommendations for a three-part recombination with human cytomegalovirus promoter and C-terminal eGFP tag (ViraPower HiPerform Lentiviral Expression Systems, Invitrogen). Lentivirus was produced in 293FT cells, and the cell supernatant was used to infect zyxin-null fibroblasts. After at least 1 wk in culture, cells were FACS sorted for GFP expressors. Zyxin and GFP epitopes were confirmed for constructs containing 1–564, 139–564, 1–138, 309–564, or 1–372, but no antibodies were available for zyxin sequences in 160–340 and 373–564.

Zyxin mutant 43–564, previously described (Smith et al., 2010), was subcloned into Gateway pLentivirus expression (Invitrogen) and cells sorted for GFP expression. Site-directed mutagenesis of four phenylalanines in the Ena/VASP-binding region of zyxin (zyx4F>A; F71A, F93A, F105A, F115A) was performed with the QuikChange II Mutagenesis Kit (Invitrogen). Mutant zyx^{F71,93,105,115A} was subcloned with eGFP tag into the retroviral vector pLINX using methylation-sensitive *Clal* restriction sites (Hoshimaru et al., 1996). Retrovirus was made in Phoenix-Eco producer cells (American Type Culture Collection, Manassas, VA) and used to infect zyxin-null fibroblasts. Stable cell lines expressing GFP-zyx^{F71,93,105,115A} were selected for GFP expression by FACS. GFP- α -actinin nucleofection followed manufacturer recommendations (Amaxa Biosystems, Lonza, Cologne, Germany).

Cell stretching, protein detection, and SFTI analysis

Cells were seeded onto precoated silicone membranes (25 μ g/ml collagen I, 2 μ g/ml fibronectin) as previously described (Yoshigi et al., 2005). Briefly, three 26 \times 33 mm membranes in a 100-mm dish were seeded with 1.2–1.5 million cells. After 24 h growth in DMEMc and 10% serum, cells were subjected to uniaxial cyclic stretch (15%, 0.5 Hz, up to 2 h) using a custom-made stretch device driven by a step motor (Yoshigi et al., 2003). At specified times, cells were fixed (15 min, 3.7% formaldehyde) and permeabilized (5 min, 0.5% Triton X-100) directly on membranes, followed by staining and imaging, or cells were lysed on membranes for protein analysis (150–300 μ l/membrane; 50 mM Tris-HCl, pH 8, 150 mM NaCl, 0.5% NP-40, 0.1% SDS, 0.1 mM NaF, 0.2 mM sodium orthovanadate with protease inhibitors [Boehringer-Mannheim, Mannheim, Germany]). Cell images are always shown with the stretch vector maintained in the horizontal direction (double-headed arrow). SFs within 30° of perpendicular to the horizon were considered aligned (Yoshigi et al., 2005). For inhibition of transcription and translation, cells on membranes were preincubated for 30 min before stretch and for the duration of a 1-h stretch with actinomycin D (1 μ g/ml) or cycloheximide (10 μ g/ml; Tamura et al., 2000; Sun et al., 2001; Momberger et al., 2005), concentrations that are sufficient to inhibit >90% transcription (Sawicki and Godman, 1971) and >90% protein translation in this time frame (Sundell and Singer, 1990). For Table 1 showing the zyxin domain analysis, cells were scored for GFP-zyxin signal localization at FAs and along SFs. SF thickening was phalloidin signal/cell increased by stretch, comparison (relative to zyx-null and wild-type cells) between independent stretch experiments.

For SFTI measurements, images of phalloidin-stained F-actin (using concomitant GFP signal to confirm expression) were analyzed with a custom erosion/brightness decay software (Yoshigi et al., 2005) written in LabVIEW (National Instruments, Austin, TX). Exposure of GFP signal was held constant for image capture, and cells

with comparable expression levels were selected for SFTI analysis of phalloidin signal. For each cell type, multiple stress fibers/cell in >10 fields (Zeiss 40 \times ; Carl Zeiss, Jena, Germany) were evaluated ($n > 100$ measurements); statistical analysis (means \pm SEMs, unpaired *t* tests, analysis of variance) and graphing were performed with Prism software (GraphPad, La Jolla, CA). At least three independent stretch experiments were performed for each construct and cell type, and the relative SFTI values within each experiment were compared.

Cell microscopy

Cells were seeded onto glass coverslips and grown for 18 h in complete DMEM and 10% serum, followed by fixation (15 min, 3.7% formaldehyde) and permeabilization (5 min, 5% Triton X-100). Proteins were localized by antibody immunostaining and phalloidin. Cell images were captured with a CoolSnap HQ camera and Zeiss Axiophot fluorescence microscope (Plan-Apochromat 63 \times , 1.40 numerical aperture [NA], oil objective; 40 \times , 0.75 NA, dry objective) and OpenLab software (Improvision, PerkinElmer, Waltham, MA) or ImageQuant software (Andor Technology, South Windsor, CT). A Zeiss Axioskop2 mot plus microscope (40 \times , 0.75 NA, dry objective) with automatic shutter and a Zeiss AxioCamMRm camera with Zeiss AxioVision 4.8.1 software were also used to capture images. Time-lapse imaging used a stage heater (Bioptechs, Butler, PA) on an Olympus microscope (60 \times , 1.45 NA, objective; Olympus, Center Valley, PA), a digital camera (Orca; Hamamatsu, Hamamatsu, Japan), and MetaMorph software (Molecular Devices, Sunnyvale, CA). Photoshop, version 8 (Adobe, San Jose, CA), was used for image processing and Adobe Illustrator, version 11.0, for figure preparation.

Electrophoresis and Western immunoblots

Cell lysates (10–25 μ g/lane) were electrophoresed through denaturing 10% polyacrylamide gels (Bio-Rad, Hercules, CA) with prestained Precision Plus molecular weight markers (Bio-Rad) and then electroblotted onto nitrocellulose filters, probed with HRP-conjugated antibodies, and detected by enhanced chemiluminescence (GE Healthcare). For phosphatase experiments, cell lysates were incubated with calf intestinal phosphatase or lambda phosphatase (New England Biolabs, Ipswich, MA) for 30 min before electrophoresis.

ACKNOWLEDGMENTS

We are grateful to Hiroaki Honda, Hisamura Hirai, and Carol Otey for cell lines and constructs. We thank Martial Hery and Mark Toda, who participated in early stages of this work, and Mark Smith and Diana Lim for help with manuscript preparation. A National Cancer Institute Cancer Center Support Grant (2 P30 CA042014) provided essential shared resources. This work was supported by National Institutes of Health Grant GM50877 (to M.C.B.) and the Huntsman Cancer Institute.

REFERENCES

- Banes AJ, Gilbert J, Taylor D, Monbureau O (1985). A new vacuum-operated stress-providing instrument that applies static or variable duration cyclic tension or compression to cells in vitro. *J Cell Sci* 75, 35–42.
- Beckerle MC (1986). Identification of a new protein localized at sites of cell-substrate adhesion. *J Cell Biol* 103, 1679–1687.
- Bubb MR, Spector I, Beyer BB, Fosen KM (2000). Effects of jasplakinolide on the kinetics of actin polymerization. An explanation for certain in vivo observations. *J Biol Chem* 275, 5163–5170.
- Byers HR, White GE, Fujiwara K (1984). Organization and function of stress fibers in cells in vitro and in situ. A review. *Cell Muscle Motil* 5, 83–137.
- Call GS, Chung JY, Davis JA, Price BD, Primavera TS, Thomson NC, Wagner MV, Hansen MD (2011). Zyxin phosphorylation at serine 142 modulates the zyxin head-tail interaction to alter cell-cell adhesion. *Biochem Biophys Res Commun* 404, 780–784.

- Chodniewicz D, Klemke RL (2004). Regulation of integrin-mediated cellular responses through assembly of a CAS/Crk scaffold. *Biochim Biophys Acta* 1692, 63–76.
- Cohen TS, Gray Lawrence G, Khasgiwala A, Margulies SS (2010). MAPK activation modulates permeability of isolated rat alveolar epithelial cell monolayers following cyclic stretch. *PLoS One* 5, e10385.
- Colombelli J, Besser A, Kress H, Reynaud EG, Girard P, Caussinus E, Haselmann U, Small JV, Schwarz US, Stelzer EH (2009). Mechanosensing in actin stress fibers revealed by a close correlation between force and protein localization. *J Cell Sci* 122, 1665–1679.
- Cramer LP (1999). Role of actin-filament disassembly in lamellipodium protrusion in motile cells revealed using the drug jasplakinolide. *Curr Biol* 9, 1095–1105.
- Crawford AW, Beckerle MC (1991). Purification and characterization of zyxin, an 82,000-dalton component of adherens junctions. *J Biol Chem* 266, 5847–5853.
- Davies PF (1995). Flow-mediated endothelial mechanotransduction. *Physiol Rev* 75, 519–560.
- Defilippi P, Di Stefano P, Cabodi S (2006). p130Cas: a versatile scaffold in signaling networks. *Trends Cell Biol* 16, 257–263.
- del Rio A, Perez-Jimenez R, Liu R, Roca-Cusachs P, Fernandez JM, Sheetz MP (2009). Stretching single talin rod molecules activates vinculin binding. *Science* 323, 638–641.
- Dobrin PB (1978). Mechanical properties of arteries. *Physiol Rev* 58, 397–460.
- Drees B, Friederich E, Fradelizi J, Louvard D, Beckerle MC, Golsteyn RM (2000). Characterization of the interaction between zyxin and members of the Ena/vasodilator-stimulated phosphoprotein family of proteins. *J Biol Chem* 275, 22503–22511.
- Drees BE, Andrews KM, Beckerle MC (1999). Molecular dissection of zyxin function reveals its involvement in cell motility. *J Cell Biol* 147, 1549–1560.
- Eldib M, Dean DA (2011). Cyclic stretch of alveolar epithelial cells alters cytoskeletal micromechanics. *Biotechnol Bioeng* 108, 446–453.
- Eyckmans J, Boudou T, Yu X, Chen CS (2011). A hitchhiker's guide to mechanobiology. *Dev Cell* 21, 35–47.
- Faust U, Hampe N, Rubner W, Kirchgessner N, Safran S, Hoffmann B, Merkel R (2011). Cyclic stress at mHz frequencies aligns fibroblasts in direction of zero strain. *PLoS One* 6, e28963.
- Geiger B, Spatz JP, Bershadsky AD (2009). Environmental sensing through focal adhesions. *Nat Rev Mol Cell Biol* 10, 21–33.
- Geiger RC, Taylor W, Glucksberg MR, Dean DA (2006). Cyclic stretch-induced reorganization of the cytoskeleton and its role in enhanced gene transfer. *Gene Ther* 13, 725–731.
- Golsteyn RM, Beckerle MC, Koay T, Friederich E (1997). Structural and functional similarities between the human cytoskeletal protein zyxin and the ActA protein of *Listeria monocytogenes*. *J Cell Sci* 110, Pt 161893–1906.
- Grunewald TG, Kammerer U, Winkler C, Schindler D, Sickmann A, Honig A, Butt E (2007). Overexpression of LASP-1 mediates migration and proliferation of human ovarian cancer cells and influences zyxin localisation. *Br J Cancer* 96, 296–305.
- Guilluy C, Garcia-Mata R, Burridge K (2011a). Rho protein crosstalk: another social network? *Trends Cell Biol* 21, 718–726.
- Guilluy C, Swaminathan V, Garcia-Mata R, O'Brien ET, Superfine R, Burridge K (2011b). The Rho GEFs LARG and GEF-H1 regulate the mechanical response to force on integrins. *Nat Cell Biol* 13, 722–727.
- Guo WH, Wang YL (2007). Retrograde fluxes of focal adhesion proteins in response to cell migration and mechanical signals. *Mol Biol Cell* 18, 4519–4527.
- Henvy M, Hoffman LM, Jensen CC, Smith MA, Beckerle MC (2010). The LIM protein Zyxin binds CARP-1 and promotes apoptosis. *Genes Cancer* 1, 506–515.
- Hirata H, Tatsumi H, Sokabe M (2008). Mechanical forces facilitate actin polymerization at focal adhesions in a zyxin-dependent manner. *J Cell Sci* 121, 2795–2804.
- Hoffman LM, Jensen CC, Kloeker S, Wang CL, Yoshigi M, Beckerle MC (2006). Genetic ablation of zyxin causes Mena/VASP mislocalization, increased motility, and deficits in actin remodeling. *J Cell Biol* 172, 771–782.
- Hoffman LM *et al.* (2003). Targeted disruption of the murine zyxin gene. *Mol Cell Biol* 23, 70–79.
- Honda H *et al.* (1998). Cardiovascular anomaly, impaired actin bundling and resistance to Src-induced transformation in mice lacking p130Cas. *Nat Genet* 19, 361–365.
- Hoshimaru M, Ray J, Sah DW, Gage FH (1996). Differentiation of the immortalized adult neuronal progenitor cell line HC2S2 into neurons by regulatable suppression of the v-myc oncogene. *Proc Natl Acad Sci USA* 93, 1518–1523.
- Jaalouk DE, Lammerding J (2009). Mechanotransduction gone awry. *Nat Rev Mol Cell Biol* 10, 63–73.
- Jaffe AB, Hall A (2005). Rho GTPases: biochemistry and biology. *Annu Rev Cell Dev Biol* 21, 247–269.
- Jungbauer S, Gao H, Spatz JP, Kemkemer R (2008). Two characteristic regimes in frequency-dependent dynamic reorientation of fibroblasts on cyclically stretched substrates. *Biophys J* 95, 3470–3478.
- Kaunas R, Nguyen P, Usami S, Chien S (2005). Cooperative effects of Rho and mechanical stretch on stress fiber organization. *Proc Natl Acad Sci USA* 102, 15895–15900.
- Kessler D, Dethlefsen S, Haase I, Plomann M, Hirsch F, Krieg T, Eckes B (2001). Fibroblasts in mechanically stressed collagen lattices assume a synthetic phenotype. *J Biol Chem* 276, 36575–36585.
- Kito H, Chen EL, Wang X, Ikeda M, Azuma N, Nakajima N, Gahtan V, Sumpio BE (2000). Role of mitogen-activated protein kinases in pulmonary endothelial cells exposed to cyclic strain. *J Appl Physiol* 89, 2391–2400.
- Krause M, Dent EW, Bear JE, Loureiro JJ, Gertler FB (2003). Ena/VASP proteins: regulators of the actin cytoskeleton and cell migration. *Annu Rev Cell Dev Biol* 19, 541–564.
- Lee CF, Haase C, Deguchi S, Kaunas R (2010). Cyclic stretch-induced stress fiber dynamics—dependence on strain rate, Rho-kinase and MLCK. *Biochem Biophys Res Commun* 401, 344–349.
- Lee E, Shelden EA, Knecht DA (1998). Formation of F-actin aggregates in cells treated with actin stabilizing drugs. *Cell Motil Cytoskeleton* 39, 122–133.
- Lele TP, Pendse J, Kumar S, Salanga M, Karavitis J, Ingber DE (2006). Mechanical forces alter zyxin unbinding kinetics within focal adhesions of living cells. *J Cell Physiol* 207, 187–194.
- Li B, Trueb B (2001). Analysis of the alpha-actinin/zyxin interaction. *J Biol Chem* 276, 33328–33335.
- Li B, Zhuang L, Trueb B (2004). Zyxin interacts with the SH3 domains of the cytoskeletal proteins LIM-nebulette and Lasp-1. *J Biol Chem* 279, 20401–20410.
- Machner MP, Urbanke C, Barzik M, Otten S, Sechi AS, Wehland J, Heinz DW (2001). ActA from *Listeria monocytogenes* can interact with up to four Ena/VASP homology 1 domains simultaneously. *J Biol Chem* 276, 40096–40103.
- Miyoshi T, Tsuji T, Higashida C, Hertzog M, Fujita A, Narumiya S, Scita G, Watanabe N (2006). Actin turnover-dependent fast dissociation of capping protein in the dendritic nucleation actin network: evidence of frequent filament severing. *J Cell Biol* 175, 947–955.
- Momberger TS, Levick JR, Mason RM (2005). Hyaluronan secretion by synovial cells is mechanosensitive. *Matrix Biol* 24, 510–519.
- Moody JD, Grange J, Ascione MP, Boothe D, Bushnell E, Hansen MD (2009). A zyxin head-tail interaction regulates zyxin-VASP complex formation. *Biochem Biophys Res Commun* 378, 625–628.
- Naumanen P, Lappalainen P, Hotulainen P (2008). Mechanisms of actin stress fibre assembly. *J Microsc* 231, 446–454.
- Nguyen TN, Uemura A, Shih W, Yamada S (2010). Zyxin-mediated actin assembly is required for efficient wound closure. *J Biol Chem* 285, 35439–35445.
- Niebuhr K, Ebel F, Frank R, Reinhard M, Domann E, Carl UD, Walter U, Gertler FB, Wehland J, Chakraborty T (1997). A novel proline-rich motif present in ActA of *Listeria monocytogenes* and cytoskeletal proteins is the ligand for the EVH1 domain, a protein module present in the Ena/VASP family. *EMBO J* 16, 5433–5444.
- Nix DA, Beckerle MC (1997). Nuclear-cytoplasmic shuttling of the focal contact protein, zyxin: a potential mechanism for communication between sites of cell adhesion and the nucleus. *J Cell Biol* 138, 1139–1147.
- Nix DA, Fradelizi J, Bockholt S, Menichi B, Louvard D, Friederich E, Beckerle MC (2001). Targeting of zyxin to sites of actin membrane interaction and to the nucleus. *J Biol Chem* 276, 34759–34767.
- Orr AW, Helmke BP, Blackman BR, Schwartz MA (2006). Mechanisms of mechanotransduction. *Dev Cell* 10, 11–20.
- Otey CA, Carpen O (2004). Alpha-actinin revisited: a fresh look at an old player. *Cell Motil Cytoskeleton* 58, 104–111.
- Parsons JT, Horwitz AR, Schwartz MA (2010). Cell adhesion: integrating cytoskeletal dynamics and cellular tension. *Nat Rev Mol Cell Biol* 11, 633–643.

- Pavalko FM, Schneider G, Burridge K, Lim SS (1995). Immunodetection of alpha-actinin in focal adhesions is limited by antibody inaccessibility. *Exp Cell Res* 217, 534–540.
- Perez-Alvarado GC, Miles C, Michelsen JW, Louis HA, Winge DR, Beckerle MC, Summers MF (1994). Structure of the carboxy-terminal LIM domain from the cysteine rich protein CRP. *Nat Struct Biol* 1, 388–398.
- Puklin-Faucher E, Sheetz MP (2009). The mechanical integrin cycle. *J Cell Sci* 122, 179–186.
- Purich DL, Southwick FS (1997). ABM-1 and ABM-2 homology sequences: consensus docking sites for actin-based motility defined by oligoproline regions in *Listeria* ActA surface protein and human VASP. *Biochem Biophys Res Commun* 231, 686–691.
- Reinhard M, Zumbunn J, Jaquemar D, Kuhn M, Walter U, Trueb B (1999). An alpha-actinin binding site of zyxin is essential for subcellular zyxin localization and alpha-actinin recruitment. *J Biol Chem* 274, 13410–13418.
- Renfranz PJ, Beckerle MC (2002). Doing (F/L)PPPPs: EVH1 domains and their proline-rich partners in cell polarity and migration. *Curr Opin Cell Biol* 14, 88–103.
- Renfranz PJ, Siegrist SE, Stronach BE, Macalma T, Beckerle MC (2003). Molecular and phylogenetic characterization of Zyx102, a *Drosophila* orthologue of the zyxin family that interacts with *Drosophila* Enabled. *Gene* 305, 13–26.
- Ridley AJ, Hall A (1992). The small GTP-binding protein rho regulates the assembly of focal adhesions and actin stress fibers in response to growth factors. *Cell* 70, 389–399.
- Sawada Y *et al.* (2001). Rap1 is involved in cell stretching modulation of p38 but not ERK or JNK MAP kinase. *J Cell Sci* 114, 1221–1227.
- Sawada Y, Sheetz MP (2002). Force transduction by Triton cytoskeletons. *J Cell Biol* 156, 609–615.
- Sawada Y, Tamada M, Dubin-Thaler BJ, Cherniavskaya O, Sakai R, Tanaka S, Sheetz MP (2006). Force sensing by mechanical extension of the Src family kinase substrate p130Cas. *Cell* 127, 1015–1026.
- Sawicki SG, Godman GC (1971). On the differential cytotoxicity of actinomycin D. *J Cell Biol* 50, 746–761.
- Schmeichel KL, Beckerle MC (1994). The LIM domain is a modular protein-binding interface. *Cell* 79, 211–219.
- Schwartz MA (2010). Integrins and extracellular matrix in mechanotransduction. *Cold Spring Harb Perspect Biol* 2, a005066.
- Seibel NM, Eljouni J, Nalaskowski MM, Hampe W (2007). Nuclear localization of enhanced green fluorescent protein homomultimers. *Anal Biochem* 368, 95–99.
- Smith MA, Blankman E, Gardel ML, Luetjohann L, Waterman CM, Beckerle MC (2010). A zyxin-mediated mechanism for actin stress fiber maintenance and repair. *Dev Cell* 19, 365–376.
- Sukharev S, Corey DP (2004). Mechanosensitive channels: multiplicity of families and gating paradigms. *Sci STKE* 2004, re4.
- Sun R, Chen X, Yang VW (2001). Intestinal-enriched Kruppel-like factor (Kruppel-like factor 5) is a positive regulator of cellular proliferation. *J Biol Chem* 276, 6897–6900.
- Sundell CL, Singer RH (1990). Actin mRNA localizes in the absence of protein synthesis. *J Cell Biol* 111, 2397–2403.
- Tamada M, Sheetz MP, Sawada Y (2004). Activation of a signaling cascade by cytoskeleton stretch. *Dev Cell* 7, 709–718.
- Tamura K *et al.* (2000). Molecular mechanism of fibronectin gene activation by cyclic stretch in vascular smooth muscle cells. *J Biol Chem* 275, 34619–34627.
- Uemura A, Nguyen TN, Steele AN, Yamada S (2011). The LIM domain of zyxin is sufficient for force-induced accumulation of zyxin during cell migration. *Biophys J* 101, 1069–1075.
- Wang N, Tytell JD, Ingber DE (2009). Mechanotransduction at a distance: mechanically coupling the extracellular matrix with the nucleus. *Nat Rev Mol Cell Biol* 10, 75–82.
- Wille JJ, Ambrosi CM, Yin FC (2004). Comparison of the effects of cyclic stretching and compression on endothelial cell morphological responses. *J Biomech Eng* 126, 545–551.
- Wojtowicz A, Babu SS, Li L, Gretz N, Hecker M, Cattaruzza M (2010). Zyxin mediation of stretch-induced gene expression in human endothelial cells. *Circ Res* 107, 898–902.
- Wong AJ, Pollard TD, Herman IM (1983). Actin filament stress fibers in vascular endothelial cells in vivo. *Science* 219, 867–869.
- Yi J, Kloeker S, Jensen CC, Bockholt S, Honda H, Hirai H, Beckerle MC (2002). Members of the zyxin family of LIM proteins interact with members of the p130Cas family of signal transducers. *J Biol Chem* 277, 9580–9589.
- Yoshigi M, Clark EB, Yost HJ (2003). Quantification of stretch-induced cytoskeletal remodeling in vascular endothelial cells by image processing. *Cytometry A* 55, 109–118.
- Yoshigi M, Hoffman LM, Jensen CC, Yost HJ, Beckerle MC (2005). Mechanical force mobilizes zyxin from focal adhesions to actin filaments and regulates cytoskeletal reinforcement. *J Cell Biol* 171, 209–215.

CHAPTER 5

MOLECULAR DISSECTION OF THE MECHANISM BY WHICH EWS/FLI EXPRESSION COMPROMISES ACTIN CYTOSKELETAL INTEGRITY AND CELL ADHESION IN EWING SARCOMA

Aashi Chaturvedi, Laura M. Hoffman, Christopher C. Jensen,
Yi-Chun Lin, Allie H. Grossmann, Lor R. Randall, Stephen L. Lessnick,
Alana L. Welm, Mary C. Beckerle.

This Chapter describes my contributions to the above mentioned manuscript.

Dr. Laura Hoffman helped with the figures and the writing of this manuscript.

Christopher Jensen performed the western blot analysis and

with Figures 5.3G, 5.5C and 5.5D.

Yi-Chun Lin performed sectioning and H&E staining of mouse lung tissue.

Dr. Allie Grossmann is the independent pathologist for this work.

Dr. Lor Randall performed the radiographic analysis of mice tibia.

Dr. Alana Welm performed the tail vein injections for the *in vivo* lung adhesion assay.

Abstract

The uncertain histogenesis and aggressive biological behavior of Ewing sarcoma has always been a subject of interest among clinicians and researchers alike. This malignant disease is driven by the fusion oncogene EWS/FLI which is necessary for transformation. The role of basic cellular features like actin cytoskeleton and focal adhesion sites are not very well understood in Ewing sarcoma tumor growth and metastasis. Here, we have used the RNAi-based silencing of EWS/FLI oncogene that result in dramatic cytoskeletal changes and reduced cellular spreading and adhesion, potentially through downregulation of the genes regulating these cellular features. Microarray analysis revealed hundreds of such genes that are associated with focal adhesion proteins, ECM-receptor interactions and cell adhesions. Our study demonstrates that focal adhesion protein zyxin and $\alpha 5$ integrin are downregulated by EWS/FLI to compromise the actin cytoskeleton, cell adhesion and, cell spreading of Ewing sarcoma cells as revealed by immunofluorescence microscopy. We hypothesize that EWS/FLI mediated changes in these cellular features facilitates cell transformation. To test this, the current study establishes an intratibial orthotopic mouse model and shows successful Ewing sarcoma tumor growth, progression and metastasis in NOD/SCID mice. To our knowledge, this is the first report of spontaneous metastasis to lungs and other bones from a primary Ewing sarcoma tumor in the mouse tibia. Using this mouse model we characterized the tumor progression and metastasis by Ewing sarcoma cells engineered to reexpress zyxin or $\alpha 5$ integrin or both zyxin and $\alpha 5$ integrin. In this mouse model the rate of tumor growth significantly decreases when both zyxin and $\alpha 5$ integrin are reexpressed in Ewing sarcoma cells, but the rate of metastasis to lungs is significantly higher when $\alpha 5$ integrin is expressed. These results suggest that EWS/FLI mediated downregulation of

adhesion proteins is required for tumor progression, but could compromise tumor cell metastasis. The current study highlights the contributions of adhesion proteins (zyxin and $\alpha 5$ integrin) in modulating cell-ECM interactions, actin cytoskeleton, cell adhesion and spreading to achieve small round cell morphology and guiding tumor progression and metastasis in Ewing sarcoma.

Introduction

Ewing sarcoma is a round-cell malignant neoplasm of the bone that typically affects adolescents and young adults. It usually develops in the diaphysis or metaphysis of long bones, most commonly in femur, tibia and humerus (Kimber et al., 1998; Spraker et al., 2012). Ewing sarcoma is an aggressive cancer that grows rapidly and metastasizes to lungs and bones (Karosas, 2010). Treatment of apparently localized primary tumors involves surgery and chemotherapy. Despite these interventions, the vast majority of patients relapse even after definitive surgical removal of the primary tumor, illustrating the fact that most patients have occult disseminated disease upon presentation (McAllister and Lessnick, 2005; Spraker HL et al., 2012). Patients with metastatic or recurrent disease face poor prognosis with less than 15% 5-year survival rate. Knowledge of the molecular mechanisms that determine Ewing sarcoma cell behavior will be crucial in understanding disease progression.

Ewing sarcoma is caused by a reciprocal chromosomal translocation involving the *EWSR1* gene on chromosome 22 and a member of the *FLI* gene on chromosome 11 (Delattre et al., 1992; Turc-Carel et al., 1988). In approximately 85% of cases, a t(11;22)(q24;q12) translocation results in the expression of chimeric transcription factor in which a strong transcription regulatory domain found in EWS is fused in-frame to a

portion of FLI-1 that includes a DNA-binding domain (Aurias et al., 1984; Delattre et al., 1992; Lessnick et al., 1995; May et al., 1993a). EWS/FLI acts as a master transcriptional regulator that modulates the expression of several hundred genes. Several upregulated targets of EWS/FLI have been extensively studied including NKX2.2, NR0B1 and Caveolin1 (Kinsey et al., 2006; Owen et al., 2008; Tirado et al., 2006). Although predicted to aberrantly activate transcription, EWS/FLI also causes repression of hundreds to thousands of genes (Kinsey et al., 2006; Owen et al., 2008; Smith et al., 2006). With a few exceptions (Borinstein et al., 2011; Herrero-Martin et al., 2009; Mateo-Lozano et al., 2003), the downregulated targets of EWS/FLI have not been extensively characterized, even though the repression of specific gene expression could lead to loss of key regulators of normal cell growth and behavior.

Recent studies suggest that EWS/FLI is not only required for tumorigenesis, but also modulates key cellular properties such as cell adhesion, motility and invasion (Amsellem et al., 2005; Cerisano et al., 2004; Chaturvedi et al., 2012). For example, RNA interference based knockdown of EWS/FLI expression revealed that EWS/FLI expression promotes loss of tumor cell adhesion (Chaturvedi et al., 2012). EWS/FLI - mediated regulation of adhesion genes could affect two stages of Ewing sarcoma metastasis: tumor cell dissemination and/or readhesion of these cells at a secondary site for effective colonization. Here, we identify specific EWS/FLI target genes that regulate the tumor cell adhesion to extracellular matrix and contribute towards maintenance of actin cytoskeleton. In the current study we investigate the contributions of two EWS/FLI targets, zyxin and $\alpha 5$ integrin, to the actin cytoskeleton, cell spreading and adhesion of Ewing sarcoma cells. We extend the results from *in vitro* studies into an experimental mouse model that effectively recapitulates the clinical manifestations of Ewing sarcoma

observed in patients, including rapid formation of osteolytic tumors and aggressive metastasis to lungs and other bones.

Results

EWS/FLI expression compromises the cytoskeleton of Ewing sarcoma cells

The cell of origin that gives rise to Ewing sarcoma has not yet been definitively identified (Cavazzana et al., 1987; Ewing, 1921; Jedlicka, 2010; Kovar, 2005; Tirode et al., 2007). Consequently, the approach of ectopic EWS/FLI expression as a way to model oncogene impact on cell behavior is fraught with difficulty, owing to the uncertain effect of inappropriate cellular context (Braunreiter et al., 2006; Owen and Lessnick, 2006). To circumvent this challenge, we studied how the EWS/FLI oncoprotein influences cellular behavior by using an RNA interference approach to knockdown EWS/FLI expression in patient-derived Ewing sarcoma cells (A673 and EWS502).

We used retrovirally-encoded short hairpin RNA directed against EWS/FLI transcripts to knockdown the expression of EWS/FLI (EWS/FLI RNAi) and RNA interference against luciferase served as Control RNAi and compared their cellular behavior. Knockdown of EWS/FLI expression in multiple human Ewing sarcoma cell lines resulted in dramatic effects on cell phenotype including alterations in adhesion and motility (Chaturvedi et al., 2012). In an effort to provide an extracellular matrix ligand that is prominent in bone, the cells were plated on fibronectin (Rodan and Rodan, 1997). Ewing sarcoma cells displayed a profound cytoskeletal deficit (Figure 5.1A). Both A673 cells and EWS502 cells appeared small and poorly spread, with thin and short actin stress fibers. In contrast, when EWS/FLI expression was knocked down by RNA interference, the Ewing sarcoma cells underwent a dramatic morphological transformation in which

they exhibited pronounced adhesion and spreading to the fibronectin substratum and displayed robust actin stress fibers. These results illustrated a profound effect of EWS/FLI expression on adhesion and cytoarchitecture, prompting us to explore the mechanism by which EWS/FLI influences these phenotypic attributes of the tumor cells.

EWS/FLI is a transcription factor that modulates the expression of hundreds to thousands of genes (Owen et al., 2008). To identify candidate targets of EWS/FLI that might influence adhesion and cytoarchitecture, we analyzed a previously published microarray analysis of EWS/FLI regulated genes (Owen et al., 2008). Selection of genes whose expression was decreased at least 1.8 fold by EWS/FLI revealed 222 genes that were downregulated by EWS/FLI by this criterion. Kyoto Encyclopedia of Genes and Genomes (KEGG) analysis revealed that the top three classes of genes downregulated by EWS/FLI were those encoding focal adhesion proteins, modulators of extracellular matrix and receptor interactions, and regulators of the actin cytoskeleton (Table 5.1), consistent with the major cellular phenotypes we observed by microscopic analysis of cells in Figure 5.1A. Inspection of the EWS/FLI downregulated genes revealed that more than one-third would be expected to influence the actin cytoskeleton, cell-matrix communication, or cell adhesion and migration based on their annotated functions (Supplemental Table S.1). The largest single class of genes downregulated by EWS/FLI expression encodes focal adhesion proteins. Focal adhesions are regions of the cell surface specialized for cell-matrix adhesion and transmembrane communication, known to convey information about extracellular matrix composition, as well as mechanical stress to the cell interior. Focal adhesions are themselves complex multicomponent structures with over 100 known protein constituents (Geiger and Yamada, 2011; Zaidel-Bar et al., 2007).

From the list of genes that are down-regulated by EWS/FLI, we selected the genes encoding zyxin and $\alpha 5$ integrin for further study because of their known influence on cytoskeleton and cell-matrix interactions. Zyxin is an important regulator of the actin cytoskeleton that is required for maintenance and repair of actin stress fibers (Hoffman et al., 2012; Smith et al., 2010; Yoshigi et al., 2005). Importantly, zyxin was previously implicated as a regulator of cytoskeletal function in Ewing sarcoma models (Amsellem et al., 2005; Cerisano et al., 2004). Integrins are transmembrane $\alpha 5$ heterodimeric receptors for extracellular matrix that are critical for cell-substratum adhesion as well as stress fiber anchorage and integrity (Campbell and Humphries, 2011; Hynes, 2002; Lotz et al., 2000). $\alpha 5$ integrin is a known modulator of cell adhesion, migration and cell-matrix communication that dimerizes with $\alpha 5$ integrin subunit to confer adhesion to fibronectin (Gupton et al., 2012; Margadant et al., 2011; Mostafavi-Pour et al., 2003; Nagae et al., 2012). Fibronectin expression is also reduced in EWS/FLI-expressing cells (Supp. Table S.1), consistent with the proposal that the EWS/FLI oncogene acts, at least in part, by abrogating cell-matrix adhesion and the associated actin cytoskeleton.

Validating the microarray findings, Western immunoblot analysis comparing the protein complements in control and EWS/FLI knockdown cells, revealed that both zyxin and $\alpha 5$ integrin are downregulated ~two-fold by EWS/FLI expression (Figure 5.1B). Evidence that the RNA interference was effective in abrogating EWS/FLI expression is shown in Figure 5.1B in which FLI1 antibody detects reduced EWS/FLI fusion protein. Tubulin expression serves as a surrogate for cell number and controls for equivalent sample loading in this experiment.

Reexpression of zyxin and $\alpha 5$ integrin in Ewing sarcoma cells influences the actin cytoskeleton, cell adhesion and spreading

To study the impact of reduced expression of zyxin and $\alpha 5$ integrin in Ewing sarcoma, we reexpressed these downregulated targets in patient-derived Ewing sarcoma cells using retrovirus to program the cells to express these cDNAs of interest. As can be seen in Figure 5.1C, by Western immunoblot analysis, we detect increases in zyxin and/or $\alpha 5$ integrin. Expression of these proteins does not detectably alter the levels of EWS/FLI in the cells, as detected with anti FLI1 antibody.

Although EWS/FLI affects the expression of hundreds of genes, the reexpression of just one or two of these, zyxin and/or $\alpha 5$ integrin, in the Ewing sarcoma cells resulted in dramatic phenotypic alterations in the cells. Importantly, these genes induced distinct alterations in cell morphology and cytoarchitecture. Compared to the parental A673 cells infected with the empty retroviral vector, which were poorly spread and exhibited only rudimentary stress fibers (Figure 5.1D), Ewing sarcoma cells programmed to express zyxin displayed a profound elaboration of actin stress fibers, with an increase in cell spreading as well (Figure 5.1E). Expression of $\alpha 5$ integrin alone appeared to improve cell spreading without resulting in enhancement of actin cytoskeletal arrays (Figure 5.1F). When these proteins were coexpressed, the Ewing sarcoma cells are marked by both well formed actin stress fibers and enhanced cell spreading (Figure 5.1G). Similar results were obtained in both A673 and EWS502 cells (data not shown).

Higher magnification and quantitative analysis of these initial findings confirmed the significant and unique impacts of zyxin and $\alpha 5$ integrin on Ewing sarcoma cell morphology and cytoarchitecture (Figure 5.2). The cells were double labeled with phalloidin to visualize filamentous actin (Figures 5.2A-D) and antipaxillin antibody to

mark focal adhesions (Figures 5.2E-H). The size (Figure 5.2I) and number (Figure 5.2J) of focal adhesions was quantitated for each condition. Knockdown of EWS/FLI expression in Ewing sarcoma cells resulted in a statistically significant increase in the average focal adhesion size from $1.3 \mu\text{m}^2$ to $1.8 \mu\text{m}^2$ (Figure 5.2I). Reexpression of either zyxin, $\alpha 5$ integrin, or both zyxin and $\alpha 5$ integrin restored the size of paxillin-rich focal adhesions to a level that is not statistically different from what is observed when EWS/FLI is knocked down in Ewing sarcoma cells by RNAi (Figure 5.2I).

Ewing sarcoma cells or those with control RNAi had fewer focal adhesions (~50 per cell) compared to cells in which EWS/FLI expression was knocked down, which displayed an average of 177 focal adhesions per cell (Figure 5.2J). Expression of zyxin and/or $\alpha 5$ integrin in Ewing sarcoma cells resulted in a statistically significant increase of focal adhesion number (Figure 5.2J). Interestingly, however, zyxin expression had a much more significant impact on focal adhesion number than did expression of $\alpha 5$ integrin. For example, expression of $\alpha 5$ integrin led to moderate increase in number of focal adhesions from an average of 50 to 70 per cell (Figure 5.2J). However, expression of zyxin alone or $\alpha 5$ integrin led to dramatic increase in the focal adhesion number to more than 150 focal adhesions per cell (Figure 5.2J), highlighting the differential impact of zyxin and $\alpha 5$ integrin on establishment of number of focal adhesions.

Given the established link between focal adhesion development and cell spreading (Salsmann et al., 2006; Smilenov et al., 1999), the increased focal adhesion size and number observed upon reexpression of zyxin and/or $\alpha 5$ integrin was consistent with low magnification analysis which suggested that reexpression of either zyxin or $\alpha 5$ integrin enhanced cell spreading. To test this possibility quantitatively, we measured the areas of phalloidin stained cells (e.g. cells such as those represented in Figure 5.2A-D).

Expression of zyxin and/or $\alpha 5$ integrin resulted in statistically significant increase in cell spreading, illustrated by increased cell area (Figure 5.2K). Measured cell area more than doubled from $950 \mu\text{m}^2$ for Ewing sarcoma cells harboring empty vector to $>1500 \mu\text{m}^2$ for cells expressing the adhesion proteins (Figure 5.2K). Reexpression of zyxin induced a more robust spreading response than what occurred with reexpression of $\alpha 5$ integrin, although both displayed more extensive cell spreading than the parental Ewing sarcoma cells. Interestingly, the cell area for Ewing sarcoma cells with knockdown of EWS/FLI ($\sim 2200 \mu\text{m}^2$) was indistinguishable from the average area of cells expressing either zyxin alone or in combination with $\alpha 5$ integrin, illustrating that reexpression of zyxin is sufficient to fully rescue the cell spreading deficit observed in Ewing sarcoma cells.

The increased cell spreading and focal adhesion assembly was associated with enhanced adhesion, as measured in a quantitative, short time course cell adhesion assay (Figure 5.2L). In this 2 hour adhesion assay the cells were allowed to adhere to an uncoated plastic tissue culture dish. Knockdown of EWS/FLI expression resulted in a statistically significant 2-fold increase in cell adhesion (Figure 5.2L). Reexpression of $\alpha 5$ integrin alone or with zyxin enhanced cellular adhesion comparable to cells in which EWS/FLI expression was knocked down by RNAi. Although Ewing sarcoma cells reexpressing zyxin also increased cell adhesion, the effect was not as dramatic as in the presence of $\alpha 5$ integrin (Figure 5.2L). The profound, yet differential capacity of zyxin and $\alpha 5$ integrin to restore cell adhesion, spreading, actin cytoskeleton and focal adhesion number is summarized in the schematic representation in Figure 5.2M.

Intratibial orthotopic mouse model for Ewing sarcoma recapitulates features of the human disease

The ultimate goal of our studies was to understand both the critical cellular mechanisms that are compromised in EWS/FLI-transformed cells and to decipher the consequences of these alterations for tumor biology. To test whether increasing cellular adhesion by the reexpression of zyxin and $\alpha 5$ integrin in Ewing sarcoma cells would affect tumor cell behavior *in vivo*, we first established an orthotopic xenograft model that faithfully replicates key aspects of Ewing sarcoma behavior. In brief, we injected A673 Ewing sarcoma cells that were suspended in extracellular matrix (Matrigel) into the right tibias of NOD/SCID immunodeficient mice. The tumor cells were programmed to constitutively express luciferase, enabling continuous detection of viable cells *in situ*. Tumor growth and progression, including histopathology, osteolysis, and metastasis, were systematically monitored (Figure 5.3A).

Under our experimental conditions, tumors grew rapidly and were highly osteolytic. Most of the mice (14 out of 15) formed tumors in the injected tibia within four weeks. Using *in vivo* luciferase imaging we observed aggressive growth of these tumors between weeks 3 and 4 (Figure 5.3B). Tibial radiographs revealed extensive osteolysis (Figure 5.3C) a characteristic of Ewing sarcoma progression in human patients. Radiographic analysis revealed that 85% of mice displayed cortical bone destruction and massive bone loss by week 4, warranting a classification of grade 3 or 4 osteolysis (Figure 5.3D). Ewing sarcoma is distinguished by its small round blue cell morphology when tissue biopsy sections are stained with hematoxylin and eosin (H&E) as well as distinct membrane labeling with antibodies directed against CD99, a transmembrane glycoprotein that serves as a diagnostic biomarker for Ewing sarcoma (Ambros et al.,

1991; Fellingner et al., 1991; Perlman et al., 1994). Consistent with features observed in clinical samples, The histological presentation and positive CD99 staining of Ewing sarcoma cells in the mouse model were indistinguishable from what is observed in human patient samples (Figure 5.3E), illustrating preservation of key morphological properties of the human tumor cells in the context of the murine host.

In patients, Ewing sarcoma arises in bone and has a propensity to metastasize to lung and other bones (Arndt and Crist, 1999; Spraker et al., 2012). This feature is also preserved in our mouse orthotopic model (Figure 5.3F-G). *In vivo* imaging of the luciferase tagged Ewing sarcoma cells in the mice revealed that half exhibited positive signal in the chest area, suggesting potential metastasis to the lungs. Upon dissection and histopathological analysis, lungs that were luciferase-positive exhibited small round blue cells by H&E staining and positive anti-CD99 labeling, confirming the presence of metastatic Ewing sarcoma cells (Figure 5.3F). Luciferase imaging of the mouse carcass revealed metastasis to other sites, such as the left tibia or upper limb and occasionally to ribs and spine (Figure 5.3G). The development of a robust mouse model system for Ewing sarcoma that recapitulates key clinical features of the human disease set the stage for studies of the impact of EWS/FLI dependent gene regulation *in vivo*.

EWS/FLI dependent repression of zyxin and $\alpha 5$ integrin expression enhances anchorage independent growth of Ewing sarcoma cells

To probe the impact of EWS/FLI-dependent repression of zyxin and $\alpha 5$ integrin expression, we introduced Ewing sarcoma cells that were engineered to reexpress one or both of these proteins into recipient mice via intratibial injection, as described above, and compared the growth of the resulting primary tumors with those derived from parental A673 cells. In all four groups (A673 parental; zyxin reexpression, $\alpha 5$ integrin

reexpression, or zyxin plus $\alpha 5$ integrin reexpression), 90-100% of the mice formed luciferase positive tumors within 4 weeks after intratibial injection (Figure 5.4A). Histological analysis of tissue sections taken at week 4 revealed that all of the tumors exhibit small round blue cell morphology characteristic of Ewing sarcoma and were CD99-positive by immunohistochemistry (Supp Fig S.1). Light microscopic examination revealed no differences among the four tumor groups. Likewise, significant osteolysis (>Grade 3) was evident in radiographs of the affected tibias at 4 weeks for tumors derived from all four cell variants (Figure 5.4B).

Although all four tumor cell variants formed palpable tumors and osteolytic lesions, *in vivo* luciferase based imaging of tumors derived from A673 cells coexpressing zyxin and $\alpha 5$ integrin revealed slower tumor growth than tumors derived from either parental A673 cells or cells expressing just one of the transgenes (Figure 5.4C). This observation suggests that EWS/FLI mediated downregulation of zyxin and $\alpha 5$ integrin synergistically facilitates tumor growth.

The reduction in primary tumor growth by Ewing sarcoma cells that expressed both zyxin and $\alpha 5$ integrin raised the possibility that reexpression of these two focal adhesion proteins might impact cell proliferation rate. To test this possibility directly, we measured cell growth in culture (Figure 5.4D). The three reexpression lines displayed growth curves that were indistinguishable from that of the parental A673 Ewing sarcoma cells, indicating that anchorage-dependent cell proliferation was not detectably influenced by altering zyxin or $\alpha 5$ integrin levels. In striking contrast, simultaneous reexpression of zyxin and $\alpha 5$ integrin in A673 cells results in ~40% reduction in the number of cell colonies in a soft agar transformation assay, whereas neither individual protein resulted in a statistically significant impact (Figure 5.4E). Consistent with our quantitative analysis

of viable tumor cells by *in vivo* luciferase monitoring in Figure 5.4C, coexpression of zyxin and $\alpha 5$ integrin synergistically retards cell growth in soft agar. In particular, the reduction in zyxin and $\alpha 5$ integrin that occurs in response to EWS/FLI expression enhances the cells' capacity to proliferate under anchorage-independent growth conditions.

EWS/FLI-dependent repression of $\alpha 5$ integrin, expression
abrogates metastatic lung colonization

Because of the impact of cell adhesion in establishing metastatic potential (Arjonen et al., 2011; Patel et al., 2011), it was of interest to evaluate whether repression of zyxin and/or $\alpha 5$ integrin expression influences this process. The tibial injection model we developed, in which metastasis of Ewing sarcoma cells follows the pattern of sites observed clinically in patients, enabled us to probe the roles of zyxin and/or $\alpha 5$ integrin in the spatial and temporal regulation of metastasis. A673 parental Ewing sarcoma cells, or cells engineered to reexpress zyxin and/or $\alpha 5$ integrin were introduced into recipient mice by intratibial injection and were followed by weekly *in vivo* luciferase imaging for 4 weeks, to evaluate the rate at which metastasis (positive chest signal) developed for each A673 sarcoma cell variant (Figure 5.5A). Interestingly, mice injected with Ewing sarcoma cells that reexpressed $\alpha 5$ integrin alone or in concert with zyxin revealed positive luciferase signal in the chest earlier than mice injected with Ewing sarcoma cells harboring empty vector or zyxin only (Figure 5.5A). By 3 weeks after intratibial injection, intravital imaging revealed evidence of tumor burden beyond the initial site of tumor cell injection, for Ewing sarcoma cells expressing empty vector. At this time, differential levels of metastasis were already evident for the different molecular variants of A673 Ewing sarcoma cells. Metastasis was observed in approximately 20% of animals

harboring the parental A673 tumor cells or A673 cells programmed to reexpress zyxin, whereas tumor cells programmed to reexpress $\alpha 5$ integrin either alone or with zyxin, more than tripled the frequency of evident metastases. By week 4, differences in the behavior of the tumor cell variants was further accentuated, with metastasis evident in approximately 90-100% of the animals injected with A673 sarcoma cells that reexpressed $\alpha 5$ integrin alone or with zyxin, and 40% of animals injected with A673 cells programmed to reexpress zyxin, and 50% of animals injected with parental A673 cells (Figure 5.5A-5.5B)

We examined the propensity of the metastatic tumor cells to colonize the lung, a common site of metastasis in human Ewing sarcoma patients. When animals were sacrificed at 4 weeks post injection, lungs were isolated by dissection, examined macroscopically, and prepared for histological staining and immunohistochemistry. Although dissected lungs had macroscopically visible metastatic lesions, lungs derived from mice injected with cells expressing $\alpha 5$ integrin either alone or with zyxin were extensively riddled with lesions at high frequency (Figure 5.5C). Stained sections of lung tissue displayed small round blue cells that were positive for the Ewing sarcoma marker, CD99 (Figure 5.5C). When dissected bones and organs of sacrificed mice were examined for presence of metastasis by luciferase imaging, mice across all four groups showed presence of bone metastasis in addition to lung metastasis (Figure 5.5D). Common sites for presence of bone metastasis were uninjected leg, upper limb, spine and ribs. These results illustrate that in our model EWS/FLI-mediated downregulation of zyxin and $\alpha 5$ integrin still led to detectable metastasis to lungs and bones, consistent with metastatic sites reported in the human disease.

Reexpression of adhesion proteins in Ewing sarcoma cells increases the cellular adherence to lung parenchyma *in vivo*

To test if the increased adhesion of Ewing sarcoma cells reexpressing zyxin and/or $\alpha 5$ integrin (as in Figure 5.2L) could explain the high incidence of lung lesions in our mouse experiments, we used a lung colonization assay wherein we differentially labeled Ewing sarcoma cells harboring empty vector using the red lipophilic dye (DiI), and cells reexpressing zyxin and/or $\alpha 5$ integrin were marked green using the lipophilic dye (DiO). An equal mix of control cells and cells reexpressing zyxin and/or $\alpha 5$ integrin were injected into the bloodstream of immunodeficient mice via tail vein (Padua et al., 2008). Lungs were harvested 24 hours post injection and scanned for the presence of fluorescently labeled red or green cells adhering to lung parenchyma (Figure 5.6A-C). Although Ewing sarcoma cells adhered to the lung tissue, they exhibited higher adhesion when these tumor cells reexpressed zyxin and/or $\alpha 5$ integrin. This was clearly indicated by increased ratio of green cells in the lung parenchyma compared to red cells (Figure 5.6). Expression of zyxin (Figure 5.6A), $\alpha 5$ integrin (Figure 5.6B), or both zyxin and $\alpha 5$ integrin (Figure 5.6C) significantly increased adhesion of cells to lung parenchyma (Figure 5.6D). Therefore, Ewing sarcoma cells expressing zyxin and/or $\alpha 5$ integrin exhibited high adhesion in our *in vitro* and *in vivo* experiments, suggesting that EWS/FLI mediated downregulation of zyxin and $\alpha 5$ integrin reduces tumor cell adhesion which could determine Ewing sarcoma cell behavior and metastasis.

Discussion

Nearly all cases of Ewing sarcoma harbor the t(11;22) chromosomal translocation and are micrometastatic at presentation. However, very little is understood about how EWS/FLI expression - which represses many more genes than it activates - affects

complex cell behaviors that dictate Ewing sarcoma tumor progression and metastasis (May et al., 1993b; Owen et al., 2008; Smith et al., 2006). In order to dissect the mechanism by which EWS/FLI affects tumor cell properties such as cytoarchitecture and cell adhesion, we used patient-derived Ewing sarcoma cell lines to identify the misregulated genes responsible for the tumor phenotypes.

It should be noted that this is the first study that examines multiple downregulated targets of EWS/FLI to evaluate tumor cell behavior, revealing that the knockdown of EWS/FLI leads to compromised cytoskeletal integrity and adhesiveness of Ewing sarcoma cells. Analysis of the gene expression signature of EWS/FLI using a previously published microarray (Owen et al., 2008) showed that the targets that were most downregulated by EWS/FLI were focal adhesion proteins, extracellular matrix (ECM)-receptor proteins and the regulators of actin cytoskeleton. We therefore proposed that such genes could play a critical role in modulating tumor cell adhesion, cell spreading, and interaction of tumor cells with their environment, hence affecting tumor progression and metastasis. These processes have not been well studied in Ewing Sarcoma, but could explain unique cellular properties of this micrometastatic tumor. Here, we have dissected the impact of two such EWS/FLI downregulated targets: zyxin (a focal adhesion protein) and $\alpha 5$ integrin which, along with $\beta 1$ integrin subunit, forms the receptor for binding fibronectin - a prominent bone matrix component. We reexpressed these proteins in patient-derived Ewing sarcoma cells either alone or in combination with each other to identify the unique and distinct contributions of zyxin and $\alpha 5$ integrin in Ewing sarcoma biology.

We propose that downregulation of these adhesion proteins and inhibition of the ECM-receptor mediated cell signaling is relevant to the transformation of Ewing sarcoma

cells. In the current study we show that reexpression of $\alpha 5$ integrin in the small round Ewing sarcoma cells improves cell spreading which could be attributed to increased size of focal adhesions, but when zyxin is reexpressed in these cells, either alone or along with $\alpha 5$ integrin, dramatic change in the actin cytoskeleton coincides with increased cell spreading. This difference could be attributed to the increased number and size of focal adhesions required for stabilizing the actin stress fiber network in cells. We also report an increase in the number of focal adhesions when zyxin is expressed in cells, either alone or with $\alpha 5$ integrin to greatly foster robust actin stress fiber network in Ewing sarcoma cells with a modest improvement in cell adhesion. This compromised cell adhesion due to downregulation of zyxin and disruption of $\alpha 5$ integrin-fibronectin interaction could be critical for Ewing sarcoma tumor growth, as observed by reduction in number of colonies in soft agar transformation assays when both zyxin and $\alpha 5$ integrin are reexpressed in Ewing sarcoma cells. Interestingly, similar to increased cell adhesion and well spread fibroblast-like morphology seen in Ewing sarcoma cells reexpressing $\alpha 5$ integrin, it is well known that expression of $\alpha 5\beta 1$ integrin promotes fibroblast like morphology of cells (Truong and Danen, 2009). This observation contributes to the increasing body of evidence that mesenchymal cells could be the cell of origin for Ewing sarcoma (Riggi et al., 2008; Tirode et al., 2007), potentially by disrupting the interaction between $\alpha 5$ integrin and fibronectin in the bone.

Knowing that bone is the most common site for occurrence of Ewing sarcoma, in the present study, we injected the patient derived Ewing sarcoma cells into the mouse tibia to study tumor growth and metastasis of Ewing sarcoma from long bones of mice. This mouse model recapitulated several features of the human disease by showing rapid growth of the tumor with extensive osteolysis and spontaneous metastasis to other bones

and lungs but not to liver or other vital organs. To our knowledge, this is the first report that shows spontaneous metastasis of Ewing sarcoma from the primary boney site to other bones. Using RT-PCR analysis we detected Ewing sarcoma cells in the blood (data not shown), confirming that these cells metastasized hematogenously similar to that in human patients. Observations like the tissue specific metastasis of Ewing sarcoma to lung and bones but not the liver, despite using blood circulation for metastasis highlight the role of tumor microenvironment in Ewing sarcoma (Kerbel, 1995; Mundy, 2002). We therefore consider this mouse model highly relevant for studying Ewing sarcoma. For example, this mouse model will adequately represent the interaction of $\alpha 5 \beta 1$ integrin to the fibronectin matrix, which is so abundantly present in the bone.

Reexpression of $\alpha 5$ integrin and zyxin together (but not alone) in Ewing sarcoma cells, reduces the rate of growth for tibial tumors, similar to loss of transformation seen in soft agar assays, but also had increased rate of metastasis. Interestingly though, reexpression of $\alpha 5$ integrin alone or in combination with zyxin, led to early metastasis of Ewing sarcoma cells to the chest area consequently leading to larger lesions in the mouse lungs. These results raise an interesting concept that EWS/FLI mediated repression of zyxin and $\alpha 5$ integrin affects cellular morphology and cell adhesion to facilitate tumor cell growth and transformation, but the same repression also appears to compromise at least one step of metastasis, such as the ability of these cells to adhere and colonize at a secondary site, such as lungs in the current mouse model. Such uncoupling of tumor progression and metastasis by an oncogene has been suggested previously by other researchers as well (Bernards and Weinberg, 2002).

The reasons for the micrometastatic nature of Ewing sarcoma cells could be many. The EWS/FLI mediated transformation could also simultaneously lead to tumor

cell dissemination (Chaturvedi et al., 2012), or regulate expression of EWS/FLI based on growth factors in the tumor microenvironment (Girnita et al., 2000) or even be correlated to size of the primary tumor (Rodriguez-Galindo et al., 2008). Based on these findings, as the solid tumor grows, the tumor microenvironment could induce changes in gene expression or matrix availability. It has been shown that microenvironmental changes such as hypoxia increases the expression of $\alpha 5$ integrin, which in turn increases the adhesion of cells to fibronectin affecting downstream signaling and hence cell metastasis (Indovina et al., 2008). Such a situation is duplicated in our experiments with reexpression of $\alpha 5$ integrin (either alone or with zyxin) in Ewing sarcoma cells, and that could explain early metastasis as seen in mice injected with these cell variants. Once in circulation, the cells show increased adhesion to lung parenchyma, as seen in the *in vivo* lung colonization assay by increasing cell adhesion.

The present study identifies a potentially crucial role of actin cytoskeleton and focal adhesion based cell-ECM interactions in Ewing sarcoma growth and metastasis. Higher expression of $\alpha 5\beta 1$ integrin in certain cancer cells improves the actin cytoskeleton, increases cell spreading and improves the interaction of $\alpha 5\beta 1$ expressing cells to the available fibronectin and collagen matrix, thereby increasing contractile forces and cellular invasion (Mierke et al., 2011). In our study, we found that expression of zyxin significantly improves actin cytoskeleton and makes a modest contribution to cell adhesion, whereas expression of $\alpha 5$ integrin improves cell adhesion and spreading without much contribution to the actin cytoskeleton. When these proteins are expressed together, the Ewing sarcoma cells show higher cell adhesion, spreading and a strong stress fiber network. We therefore propose that reexpression of zyxin improves the actin cytoskeleton required for generation of contractile forces through increase in number and

size of focal adhesions, and expression of $\alpha 5$ integrin improves the interaction to fibronectin matrix present in the bone.

Our findings illustrate that the causative oncogene for Ewing sarcoma simultaneously affects both cell proliferative capacity as well as a wide range of cellular phenotypes that could influence tumor cell dissemination or metastatic colonization. Understanding how EWS/FLI mediated downregulation of adhesion genes, integrins and cytoskeletal proteins affects early and late tumor cell dissemination or affects tumor cell adhesion and colonization at secondary sites, through its effects on the actin cytoskeleton and cell adhesion invasion and metastasis is critical to understanding the micrometastatic nature of this disease. The loss in cellular adhesion observed in EWS/FLI transformed cells could prevent formation of multilayer foci required for formation of solid tumors (Taverna et al., 1998, Hynes 1998), and it could simultaneously promote early dissemination of tumor cells (Chaturvedi et al., 2012). We also suggest that Ewing sarcoma cells and/or EWS/FLI expression is especially sensitive to microenvironmental cues and through changes in downstream gene expression influences tumor cell behavior to establish successful metastatic lesions. Evaluating the effect of adhesion proteins on the rate of tumor cell dissemination will be the focus of future studies in which a higher degree of temporal resolution and detection of circulating tumor cells is possible.

These studies illustrate the need to study tumors in their relevant microenvironment to understand how the tumor cell behaviors observed in cell culture experiments affect disease progression. In addition, our findings demonstrate the existence of ‘tradeoffs’ that occur within oncogenic programs. For example, in the case of Ewing sarcoma, downregulation of zyxin and $\alpha 5$ integrin expression confers an apparent advantage to the tumor by enhancing anchorage independent cell growth, while

at the same time reducing the capacity for metastatic lung colonization. These findings illustrate the multifactorial complexity of tumor biology and remind us that not all gene expression changes observed in tumors are advantageous for all aspects of tumor initiation and progression.

Materials and Methods

Reagents and antibodies

Antibodies were used for Western immunoblots, indirect immunofluorescence microscopy, and immunohistochemistry as per manufacturer's instructions: paxillin mouse antibody (Transduction Laboratories P13520), FLI-1 rabbit antibody (AbCam 15289), zyxin rabbit antibody (Beckerle Lab B71), $\alpha 5$ integrin (BD Bioscience), β -actin AC-74 mouse antibody (Sigma-Aldrich), β -tubulin mouse antibody (Developmental Studies Hybridoma Bank 12G10), CD99 (clone 0-13) mouse antibody (Signet #620-01). Secondary antibodies were HRP-conjugated antibodies for immunoblots (GE Healthcare), the Alexa-Fluor antibodies and phalloidin for microscopy (Molecular Probes/Invitrogen), and biotinylated rabbit antimouse antibody (Dako #E0413) for immunohistochemistry. Fibronectin to coat coverslips and Mowiol to mount coverslips (Sigma-Aldrich), Vybrant Cell-Labeling solutions DiI and DiO (Molecular Probes/Invitrogen) were used as per manufacturer's instructions. D-Luciferin (Gold Biotech #Luck) was injected for bioluminescence detection. Prolong Gold antifade reagent with DAPI (Invitrogen/Gibco Life Technologies #P-36931) was used for mounting lung sections.

Cell culture

Ewing sarcoma cell lines A673 and EWS502 were grown in DMEM media with 10%FBS, and RPMI media with 15% FBS, respectively, as previously published (Owen and Lessnick, 2006). Selection antibiotics puromycin (Sigma), neomycin (Gibco), hygromycin (Invitrogen) were used at (puromycin 2 μ g/ml, neomycin 300 μ g/ml, hygromycin 100 μ g/ml).

Constructs and retroviruses

Knockdown experiments used the luciferase-RNAi (as control RNAi), and EF-2-RNAi (as EWS/FLI RNAi) constructs in pSRP retroviral vector with a puromycin resistance marker previously described (Chaturvedi A et al., 2012; Smith et al., 2006). For expression constructs, the human zyxin cDNA was cloned into pMSCV-neomycin retroviral vector (Clontech). The α 5 integrin cDNA cloned in pMSCV-puromycin retroviral vector was a kind donation from Dr. Christopher Stipp (University of Iowa). For luciferase expression in mice, pMMP-LucNeo or pMMP-LucHygro retroviruses were used as previously described (Owen and Lessnick, 2006). Following retroviral infection for 2 days, cells were selected (puromycin, neomycin, or hygromycin) for 2 days prior to use and maintained for up to 5 weeks.

Western blots

Whole cell lysates in RIPA buffer (10 mM Tris-HCl pH7, 100 mM NaCl, 1 mM ETA, 1% TritonX-100, 0.5% Na-Deoxycholate, 0.1% SDS) with Complete Mini-EDTA free protease inhibitor cocktail tablets (Roche Diagnostics GmbH, Cat#11836153001) were electrophoresed (15-30 μ g/lane) on 10% SDS-PAGE gels and transferred onto nitrocellulose membranes. Proteins were detected with antibodies for FLI-1 (1:2,000),

zyxin (1:10,000), $\alpha 5$ integrin (1:5,000), tubulin (1:10,000) and HRP-conjugated secondary antibodies followed by Enhanced ChemiLuminescence detection (GE Healthcare).

Immunofluorescence microscopy

The staining, microscopy, imaging and analysis of fluorescently labeled cells was done as previously described (Chaturvedi A et al., 2012). A673 cells (75,000 cells) were plated on fibronectin-coated (10 μ g/ml) coverslips in 12 well plates for 24 hrs, fixed in 3.7% formaldehyde for 15 min. and permeabilized in 0.2% Triton X-100/PBS for 5 min. Cells were incubated with paxillin antibody (1:100) for 1 h at 37°C, washed (PBS), stained with AlexaFluor antimouse antibody (1:200), AlexaFluor phalloidin (1:100) and DAPI (1:600) for 1 h at 37°C, washed (PBS) and mounted in Mowiol medium. Cells images were captured with a Zeiss Axioskop2 mot plus microscope with a 40X objective (NA 0.75 NeoFluor), AxioCam MR camera, and Axiovision v4.8.1 software (Carl Zeiss MicroImaging, Inc.) or with a Nikon A1R Ti inverted microscope, 60X oil objective (NA1.4 Plan Apo DIC N2) and Nikon Elements v3 software).

Cell area, number and size of focal adhesions

To quantify these cellular features, Ewing sarcoma cells stained with paxillin antibody and phalloidin were analyzed using immunofluorescent images (Nikon A1R Ti inverted microscope with 60X Oil objective) as previously described (Chaturvedi et.al, 2012). Briefly, using the trace tool the boundaries of phalloidin-stained cells were outlined and area of the selected region measured (Metamorph v7.5 software). To count and measure the size of the paxillin-rich focal adhesions, single-cell images were first processed (despeckle, remove noise, background subtracted with rolling ball) in NIH

freeware Image J. Image threshold was set in single cell images and the area of the thresholded region represented the size of focal adhesions (Metamorph imaging v 7.5 software). At least 35 cells were analyzed for each cell type.

Cell growth assays

3T5 Cell growth assays were performed as described in (Smith et al., 2006). Briefly, 5×10^5 cells were seeded into 10 cm dishes for growth in tissue culture and counted every third day to determine the rate of cell proliferation and population doubling time calculated.

Soft agar transformation assays

These assays were performed in triplicates as previously described (Chaturvedi A et al., 2012; Lessnick et al., 2002). In short, 1×10^5 cells were seeded in 0.35% agarose made in Iscove's modification Eagle's media, penicillin/streptomycin and glutamine with or without selection, grown for 3-4 weeks, imaged and colony count noted.

Adhesion assays

Adhesion assays were performed in triplicates for each cell type following previously published protocols (Chaturvedi A et al., 2012; Hoffman et al., 2006). Ewing sarcoma cells (300,000) were seeded in triplicate onto a non-ECM coated 24 well plate for 2 hrs at 37°C, fixed in 3.7% formaldehyde (15 min), stained with 1% Toluidene Blue for 1 h, washed, air dried and dissolved in 2% SDS. O.D. is measured at 620nm.

In vivo mouse model

All animal protocols were approved by the Institutional Animal Care and Use Committee at the University of Utah. Male 5-6 weeks old NOD/SCID mice (Charles

River Labs strain code #394) were obtained and housed at Utah for 1 week prior to experiments. The intratibial model studies were modified from a previously published method (Guan et al., 2008). Mouse tibias were predrilled with a 26g needle, x-rayed to validate needle placement, then Luciferase expressing Ewing sarcoma cells (2.5×10^5 cells in 10 μ l Matrigel; control A673 cells with empty vectors, A673 cells engineered to express zyxin, or $\alpha 5$ integrin or both zyxin and $\alpha 5$ integrin together) were injected with a glass Hamilton syringe and 45° bevel 26g needle. Tumor growth was monitored weekly for 4 weeks by injecting mice intraperitoneally with Luciferin, anesthetizing (Isoflurane) the mice and measuring the emitted photons/sec (Xenogen IVIS 100 Imager and Living Image v2.50.2 software). Tumor volume was measured with calipers and calculated using the formula $0.5 \times a \times b \times c$, where a, b and c are the three maximum diameters. Weekly X-rays were recorded (Kodak DXS4000) and osteolytic destruction of injected tibias were scored in a blind study by an independent analyst (L.R.). Bone lysis was graded on a scale of 0 to 4 where grade 0 represented no bone loss, grade 1 minimal but visible, grade 2 moderate (no cortex affected), grade 3 severe (cortex disrupted) and grade 4 signifies massive bone destruction (Guan et al., 2008). After 4 weeks the mice received a final luciferin injection, were sacrificed, the lungs were perfused intratracheally with 4% paraformaldehyde, the bone tumors and lungs were removed, imaged for *ex vivo* luciferase signal and fixed in neutral buffered formalin. *Ex vivo* luciferase signal of organs (lung, liver, spleen, kidney, heart, testes, injected tibias and uninjected bones) was used to evaluate other sites of metastasis. Prior to paraffin embedding, the fixed lungs were photographed (whole lung images) to evaluate macroscopically visible lesions.

Immunohistochemical analysis

The fixed bone tumors were decalcified for 7 days before embedding in paraffin. The embedded tibias and lungs were sectioned and stained with H&E, or IHC with CD99 (ARUP Laboratories, Salt Lake City UT). The expression of CD99 was detected using clone O-13 antimouse antibody (1:200 dilution) for 2 hrs at 37°C. Biotinylated secondary antibody (1:100) was applied for 32 min at 37°C. Signals were detected with a Streptavidin-HRP system, utilizing DAB (3-3' diaminobenzidine) as the chromogen (Research DAB detection kit; Ventana Medical Systems). The slides were counterstained with hematoxylin (Ventana Medical Systems) for 8 min, gently washed in dH₂O/DAWN mixture, placed in iodine for 30 seconds, then dipped in sodium thiosulfate, dehydrated in graded alcohols (70%, 95% x2 and 100% x2), cleared in xylene, and then coverslips mounted (Sheryl Tripp at ARUP and YCL at HCI). The tibia and lung sections were evaluated by an independent clinical pathologist (A.G.) in a blind study.

In vivo lung adhesion assay

These assays were performed as previously described (Chaturvedi et al. 2012; Padua et al., 2008). Briefly, A673 cells with empty vector were labeled with Vybrant DiI (red) and A673 cells with expression of zyxin, or $\alpha 5$ integrin, or with both zyxin and $\alpha 5$ integrin were labeled with Vybrant DiO (green). The red and green cells were mixed in a 1:1 ratio and 1 million cells were injected into the tail-vein of NOD/SCID mice (Jackson Labs #1303) and allowed 24 hrs to circulate in the mouse. Mice were sacrificed after 24 hrs, lungs were perfused intratracheally with 4% paraformaldehyde, removed and cryopreserved in OTC freezing medium. Lungs were cryosectioned into 16 μ m sections

and examined on a Nikon A1R laser scanning confocal microscope (9.2 μm optical sections, PlanFluor 40X oil DIC H N2 objective). A 3 field by 3 field (2mm X 2mm) mosaic image was created (NIS Elements v3 software) and red versus green colonies counted in 15 representative fields from 3 mice. Two such biological replicates were done.

Microarray analysis

Previously published microarray data set was reanalyzed for downregulated targets of EWS/FLI (Owen et al., 2008). Expression data was filtered for a 1.8-fold change across samples and significant changes were identified using permutation testing with a p-value of 0.01 after Benjamini and Hochberg correction and significant z-score in GeneSifter analysis software.

Statistical analysis

Graphs were made in and analyzed using Prism 5 software (Graph Pad, San Diego).

Acknowledgements

We are grateful to Dr. Christopher Stipp from the University of Iowa for donating the pMSCVpuro- $\alpha 5$ integrin cDNA construct to overexpress $\alpha 5$ integrin. We would like to thank Dr. Christopher Rodesch at the University of Utah Cell Imaging and Microscopy Core Facility for help with fluorescent imaging, image processing and analysis and thank Dr. Brett Milash at Huntsman Cancer Institute for help with microarray analysis. We acknowledge Diana Lim for help with manuscript preparation. This work was supported by the NIH (R01 GM50877 to M.C.B. and R01 CA140394 to SLL) and the Huntsman

Cancer Foundation. The Cancer Center Support Grant (2 P30 CA042014) awarded to Huntsman Cancer Institute provided developmental funds and Shared Resources critical to this project.

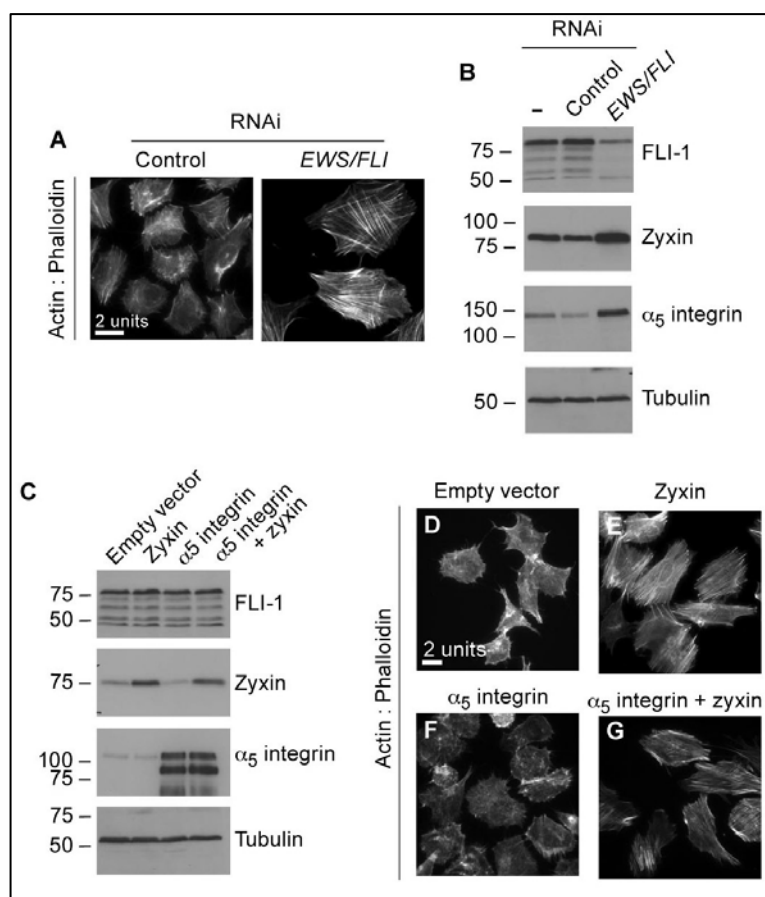


Figure 5.1: EWS/FLI-dependent changes in the actin cytoskeleton and contributions of cytoskeletal regulators. (A) Widefield fluorescent images of A673 Ewing sarcoma cells stained with phalloidin to visualize the actin filament network. A673 cells with EWS/FLI RNAi had robust actin cytoskeletons and were more spread than A673 cells with control RNAi. Scale bar 20 μ m. (B) Western immunoblot of parent Ewing sarcoma A673 cells (lane 1), A673 cells with control RNAi (lane 2) or EWS/FLI RNAi (lane 3) were probed with antibodies for FLI-1, zyxin, α_5 integrin and tubulin (loading control). EWS/FLI knockdown resulted in increased zyxin and α_5 integrin protein. (C) Western immunoblot of Ewing sarcoma cells engineered to express empty vector, zyxin, α_5 integrin, or both α_5 integrin + zyxin were probed with antibodies for FLI-1, zyxin, α_5 integrin, and tubulin (loading control). Expression of zyxin or α_5 integrin above the endogenous levels in A673 cells did not affect the level of the other protein. (D-G) Widefield fluorescent images of phalloidin-stained A673 cells engineered to express empty vector (D), zyxin (E), α_5 integrin (F) or both α_5 integrin + zyxin (G) suggest increased actin cytoskeleton and cell spreading in cells that re-express these proteins.

Figure 5.2: Zyxin and $\alpha 5$ integrin contribute to the actin cytoskeleton, focal adhesions, cell spreading and cell adhesion in Ewing sarcoma cells. (A-H) A673 cells engineered to express empty vector (A, E), zyxin (B, F), $\alpha 5$ integrin (C, G) or both $\alpha 5$ integrin + zyxin (D, H) were stained for actin filaments (phalloidin, A-D) and focal adhesions (paxillin, E-H) followed by immunofluorescent microscopy. Control A673 cells were small and round with minimal actin stress fibers and few focal adhesions. Cells that express zyxin, $\alpha 5$ integrin, or both $\alpha 5$ integrin + zyxin were well spread with prominent focal adhesions. Focal adhesion size (I) and number per cell (J) were quantitated and compared between control and EWS/FLI RNAi cells and cells that express zyxin, $\alpha 5$ integrin, or both $\alpha 5$ integrin + zyxin. EWS/FLI knockdown and expression of zyxin and $\alpha 5$ integrin increased the size of focal adhesions. (K) Total cell area was measured in phalloidin-stained cells with either RNAi (control and EWS/FLI) or that express zyxin, $\alpha 5$ integrin, or both $\alpha 5$ integrin + zyxin. Cell spreading and size increased with EWS/FLI knockdown and with expression of zyxin and $\alpha 5$ integrin. (L) Cell adhesion was evaluated by plating cells for 2 hrs, followed by colorimetric detection. Cells with control RNAi or empty vector adhered less than cells with EWS/FLI RNAi or cells that express zyxin, $\alpha 5$ integrin, or both $\alpha 5$ integrin + zyxin. (M) Model of Ewing sarcoma cell phenotypes. The actin cytoskeleton and focal adhesions, cell spreading and cell area are changed by these proteins in unique and distinct ways. EWS/FLI expression compromises Ewing sarcoma cell adhesion by influencing the actin cytoskeleton, cell morphology and spreading, perhaps due to the downregulation of cell adhesion proteins in general and of zyxin and $\alpha 5$ integrin in particular. ***p < 0.001, other comparisons were not statistically different.

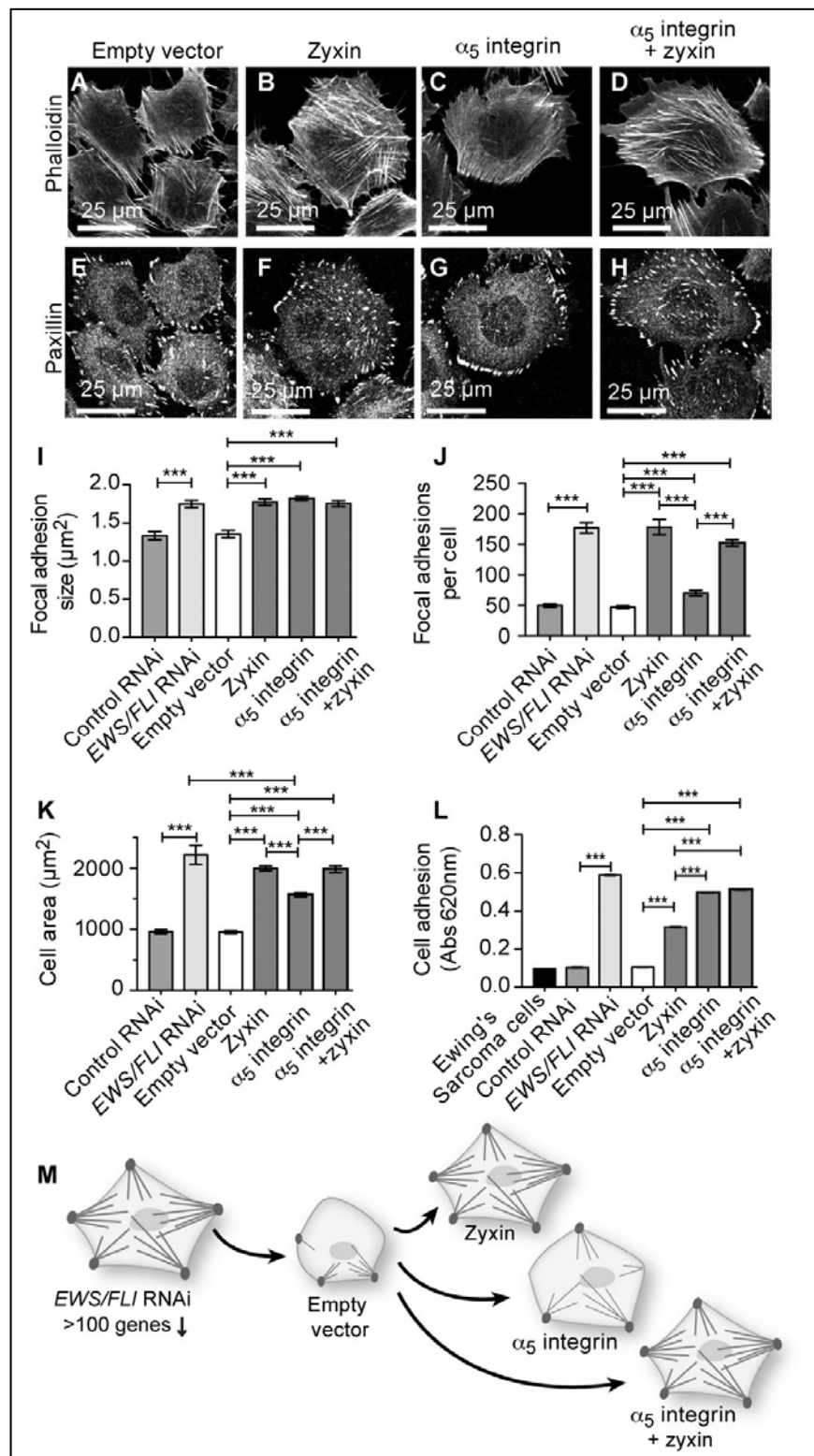


Figure 5.3: Intratibial orthotopic mouse model for Ewing sarcoma recapitulates features of the human disease. (A) Schematic diagram of the orthotopic mouse model wherein A673 Ewing sarcoma cells engineered to express luciferase were injected into the tibia, then monitored weekly for 4 weeks for tumor growth and metastasis, followed by *ex vivo* analysis and histopathology. (B) Tibial tumor growth and proliferation of Ewing sarcoma cells was measured by *in vivo* luciferase bioluminescent imaging. (C) Osteolysis (white arrows indicating regions of bone loss) increased compared to the same mouse tibia at week 1. (D) Qualitative analysis of mouse radiographs by an independent analyst revealed ~85% of mice had high grade osteolysis (Grades 3 or 4) in the injected tibias. (E) Histopathological analysis of tibial tumors showed highly invasive tumor in the tibia (5X Panel 1) and closer examination (20X-panel 2, 400X-panel 3) revealed the presence of typical small round blue Ewing sarcoma cells. Membranous staining for Ewing sarcoma marker CD99 (brown staining in panel 4) confirmed Ewing sarcoma cells in the tibial tumor. (F) Mouse lung with metastatic lesions sectioned and stained by H&E (panel 1, 2) also contained small round blue cells typical of Ewing sarcoma and the lung was positive for Ewing sarcoma marker CD99 (brown staining in panel 3). (G) Representative *ex vivo* luciferase imaging to evaluate metastasis in lungs and bones at harvest.

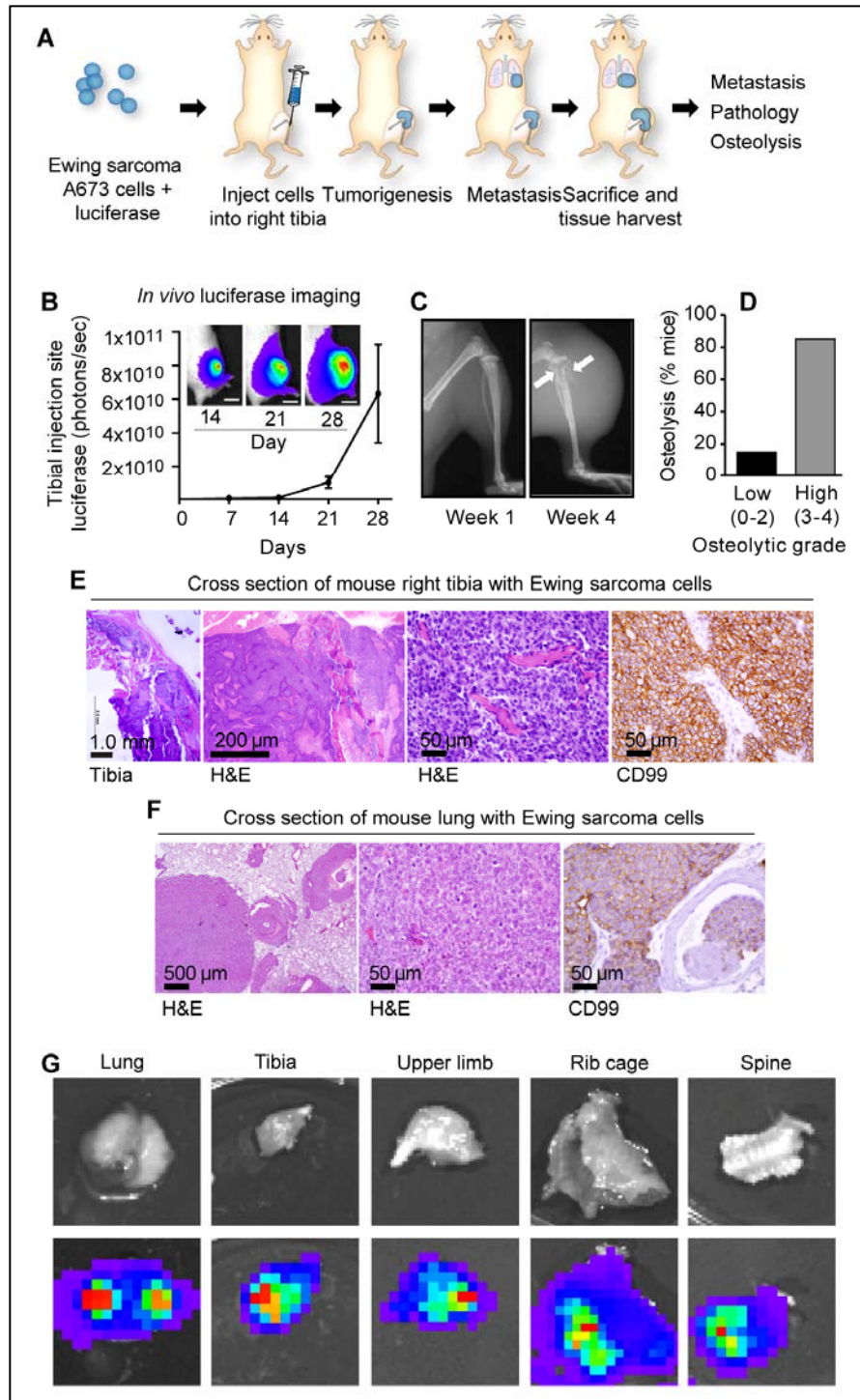


Figure 5.4: Zyxin and $\alpha 5$ integrin coexpression in Ewing sarcoma cells reduce tumor growth while osteolytic degradation of bone persists. (A) *In vivo* luciferase imaging 4 weeks after mice were injected intratibially with Ewing sarcoma A673 cells engineered to express empty vector, zyxin, $\alpha 5$ integrin, or both $\alpha 5$ integrin + zyxin. Every cell type was capable of inducing tibial tumors. (B) Radiographs of tibias 4 weeks following injections with cells that express empty vector, zyxin, $\alpha 5$ integrin, or both $\alpha 5$ integrin + zyxin revealed high grade osteolysis (white arrows) regardless of which cell type was injected. (C) *In vivo* luciferase imaging of tibial tumors for 4 weeks. Bioluminescent signals restricted to the tibial tumor region were quantitated (photons/sec) and graphed over time. Expression of $\alpha 5$ integrin + zyxin in Ewing sarcoma slowed the tumor growth compared to the other groups. (D) 3T5 cell growth assay of A673 Ewing sarcoma cells with empty vector, zyxin, $\alpha 5$ integrin or both $\alpha 5$ integrin + zyxin did not detect a difference in growth and proliferation in culture. (E) Soft agar transformation and colony formation of cells with empty vector, zyxin, or $\alpha 5$ integrin alone were not different. However, colony formation in soft agar was inhibited in A673 cells that expressed both $\alpha 5$ integrin and zyxin. * $p < 0.001$, *** $p < 0.0001$.

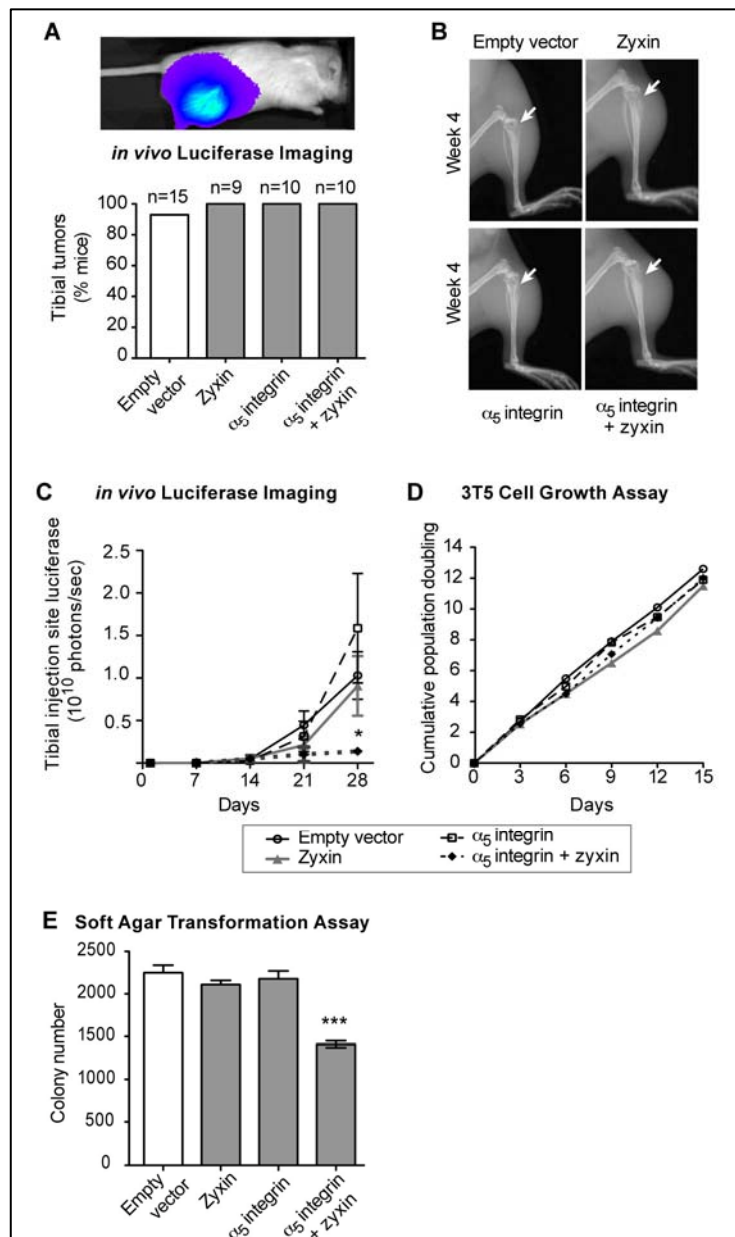
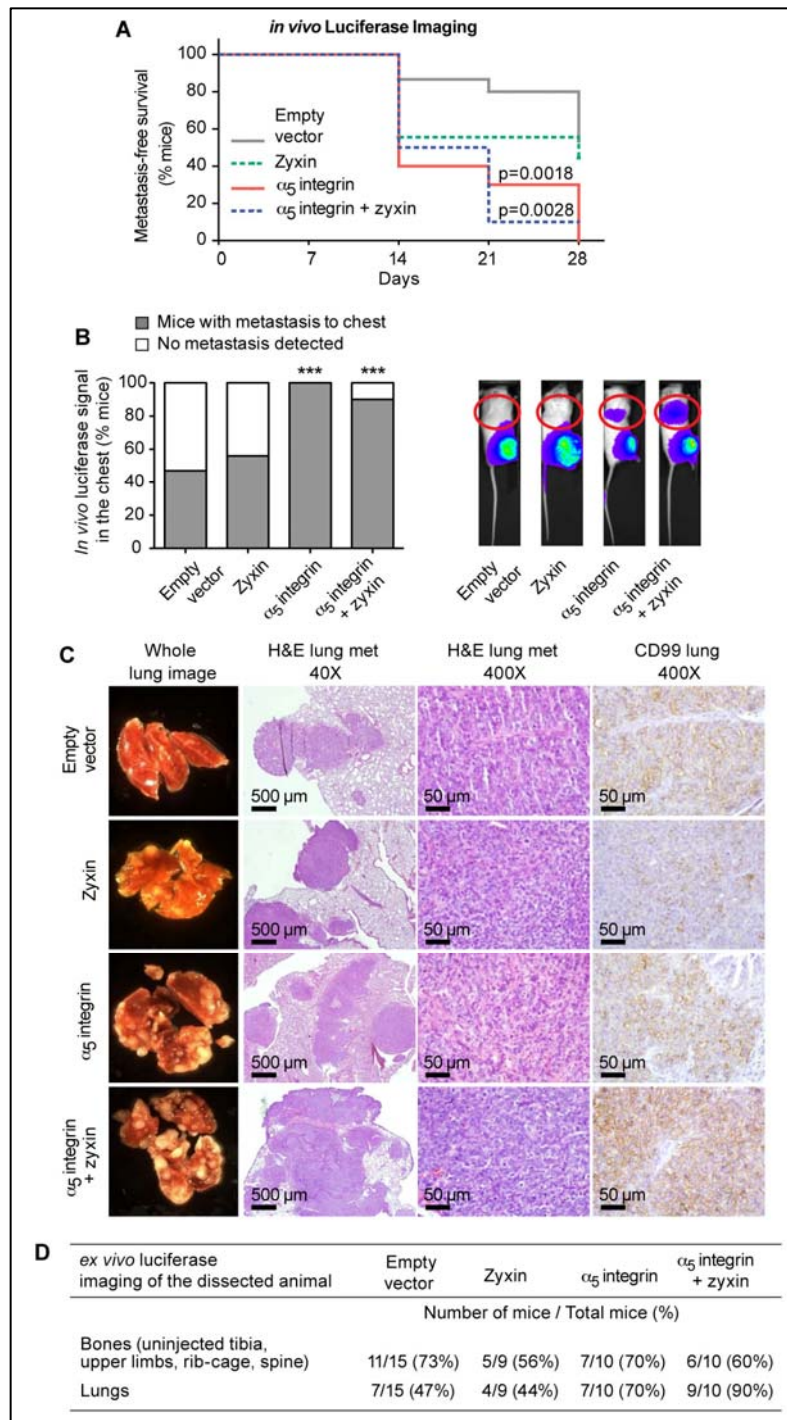


Figure 5.5: Ewing sarcoma cells that express zyxin and $\alpha 5$ integrin metastasize to lungs and bones. (A) Metastasis-free survival curve of mice evaluated by *in vivo* luciferase imaging of the four cell-type groups at weekly intervals. Metastasis was defined as appearance of bioluminescent signal other than at injection site, primarily the chest area. The mice injected with Ewing sarcoma A673 cells that expressed $\alpha 5$ integrin, alone or with zyxin, developed chest signal as early as week 2 or 3, while mice injected with control or zyxin-expressing cells developed chest signal at week 3 or 4 or not at all. (B) Week 4 endpoint images of *in vivo* luciferase signal were examined for metastasis. Almost all mice injected with Ewing sarcoma cells that expressed $\alpha 5$ integrin, either alone or in combination with zyxin, had significant metastasis by *in vivo* imaging, while only half the mice injected with empty vector control cells or with zyxin-expressing cells had *in vivo* chest signal at 4 weeks. Dissection of the mice revealed the chest signals were due to heavy involvement of lungs. (C) Lungs exhibited macroscopically visible lesions (column 1) that were obvious in every mouse. Paraffin-embedded lungs were sectioned, and H&E staining identified multiple metastases characterized by the presence of small round blue cells (columns 2,3). Immunohistochemistry for the Ewing sarcoma marker CD99 on lung sections (column 4, brown signal) confirmed the presence of Ewing sarcoma cells. (D) Immediately following dissection, *ex vivo* luciferase signals of multiple organs and skeletal regions were examined for each mouse. The number of mice displaying positive luciferase signal in bones, lungs, or other organs were scored and results are presented as % mice in each group. For all groups of mice, the preferred metastatic sites were bones and lungs.



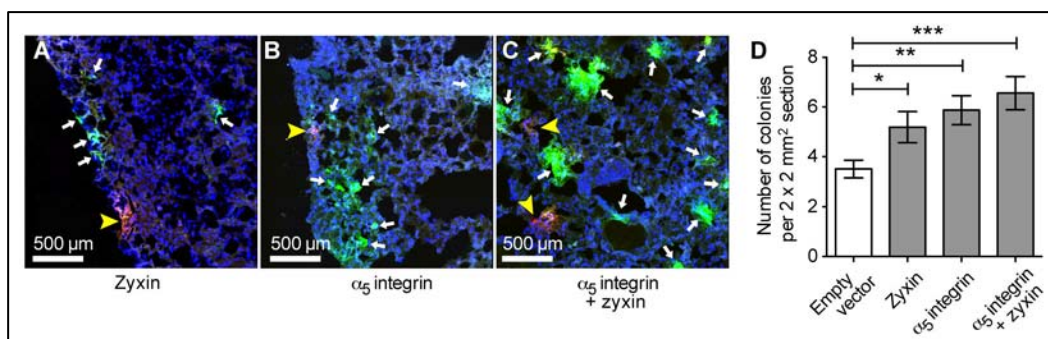


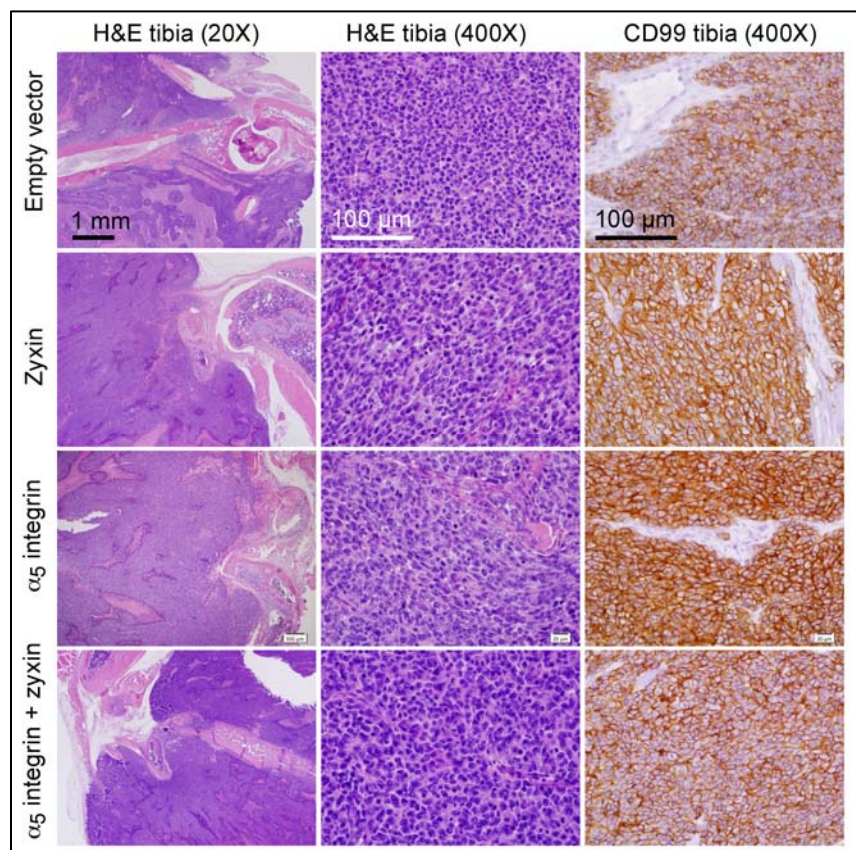
Figure 5.6: Ewing sarcoma cells that express zyxin and α_5 integrin exhibit increased adhesion to lung parenchyma. *In vivo* lung adhesion assay of Ewing sarcoma cells that express empty vector (colored red DiI) and cells that express zyxin, α_5 integrin, or both α_5 integrin + zyxin (labeled green DiO). Red and green cells were combined 1:1, 1 million cells were injected into the tail vein and given 24 hrs to circulate in the mouse. At 24 hrs, lungs were harvested, fixed, and cryosectioned. The numbers of red cell colonies and green cell colonies were evaluated by confocal microscopy of lung sections. (A-C) Maximum intensity projection of representative confocal images of lung sections, showing red cell colonies (empty vector, yellow arrowheads) versus green cell colonies (expressing zyxin and/or α_5 integrin, white block arrows) for all groups of mice. Nuclei are stained blue using DAPI. (D) Cell colonies were counted for 15 representative sections 4 mm² in area. Cells expressing zyxin or α_5 integrin accumulated more in the lung parenchyma compared to empty vector control cells. Also, cells expressing both zyxin and α_5 integrin were the most adherent group of cells with high affinity for lung parenchyma.

Table 5.1: Categories of downregulated target genes of EWS/FLI oncoprotein. The KEGG pathway groups of genes that are downregulated at least 1.8 fold by EWS/FLI are shown. The top three categories modulated by EWS/FLI are genes encoding focal adhesion-related proteins, ECM and receptor interaction proteins, and regulators of the actin cytoskeleton. The KEGG analysis therefore suggests the importance of cell adhesion and cytoskeletal pathways and components for EWS/FLI-dependent changes in Ewing sarcoma.

	KEGG Pathway	Number of genes	Gene Set	z-score
1	Focal adhesion	24	190	8.5
2	ECM-receptor interaction	14	80	8.1
3	Regulation of actin cytoskeleton	13	187	3.6
4	Amoebiasis	12	100	5.7
5	Protein processing in endoplasmic reticulum	12	144	4.2
6	Lysosome	10	109	4.1
7	Phagosome	9	139	2.7
8	Arrhythmogenic right ventricular cardiomyopathy (ARVC)	8	68	4.6
9	Cell adhesion molecules (CAMs)	8	116	2.8
10	Antigen processing and presentation	7	61	4.2
11	Natural killer cell mediated cytotoxicity	7	117	2.2
12	Protein digestion and absorption	7	70	3.7
13	Toxoplasmosis	7	118	2.1
14	Viral myocarditis	7	65	4.0
15	Adherens junction	6	71	3.0
16	Bacterial invasion of epithelial cells	6	64	3.3
17	Dilated cardiomyopathy	6	82	2.5
18	Hypertrophic cardiomyopathy (HCM)	6	79	2.7
19	Small cell lung cancer	6	83	2.5
20	Complement and coagulation cascades	5	67	2.4
21	Prion diseases	5	34	4.3
22	Shigellosis	5	55	2.9
23	Allograft rejection	4	32	3.4
24	Amino sugar and nucleotide sugar metabolism	4	42	2.7
25	Autoimmune thyroid disease	4	48	2.4
26	Bladder cancer	4	41	2.8
27	Graft-versus-host disease	4	33	3.3
28	NOD-like receptor signaling pathway	4	54	2.1
29	Type I diabetes mellitus	4	37	3.0
30	Glycosaminoglycan biosynthesis - chondroitin sulfate	2	16	2.4
31	Glycosaminoglycan degradation	2	18	2.2

Supplemental Table S.1: List of EWS/FLI downregulated target genes.

	Category	Gene Identifier	Gene ID	Fold change	p-value
Focal Adhesion-Related Genes					
1	Collagen, type VI, alpha 1	AA292373	COL6A1	15.0	0.00039
2	Collagen, type I, alpha 1	K01228	COL1A1	7.2	0.01781
3	Collagen, type I, alpha 2	NM_000089	COL1A2	6.3	0.00027
4	Placental growth factor	BC001422	PGF	4.7	0.00009
5	Baculoviral IAP repeat-containing 2	NM_0011166	BIRC2	3.7	0.00002
6	Collagen, type V, alpha 1	AI130969	COL5A1	4.3	0.00391
7	Collagen, type III, alpha 1	AU144167	COL3A1	3.9	0.00192
8	FYN oncogene related to SRC, FGR, YES	M14333	FYN	3.0	0.00017
9	Cadherin 2, type 1, N-cadherin (neuronal)	M34064	CDH2	2.7	0.00253
10	Laminin, beta 1	NM_002291	LAMB1	2.6	0.00034
11	Protein kinase C, alpha	AI471375	PRKCA	2.5	0.00676
12	Laminin, gamma 1 (formerly LAMB2)	NM_002293	LAMC1	2.5	0.00407
13	Filamin C, gamma (actin binding protein 280)	NM_001458	FLNC	2.3	0.00464
14	Integrin-linked kinase	NM_004517	ILK	2.1	0.00215
15	Zyxin	NM_003461	ZYX	2.1	0.00134
16	Calpain 2, (m/II) large subunit	M23254	CAPN2	2.0	0.00003
17	Collagen, type IV, alpha 2	AA909035	COL4A2	2.0	0.04317
18	Catenin (cadherin-associated protein), alpha 1	NM_001903	CTNNA1	1.9	0.00001
19	Vinculin	NM_014000	VCL	1.9	0.00085
20	Actinin, alpha 1	AI082078	ACTN1	1.9	0.00071
21	LIM and senescent cell antigen-like domains 1	AL110164	LIMS1	1.9	0.00443
22	Protocadherin gamma subfamily C, 3	AK026188	PCDHGC3	1.9	0.02201
23	Fermitin family homolog 2 (Drosophila)	Z24725	FERMT2	1.8	0.00040
24	Mitogen-activated protein kinase 1	NM_002745	MAPK1	1.8	0.00067
Extracellular Matrix (ECM) and Receptors					
1	CD44 molecule (Indian blood group)	AI493245	CD44	27.0	0.00012
2	Lysyl oxidase	NM_002317	LOX	18.8	0.00030
3	Periostin, osteoblast specific factor	D13665	POSTN	14.0	0.00038
4	Transforming growth factor, beta-induced, 68kDa	NM_000358	TGFBI	8.7	0.00007
5	GTP binding protein overexpressed in skeletal muscle	NM_005261	GEM	6.6	0.00001
6	Tenascin C	NM_002160	TNC	4.3	0.00035
7	Activated leukocyte cell adhesion molecule	AA156721	ALCAM	3.4	0.00011
8	Fibulin 1	NM_006486	FBLN1	3.3	0.01797
9	CD151 molecule (Raph blood group)	NM_004357	CD151	3.0	0.00006
10	Integrin, beta 5	NM_002213	ITGB5	2.7	0.01539
11	Integrin, alpha 5 (fibronectin receptor, alpha polypeptide)	NM_002205	ITGA5	2.4	0.00012
12	Fibronectin 1	BC005858	FN1	2.0	0.00016
13	Integrin, alpha V (vitronectin receptor, alpha polypeptide, antigen CD51)	AI093579	ITGAV	1.9	0.00030
14	G protein-coupled receptor 161	AI703188	GPR161	1.9	0.00054
Regulators of Actin Cytoskeleton					
1	Tropomyosin 1 (alpha)	NM_000366	TPM1	3.8	0.01856
2	Actin related protein 2/3 complex, subunit 1B, 41kDa	NM_005720	ARPC1B	3.6	0.00076
3	Gelsolin (amyloidosis, Finnish type)	NM_000177	GSN	3.1	0.00272
4	Destrin (actin depolymerizing factor)	BF697964	DSTN	3.0	0.00107
5	Coagulation factor II (thrombin) receptor	NM_001992	F2R	2.6	0.00041
6	TRIO and F-actin binding protein	AF281030	TRIOBP	2.4	0.02048
7	Guanine nucleotide binding protein (G protein), gamma 12	BG111761	GNG12	2.3	0.00005
8	Sperm specific antigen 2	NM_006751	SSFA2	2.2	0.00077
9	Caldesmon 1	AL583520	CALD1	2.2	0.00061
10	CDC42 binding protein kinase alpha (DMPK-like)	NM_003607	CDC42BPA	2.1	0.03035
11	Supervillin	NM_003174	SVIL	2.1	0.01868
12	Myosin, heavy chain 9, non-muscle	AI827941	MYH9	2.1	0.01912
13	IQ motif containing GTPase activating protein 1	NM_003870	IQGAP1	2.0	0.00718



Supplemental Figure S.1: Mouse tibial tumors of Ewing sarcoma cells engineered to express zyxin and $\alpha 5$ integrin maintain Ewing sarcoma histopathology (H&E and CD99).

References

- Ambros, I.M., Ambros, P.F., Strehl, S., Kovar, H., Gadner, H., and Salzer-Kuntschik, M. (1991). MIC2 is a specific marker for Ewing's sarcoma and peripheral primitive neuroectodermal tumors. Evidence for a common histogenesis of Ewing's sarcoma and peripheral primitive neuroectodermal tumors from MIC2 expression and specific chromosome aberration. *Cancer* 67, 1886-1893.
- Amsellem, V., Kryszke, M.H., Hervy, M., Subra, F., Athman, R., Leh, H., Brachet-Ducos, C., and Auclair, C. (2005). The actin cytoskeleton-associated protein zyxin acts as a tumor suppressor in Ewing tumor cells. *Exp. Cell Res.* 304, 443-456.
- Arjonen, A., Kaukonen, R., and Ivaska, J. (2011). Filopodia and adhesion in cancer cell motility. *Cell Adh. Migr.* 5, 421-430.
- Arndt, C.A., and Crist, W.M. (1999). Common musculoskeletal tumors of childhood and adolescence. *N. Engl. J. Med.* 341, 342-352.
- Aurias, A., Rimbaut, C., Buffe, D., Zucker, J.M., and Mazabraud, A. (1984). Translocation involving chromosome 22 in Ewing's sarcoma. A cytogenetic study of four fresh tumors. *Cancer Genet. Cytogenet.* 12, 21-25.
- Bernards, R., and Weinberg, R.A. (2002). A progression puzzle. *Nature* 418, 823.
- Borinstein, S.C., Barkauskas, D.A., Krailo, M., Scher, D., Scher, L., Schlottmann, S., Kallakury, B., Dickman, P.S., Pawel, B.R., West, D.C., *et al.* (2011). Investigation of the insulin-like growth factor-1 signaling pathway in localized Ewing sarcoma: a report from the Children's Oncology Group. *Cancer* 117, 4966-4976.
- Braunreiter, C.L., Hancock, J.D., Coffin, C.M., Boucher, K.M., and Lessnick, S.L. (2006). Expression of EWS-ETS fusions in NIH3T3 cells reveals significant differences to Ewing's sarcoma. *Cell Cycle* 5, 2753-2759.
- Campbell, I.D., and Humphries, M.J. (2011). Integrin structure, activation, and interactions. *Cold Spring Harbor Perspectives In Biology* 3.
- Cavazzana, A.O., Miser, J.S., Jefferson, J., and Triche, T.J. (1987). Experimental evidence for a neural origin of Ewing's sarcoma of bone. *Am. J. Pathol.* 127, 507-518.
- Cerisano, V., Aalto, Y., Perdichizzi, S., Bernard, G., Manara, M.C., Benini, S., Cenacchi, G., Preda, P., Lattanzi, G., Nagy, B., *et al.* (2004). Molecular mechanisms of CD99-induced caspase-independent cell death and cell-cell adhesion in Ewing's sarcoma cells: actin and zyxin as key intracellular mediators. *Oncogene* 23, 5664-5674.

Chaturvedi, A., Hoffman, L.M., Welm, A.L., Lessnick, S.L., and Beckerle, M.C. (2012). The EWS/FLI oncogene drives changes in cellular morphology, adhesion, and migration in Ewing sarcoma. *Genes Cancer* 3, 102-116.

Delattre, O., Zucman, J., Plougastel, B., Desmaze, C., Melot, T., Peter, M., Kovar, H., Joubert, I., de Jong, P., Rouleau, G., *et al.* (1992). Gene fusion with an ETS DNA-binding domain caused by chromosome translocation in human tumours. *Nature* 359, 162-165.

Ewing, J. (1921). Diffuse endothelioma of bone. *Proc. NY Pathol. Soc.* 21, 17-24.

Fellinger, E.J., Garin-Chesa, P., Triche, T.J., Huvos, A.G., and Rettig, W.J. (1991). Immunohistochemical analysis of Ewing's sarcoma cell surface antigen p30/32MIC2. *The Am. J. Pathol.* 139, 317-325.

Geiger, B., and Yamada, K.M. (2011). Molecular architecture and function of matrix adhesions. *Cold Spring Harbor Perspectives In Biology* 3.

Girnita, L., Girnita, A., Wang, M., Meis-Kindblom, J.M., Kindblom, L.G., and Larsson, O. (2000). A link between basic fibroblast growth factor (bFGF) and EWS/FLI-1 in Ewing's sarcoma cells. *Oncogene* 19, 4298-4301.

Guan, H., Zhou, Z., Gallick, G.E., Jia, S.F., Morales, J., Sood, A.K., Corey, S.J., and Kleinerman, E.S. (2008). Targeting Lyn inhibits tumor growth and metastasis in Ewing's sarcoma. *Mol. Cancer Ther.* 7, 1807-1816.

Gupton, S.L., Riquelme, D., Hughes-Alford, S.K., Tadros, J., Rudina, S.S., Hynes, R.O., Lauffenburger, D., and Gertler, F.B. (2012). Mena binds alpha5 integrin directly and modulates alpha5beta1 function. *J. Cell Biol.* 198, 657-676.

Herrero-Martin, D., Osuna, D., Ordonez, J.L., Sevillano, V., Martins, A.S., Mackintosh, C., Campos, M., Madoz-Gurpide, J., Otero-Motta, A.P., Caballero, G., *et al.* (2009). Stable interference of EWS-FLI1 in an Ewing sarcoma cell line impairs IGF-1/IGF-1R signalling and reveals TOPK as a new target. *Br. J. Cancer* 101, 80-90.

Hoffman, L.M., Jensen, C.C., Chaturvedi, A., Yoshigi, M., and Beckerle, M.C. (2012). Stretch-induced actin remodeling requires targeting of zyxin to stress fibers and recruitment of actin regulators. *Mol. Biol. Cell* 23, 1846-1859.

Hynes, R.O. (2002). Integrins: bidirectional, allosteric signaling machines. *Cell* 110, 673-687.

Indovina, P., Rainaldi, G., and Santini, M.T. (2008). Hypoxia increases adhesion and spreading of MG-63 three-dimensional tumor spheroids. *Anticancer research* 28, 1013-1022.

Jedlicka, P. (2010). Ewing sarcoma, an enigmatic malignancy of likely progenitor cell origin, driven by transcription factor oncogenic fusions. *Int. J. Clin. Exp. Pathol.* *3*, 338-347.

Karosas, A.O. (2010). Ewing's sarcoma. *Am. J. Health Syst Pharm.* *67*, 1599-1605.

Kerbel, R.S. (1995). Significance of tumor-host interactions in cancer growth and metastases. *Cancer Metastasis Rev.* *14*, 259-262.

Kimber, C., Michalski, A., Spitz, L., and Pierro, A. (1998). Primitive neuroectodermal tumours: anatomic location, extent of surgery, and outcome. *J. Pediatr. Surg.* *33*, 39-41.

Kinsey, M., Smith, R., and Lessnick, S.L. (2006). NR0B1 is required for the oncogenic phenotype mediated by EWS/FLI in Ewing's sarcoma. *Mol. Cancer Res.* *4*, 851-859.

Knowles, H.J., Schaefer, K.L., Dirksen, U., and Athanasou, N.A. (2010). Hypoxia and hypoglycaemia in Ewing's sarcoma and osteosarcoma: regulation and phenotypic effects of Hypoxia-Inducible Factor. *BMC Cancer* *10*, 372.

Kovar, H. (2005). Context matters: the hen or egg problem in Ewing's sarcoma. *Semin. Cancer Biol.* *15*, 189-196.

Lessnick, S.L., Braun, B.S., Denny, C.T., and May, W.A. (1995). Multiple domains mediate transformation by the Ewing's sarcoma EWS/FLI-1 fusion gene. *Oncogene* *10*, 423-431.

Lessnick, S.L., Dacwag, C.S., and Golub, T.R. (2002). The Ewing's sarcoma oncoprotein EWS/FLI induces a p53-dependent growth arrest in primary human fibroblasts. *Cancer Cell* *1*, 393-401.

Lotz, M.M., Rabinovitz, I., and Mercurio, A.M. (2000). Intestinal restitution: progression of actin cytoskeleton rearrangements and integrin function in a model of epithelial wound healing. *Am. J. Pathol.* *156*, 985-996.

Margadant, F., Chew, L.L., Hu, X., Yu, H., Bate, N., Zhang, X., and Sheetz, M. (2011). Mechanotransduction in vivo by repeated talin stretch-relaxation events depends upon vinculin. *PLoS Biology* *9*, e1001223.

Mateo-Lozano, S., Tirado, O.M., and Notario, V. (2003). Rapamycin induces the fusion-type independent downregulation of the EWS/FLI-1 proteins and inhibits Ewing's sarcoma cell proliferation. *Oncogene* *22*, 9282-9287.

May, W.A., Gishizky, M.L., Lessnick, S.L., Lunsford, L.B., Lewis, B.C., Delattre, O., Zucman, J., Thomas, G., and Denny, C.T. (1993a). Ewing sarcoma 11;22 translocation produces a chimeric transcription factor that requires the DNA-binding domain encoded by FLI1 for transformation. *Proc. Natl. Acad. Sci. USA* *90*, 5752-5756.

May, W.A., Lessnick, S.L., Braun, B.S., Klemsz, M., Lewis, B.C., Lunsford, L.B., Hromas, R., and Denny, C.T. (1993b). The Ewing's sarcoma EWS/FLI-1 fusion gene

encodes a more potent transcriptional activator and is a more powerful transforming gene than FLI-1. *Mol. Cell Biol.* *13*, 7393-7398.

McAllister, N.R., and Lessnick, S.L. (2005). The potential for molecular therapeutic targets in Ewing's sarcoma. *Curr. Treat Options Oncol.* *6*, 461-471.

Mierke, C.T., Frey, B., Fellner, M., Herrmann, M., and Fabry, B. (2011). Integrin alpha5beta1 facilitates cancer cell invasion through enhanced contractile forces. *J. Cell Sci.* *124*, 369-383.

Mostafavi-Pour, Z., Askari, J.A., Parkinson, S.J., Parker, P.J., Ng, T.T., and Humphries, M.J. (2003). Integrin-specific signaling pathways controlling focal adhesion formation and cell migration. *J. Cell Biol.* *161*, 155-167.

Mundy, G.R. (2002). Metastasis to bone: causes, consequences and therapeutic opportunities. *Nat. Rev. Cancer* *2*, 584-593.

Nagae, M., Re, S., Mihara, E., Nogi, T., Sugita, Y., and Takagi, J. (2012). Crystal structure of alpha5beta1 integrin ectodomain: atomic details of the fibronectin receptor. *J. Cell Biol.* *197*, 131-140.

Owen, L.A., Kowalewski, A.A., and Lessnick, S.L. (2008). EWS/FLI mediates transcriptional repression via NKX2.2 during oncogenic transformation in Ewing's sarcoma. *PLoS One* *3*, e1965.

Owen, L.A., and Lessnick, S.L. (2006). Identification of target genes in their native cellular context: an analysis of EWS/FLI in Ewing's sarcoma. *Cell Cycle* *5*, 2049-2053.

Padua, D., Zhang, X.H., Wang, Q., Nadal, C., Gerald, W.L., Gomis, R.R., and Massague, J. (2008). TGFbeta primes breast tumors for lung metastasis seeding through angiopoietin-like 4. *Cell* *133*, 66-77.

Patel, L.R., Camacho, D.F., Shiozawa, Y., Pienta, K.J., and Taichman, R.S. (2011). Mechanisms of cancer cell metastasis to the bone: a multistep process. *Future Oncol.* *7*, 1285-1297.

Perlman, E.J., Dickman, P.S., Askin, F.B., Grier, H.E., Miser, J.S., and Link, M.P. (1994). Ewing's sarcoma--routine diagnostic utilization of MIC2 analysis: a Pediatric Oncology Group/ Children's Cancer Group Intergroup Study. *Hum. Pathol.* *25*, 304-307.

Riggi, N., Suva, M.L., Suva, D., Cironi, L., Provero, P., Tercier, S., Joseph, J.M., Stehle, J.C., Baumer, K., Kindler, V., *et al.* (2008). EWS-FLI-1 expression triggers a Ewing's sarcoma initiation program in primary human mesenchymal stem cells. *Cancer Res.* *68*, 2176-2185.

Rodan, S.B., and Rodan, G.A. (1997). Integrin function in osteoclasts. *J. Endocrinol.* *154 Suppl*, S47-56.

- Rodriguez-Galindo, C., Navid, F., Liu, T., Billups, C.A., Rao, B.N., and Krasin, M.J. (2008). Prognostic factors for local and distant control in Ewing sarcoma family of tumors. *Ann. Oncol.* *19*, 814-820.
- Salsmann, A., Schaffner-Reckinger, E., and Kieffer, N. (2006). RGD, the Rho'd to cell spreading. *Eur. J. Cell Biol.* *85*, 249-254.
- Smilenov, L.B., Mikhailov, A., Pelham, R.J., Marcantonio, E.E., and Gundersen, G.G. (1999). Focal adhesion motility revealed in stationary fibroblasts. *Science* *286*, 1172-1174.
- Smith, M.A., Blankman, E., Gardel, M.L., Luettjohann, L., Waterman, C.M., and Beckerle, M.C. (2010). A zyxin-mediated mechanism for actin stress fiber maintenance and repair. *Dev. Cell* *19*, 365-376.
- Smith, R., Owen, L.A., Trem, D.J., Wong, J.S., Whangbo, J.S., Golub, T.R., and Lessnick, S.L. (2006). Expression profiling of EWS/FLI identifies NKX2.2 as a critical target gene in Ewing's sarcoma. *Cancer Cell* *9*, 405-416.
- Spraker, H.L., Price, S.L., Chaturvedi, A., Schiffman, J.D., Jones, K.B., Lessnick, S.L., Beckerle, M., and Randall, R.L. (2012). The clone wars - revenge of the metastatic rogue state: the sarcoma paradigm. *Front. Oncol.* *2*, 2.
- Taverna, D., Ullman-Cullere, M., Rayburn, H., Bronson, R.T., and Hynes, R.O. (1998). A test of the role of alpha5 integrin/fibronectin interactions in tumorigenesis. *Cancer Res.* *58*, 848-853.
- Tirado, O.M., Mateo-Lozano, S., Villar, J., Dettin, L.E., Llorca, A., Gallego, S., Ban, J., Kovar, H., and Notario, V. (2006). Caveolin-1 (CAV1) is a target of EWS/FLI-1 and a key determinant of the oncogenic phenotype and tumorigenicity of Ewing's sarcoma cells. *Cancer Res.* *66*, 9937-9947.
- Tirode, F., Laud-Duval, K., Prieur, A., Delorme, B., Charbord, P., and Delattre, O. (2007). Mesenchymal stem cell features of Ewing tumors. *Cancer Cell* *11*, 421-429.
- Truong, H., and Danen, E.H. (2009). Integrin switching modulates adhesion dynamics and cell migration. *Cell Adh. Migr.* *3*, 179-181.
- Turc-Carel, C., Aurias, A., Mugneret, F., Lizard, S., Sidaner, I., Volk, C., Thiery, J.P., Olschwang, S., Philip, I., Berger, M.P., *et al.* (1988). Chromosomes in Ewing's sarcoma. I. An evaluation of 85 cases of remarkable consistency of t(11;22)(q24;q12). *Cancer Genet. Cytogenet.* *32*, 229-238.
- Yoshigi, M., Hoffman, L.M., Jensen, C.C., Yost, H.J., and Beckerle, M.C. (2005). Mechanical force mobilizes zyxin from focal adhesions to actin filaments and regulates cytoskeletal reinforcement. *J. Cell Biol.* *171*, 209-215.

Zaidel-Bar, R., Itzkovitz, S., Ma'ayan, A., Iyengar, R., and Geiger, B. (2007). Functional atlas of the integrin adhesome. *Nat. Cell Biol.* 9, 858-867.

CHAPTER 6

SUMMARY AND PERSPECTIVES

Presence of metastatic disease is the most concerning aspect of cancer management and treatment. Most cancer-associated deaths are due to emergence of metastatic lesions in sites away from the primary tumor. Several factors, intrinsic or extrinsic to the tumor, could govern and contribute to the dissemination and colonization of tumor cells (Hanahan and Weinberg, 2011). The focus of my dissertation work has been to investigate the role of cytoskeletal features and, cell-substratum adhesions in determining tumor progression and metastasis of cancer cells. For this study I used a particularly metastatic pediatric tumor called Ewing sarcoma, which is a paradigm to investigate and understand sarcoma biology.

Ewing sarcoma is the second most common primary bone tumor in children and adolescents with ~25% of all patients presenting with metastasis at diagnosis (Gurney et al., 1999; Spraker et al., 2012). Persistent expression of EWS/FLI is necessary for maintenance of the transformed phenotype in Ewing sarcoma (Prieur et al., 2004). This fusion protein operates as an aberrant transcription factor that dysregulates the expression of a large number of target genes, many of which are crucial for malignant transformation, and several others whose relevance in Ewing sarcoma biology is not yet fully recognized (Lessnick et al., 1995; May et al., 1993a; May et al., 1993b). Therefore for my dissertation, I focused on studying the role of EWS/FLI and its downregulated

targets in affecting tumor cell behavior and cell-substratum interactions in Ewing sarcoma.

A loss-of-function approach via RNA interference was used for targeted knockdown of EWS/FLI in multiple patient-derived Ewing sarcoma cell lines which led to dramatic changes in Ewing sarcoma cell behavior. The presence of the EWS/FLI oncoprotein compromised the actin cytoskeleton, reduced cell adhesion and spreading and reduced integrin-based adhesions in a EWS/FLI-dependent manner which result in Ewing sarcoma cells maintaining low basal levels of cellular adhesion, migration and invasion *in vitro* (Chaturvedi et al., 2012). These results were consistent with other studies which described that modulation of cellular features is significant to Ewing sarcoma biology (Amsellem et al., 2005; Cerisano et al., 2004). In support of these phenotypes the transcriptional profiling data for EWS/FLI in Ewing sarcoma cells revealed the significant downregulation of focal adhesion proteins, extracellular matrix or ECM and receptor proteins, and cytoskeletal proteins (Chaturvedi et al., manuscript in preparation).

This dissertation primarily focused on characterizing the roles of two such EWS/FLI downregulated targets: zyxin (a focal adhesion protein) and $\alpha 5$ integrin, which when dimerized with $\beta 1$ subunit forms the receptor for binding fibronectin. I report in this work that zyxin and $\alpha 5$ integrin make unique and distinct contributions to Ewing sarcoma cell behavior both *in vitro* and *in vivo* (Chaturvedi et al., manuscript in preparation). Interestingly, in addition to the receptor ($\alpha 5\beta 1$), its corresponding ligand fibronectin was also downregulated by EWS/FLI highlighting the vital role of receptor-matrix interactions in Ewing sarcoma biology. However, experiments directed at understanding how changes in surrounding matrix environment drives changes in Ewing

sarcoma cell morphology and behavior are crucial in answering many important questions specific to Ewing sarcoma pathogenesis: Why do Ewing sarcoma cells have a predilection for long bones and bone marrow as the primary site of tumorigenesis? And why do Ewing sarcoma cells prefer lungs and bones for metastasis? As the next step towards answering these questions, a microarray based comparative analysis of the bulk tumor and its surrounding tissue at the primary site and secondary site will provide vital information pertinent to tumorigenesis, dissemination and colonization of Ewing sarcoma cells.

My experimental data when taken together with what we know about Ewing sarcoma from the literature and the model of “parallel tumor growth and dissemination” that I have proposed during the course of this work could help elucidate some as yet unknown mechanisms in the pathogenesis of Ewing sarcoma. For example, Ewing sarcoma is a bone malignancy and the cells therefore have easy access to the vasculature. This led me to speculate that aggressive migratory or invasive features may not be very necessary for Ewing sarcoma cells to actively metastasize from the primary site. Instead, based on low adherence of Ewing sarcoma cells I have proposed a novel mechanism for early metastasis wherein reduced cell adhesion potentially facilitates enhanced dissemination of cancer cells into the surrounding vasculature. However, future *in vivo* experiments looking at the presence of circulatory tumor cells in the bloodstream even before the presence of a detectable tumor will be a way to test this hypothesis. The realization that a “passive/stochastic” mechanism may be followed by mesenchymal tumors in contrast to the “active” multistep processes of metastasis that epithelial cancer follow is a novel contribution of this dissertation to the field of cancer research. Although the work described in this dissertation was performed on Ewing sarcoma, it lays a

foundation to verify this paradigm and define molecular mechanisms that could regulate metastasis in similar malignancies.

Although EWS/FLI largely inhibits cellular adhesion proteins, these tumor cells still need to maintain low basal levels of adhesion to be able to form tumors, and attach to and colonize secondary sites for successful metastatic lesions. Based on this discussion we can propose crucial roles for cytoskeletal proteins and receptor-matrix interactions to regulate early as well as late metastasis in Ewing sarcoma. An examination of these target genes dysregulated by EWS/FLI could point towards the molecular mechanisms required for these steps in tumor growth and metastasis.

Although future experiments are required to test the various aspects of these models this dissertation lays the foundation for techniques that enable *in vitro* and *in vivo* studies for understanding Ewing sarcoma. An important accomplishment of my dissertation work was the development of an orthotopic mouse model to study growth and progression of Ewing sarcoma in bone. This model system permitted the study of Ewing sarcoma in its most relevant tissue microenvironment (a long bone or tibia of NOD/SCID mice) that truly represented the cell-substratum interactions we intended to study. This mouse model for the first time shows Ewing sarcoma cell metastasis from a long bone to other boney sites such as bone of the upper limb, spine and ribs in addition to lungs (Chaturvedi et al., manuscript in preparation). As part of this study, a new method was developed in collaboration with Kendall Cooper to detect the presence of Ewing sarcoma cells in the blood circulation of mice using human Alu primers (unpublished results). The presence of circulating tumor cells indicated that, similar to human disease, tumor cells metastasized hematogenously. Therefore these tumors in mice

recapitulated characteristic features of the human disease and validate this orthotopic mouse model as a relevant system to study human Ewing sarcoma.

Until now, most research in Ewing sarcoma was performed in sites other than the bones. Through my research I have shown the metastasis of Ewing sarcoma tumor cells from long bones to other bones and lungs. Collaborative studies are currently underway to test the roles of genes involved in regulating the osteolytic behavior of Ewing sarcoma using this model system. Extensive osteolysis is observed in Ewing sarcoma patients and was also seen in our tibial mouse model. Future studies identifying the pathways critical to osteolysis are necessary as most patients have significant osteolysis at presentation (Spraker et al., 2012). This model can be used to test drug targets that reduce or prevent osteolysis in patients, thereby improving disease management and may lead to more effective targeted therapies for patients with this devastating disease.

After establishing the Ewing sarcoma intratibial mouse model, I used it to assess the contributions of EWS/FLI mediated downregulation of zyxin and/or $\alpha 5$ integrin in affecting tumor growth and metastasis. My results suggested that to promote tumor growth EWS/FLI upregulates some genes like NKX2.2 or NR0B1 (Kinsey et al., 2006; Smith et al., 2006) and also downregulates other genes such as zyxin and $\alpha 5$ integrin (Chaturvedi et al., manuscript in preparation). Interestingly, reexpression of $\alpha 5$ integrin either alone or along with zyxin in Ewing sarcoma cells increased the incidence of metastasis and the lesions appeared sooner in mouse lungs as well. This observation led me to propose another interesting aspect of Ewing sarcoma biology that the same oncogenic event (EWS/FLI) that downregulates genes to promote tumorigenesis could also compromise metastasis. Therefore, using my research I have proposed a mechanism by which EWS/FLI potentially uncouples tumorigenesis and metastasis, a theory that has

been speculated by some researchers in the field of tumor progression for years (Bernards and Weinberg, 2002). Alternatively, it could be deduced that not all gene expression changes caused by EWS/FLI are intentional or beneficial. This theory impresses an idea that EWS/FLI fusion gene has not yet fully evolved as an oncogene.

The cell biology techniques and the intratibial mouse model that have been developed as part of this dissertation have already been proven useful in several collaborative studies. In one such collaboration, the role of another cytoskeletal protein, the intermediate filament protein called keratin 17 (KRT17) was shown to be crucial for oncogenic transformation (Sankar et al., submitted for review). In another collaboration that employed these techniques in addition to other methods, we were able to suggest how Ewing sarcoma cells could maintain a balance between their epithelial-like and mesenchymal-like features (Wiles et al., submitted for review). This study reinforced the idea that Ewing sarcoma cells are largely undifferentiated cells. When taken together with the observations in this dissertation, it can be said that this undifferentiated nature of Ewing sarcoma cells facilitates their growth at primary and secondary sites and also explains the highly micrometastatic nature of Ewing sarcoma cells.

Furthermore, I describe that upon knockdown of EWS/FLI, the cells exhibited what we called a tumor-to-mesenchymal transition (TuMT), not only phenotypically (such as increased cell adhesion and spreading, robust actin filaments) but also in their transcriptional program (Chaturvedi et al., 2012). The loss of the characteristic round cell morphology in Ewing sarcoma cells in the absence of EWS/FLI suggests that morphological features are attributable to the presence of EWS/FLI oncogene. The appearance of more mesenchymal features upon EWS/FLI knockdown suggested that the Ewing sarcoma cells were probably being “normalized” to their original phenotype.

These findings add to the growing body of evidence and are consistent with the current school of thought that progenitor cells or mesenchymal stem cells are the most likely cell of origin for Ewing sarcoma (Riggi et al., 2008; Tirode et al., 2007).

My dissertation work is based on an important assumption that EWS/FLI expression is stable and does not change over the course of tumor growth, progression and metastasis. But at least in a couple of published reports it has been reported that the expression levels of EWS/FLI transcript changes in response to the constantly changing tumor microenvironment (Aryee et al., 2010; Girnita et al., 2000). Therefore, an alternative model needs to be considered and tested where the levels of EWS/FLI change in response to hypoxia, or tissue microenvironment or changes in matrix composition. It can then be implied that corresponding changes in the transcripts of several downstream targets of EWS/FLI will follow further influencing the behavior of Ewing sarcoma cells. Although this alternative “variable EWS/FLI expression” model needs to be tested, it could potentially account for deficits in the “stable EWS/FLI expression” model.

This “variable EWS/FLI expression” model could explain the increased rates of metastasis at both early and later stages of disease progression. For example, it is possible that upon early dissemination of the less adherent tumor cells, the cells enter circulation, where the changing composition of serum and growth factors could transiently affect EWS/FLI expression, thereby changing its transcriptional signature to increase expression of these adhesion proteins. EWS/FLI expression has been shown to be sensitive to changes in the tumor microenvironment, such as the presence of growth factors (Girnita et al., 2000). Another scenario which could result in modulating the expression of EWS/FLI is that of hypoxia, which is observed in a growing Ewing sarcoma tumor and has also been reported to change the transcriptional signature of

EWS/FLI, such as the expression of several integrins including $\alpha 5$ integrin (Knowles et al., 2010).

In conclusion, my PhD dissertation work has identified a novel role for the repressed targets of EWS/FLI in Ewing sarcoma tumor progression and metastasis. Future work will be required to identify which proteins and cell-ECM interactions are critical for oncogenesis and metastasis, and how these tumor cells disseminate and generate metastases. In this study I have defined the need for coordinating both oncogenic transformation and cellular adhesion in Ewing sarcoma. This work impresses the need to study the change in tumor cell behaviors in the context of its relevant micro-environment to understand mechanisms that affect disease progression. It needs to be determined if these mechanisms are specific to Ewing sarcoma or widely applicable to all bone tumors or to sarcomas or other tumors of uncertain origin in general. In addition, our findings highlight the complexity of oncogenic programs and remind us that not all gene expression changes observed in tumors are advantageous for all aspects of tumor initiation and progression.

References

Amsellem, V., Kryszke, M.H., Hervy, M., Subra, F., Athman, R., Leh, H., Brachet-Ducos, C., and Auclair, C. (2005). The actin cytoskeleton-associated protein zyxin acts as a tumor suppressor in Ewing tumor cells. *Exp. Cell Res.* *304*, 443-456.

Aryee, D.N., Niedan, S., Kauer, M., Schwentner, R., Bennani-Baiti, I.M., Ban, J., Muehlbacher, K., Kreppel, M., Walker, R.L., Meltzer, P., *et al.* (2010). Hypoxia modulates EWS-FLI1 transcriptional signature and enhances the malignant properties of Ewing's sarcoma cells in vitro. *Cancer Res.* *70*, 4015-4023.

Bernards, R., and Weinberg, R.A. (2002). A progression puzzle. *Nature* *418*, 823.

Cerisano, V., Aalto, Y., Perdichizzi, S., Bernard, G., Manara, M.C., Benini, S., Cenacchi, G., Preda, P., Lattanzi, G., Nagy, B., *et al.* (2004). Molecular mechanisms of CD99-

induced caspase-independent cell death and cell-cell adhesion in Ewing's sarcoma cells: actin and zyxin as key intracellular mediators. *Oncogene* 23, 5664-5674.

Chaturvedi, A., Hoffman, L.M., Welm, A.L., Lessnick, S.L., and Beckerle, M.C. (2012). The EWS/FLI oncogene drives changes in cellular morphology, adhesion, and migration in Ewing sarcoma. *Genes Cancer* 3, 102-116.

Chaturvedi, A., Hoffman, L.M., Jensen, C., Yi-Chun Lin, Grossmann, A.H., Randall, L.R., Lessnick, S.L., Welm, A.L., Beckerle, M.C. Molecular dissection of the mechanism by which EWS/FLI expression compromises actin cytoskeletal integrity and cell adhesion in Ewing sarcoma cells. Manuscript in Preparation.

Girnit, L., Girnit, A., Wang, M., Meis-Kindblom, J.M., Kindblom, L.G., and Larsson, O. (2000). A link between basic fibroblast growth factor (bFGF) and EWS/FLI-1 in Ewing's sarcoma cells. *Oncogene* 19, 4298-4301.

Gurney J.G., S.A.R., Bulterys M. (1999). Malignant bone tumors. Cancer incidence and survival among children and adolescents: US SEER Prog. 1975-95 Bethesda: NCI; 99-110.

Hanahan, D., and Weinberg, R.A. (2011). Hallmarks of cancer: the next generation. *Cell* 144, 646-674.

Hoffman, L.M., Jensen, C.C., Chaturvedi, A., Yoshigi, M., and Beckerle, M.C. (2012). Stretch-induced actin remodeling requires targeting of zyxin to stress fibers and recruitment of actin regulators. *Mol. Biol. Cell* 23, 1846-1859.

Hoffman, L.M., Jensen, C.C., Kloeker, S., Wang, C.L., Yoshigi, M., and Beckerle, M.C. (2006). Genetic ablation of zyxin causes Mena/VASP mislocalization, increased motility, and deficits in actin remodeling. *J. Cell Biol.* 172, 771-782.

Hynes, R.O. (2002). Integrins: bidirectional, allosteric signaling machines. *Cell* 110, 673-687.

Kinsey, M., Smith, R., and Lessnick, S.L. (2006). NR0B1 is required for the oncogenic phenotype mediated by EWS/FLI in Ewing's sarcoma. *Mol. Cancer Res.* 4, 851-859.

Knowles, H.J., Schaefer, K.L., Dirksen, U., and Athanasou, N.A. (2010). Hypoxia and hypoglycaemia in Ewing's sarcoma and osteosarcoma: regulation and phenotypic effects of Hypoxia-Inducible Factor. *BMC Cancer* 10, 372.

Lessnick, S.L., Braun, B.S., Denny, C.T., and May, W.A. (1995). Multiple domains mediate transformation by the Ewing's sarcoma EWS/FLI-1 fusion gene. *Oncogene* 10, 423-431.

May, W.A., Gishizky, M.L., Lessnick, S.L., Lunsford, L.B., Lewis, B.C., Delattre, O., Zucman, J., Thomas, G., and Denny, C.T. (1993a). Ewing sarcoma 11;22 translocation

produces a chimeric transcription factor that requires the DNA-binding domain encoded by FLI1 for transformation. *Proc. Natl. Acad. Sci. USA* *90*, 5752-5756.

May, W.A., Lessnick, S.L., Braun, B.S., Klemsz, M., Lewis, B.C., Lunsford, L.B., Hromas, R., and Denny, C.T. (1993b). The Ewing's sarcoma EWS/FLI-1 fusion gene encodes a more potent transcriptional activator and is a more powerful transforming gene than FLI-1. *Mol. Cell Biol.* *13*, 7393-7398.

Mierke, C.T., Frey, B., Fellner, M., Herrmann, M., and Fabry, B. (2011). Integrin $\alpha 5 \beta 1$ facilitates cancer cell invasion through enhanced contractile forces. *J. Cell Sci.* *124*, 369-383.

Owen, L.A., Kowalewski, A.A., and Lessnick, S.L. (2008). EWS/FLI mediates transcriptional repression via NKX2.2 during oncogenic transformation in Ewing's sarcoma. *PLoS One* *3*, e1965.

Prieur, A., Tirode, F., Cohen, P., and Delattre, O. (2004). EWS/FLI-1 silencing and gene profiling of Ewing cells reveal downstream oncogenic pathways and a crucial role for repression of insulin-like growth factor binding protein 3. *Mol. Cell Biol.* *24*, 7275-7283.

Riggi, N., Suva, M.L., Suva, D., Cironi, L., Provero, P., Tercier, S., Joseph, J.M., Stehle, J.C., Baumer, K., Kindler, V., *et al.* (2008). EWS-FLI-1 expression triggers a Ewing's sarcoma initiation program in primary human mesenchymal stem cells. *Cancer Res.* *68*, 2176-2185.

Sankar, S., and Lessnick, S.L. (2011). Promiscuous partnerships in Ewing's sarcoma. *Cancer Genet.* *204*, 351-365.

Smith, M.A., Blankman, E., Gardel, M.L., Luetjohann, L., Waterman, C.M., and Beckerle, M.C. (2010). A zyxin-mediated mechanism for actin stress fiber maintenance and repair. *Dev. Cell* *19*, 365-376.

Smith, R., Owen, L.A., Trem, D.J., Wong, J.S., Whangbo, J.S., Golub, T.R., and Lessnick, S.L. (2006). Expression profiling of EWS/FLI identifies NKX2.2 as a critical target gene in Ewing's sarcoma. *Cancer Cell* *9*, 405-416.

Spraker HL, Price SL, Chaturvedi A, Schiffman JD, Jones KB, Lessnick SL, Beckerle M, and RL, R. (2012). The clone wars – Revenge of the metastatic rogue state: The sarcoma paradigm. *Front. Oncol.* *2*.

Tirode, F., Laud-Duval, K., Prieur, A., Delorme, B., Charbord, P., and Delattre, O. (2007). Mesenchymal stem cell features of Ewing tumors. *Cancer Cell* *11*, 421-429.

Yoshigi, M., Hoffman, L.M., Jensen, C.C., Yost, H.J., and Beckerle, M.C. (2005). Mechanical force mobilizes zyxin from focal adhesions to actin filaments and regulates cytoskeletal reinforcement. *J. Cell Biol.* *171*, 209-215.